

No. 211

March 1980

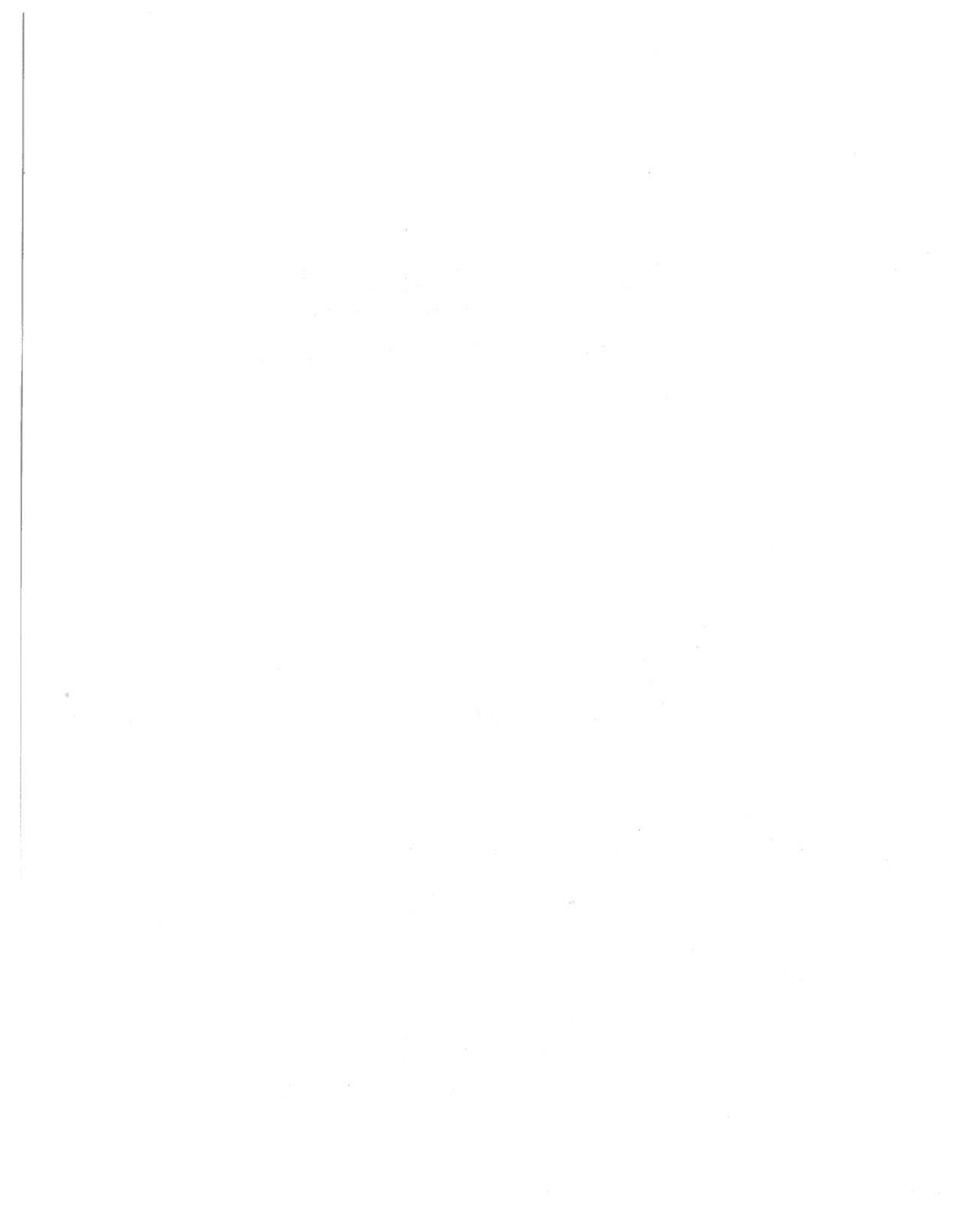
# ADAPTIVE PATH CONTROL OF SURFACE SHIPS IN RESTRICTED WATERS

Michael G. Parsons  
Hua Tu Cuong



THE DEPARTMENT OF NAVAL ARCHITECTURE AND MARINE ENGINEERING

THE UNIVERSITY OF MICHIGAN  
COLLEGE OF ENGINEERING



No. 211

March 1980

ADAPTIVE PATH CONTROL OF  
SURFACE SHIPS IN RESTRICTED WATERS

Michael G. Parsons  
Hua Tu Cuong

This research was sponsored by  
U.S. Coast Guard Contract  
DOT-CG-74843-A



Department of Naval Architecture  
and Marine Engineering  
College of Engineering  
The University of Michigan  
Ann Arbor, Michigan 48109

117

117

117

117

117

117

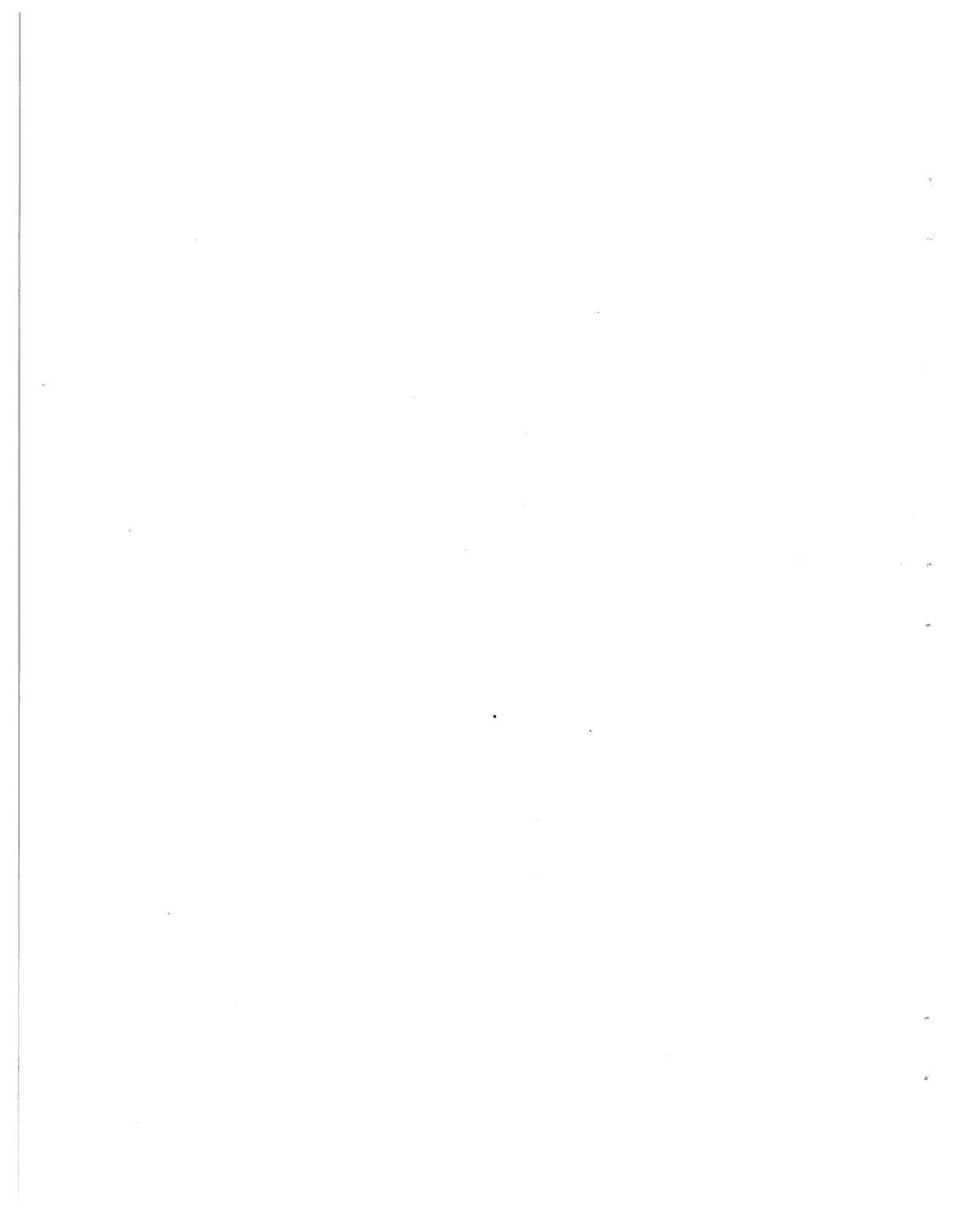
### Abstract

The feasibility and effectiveness of using an integrated system for the adaptive control of a surface ship along a prescribed path in restricted waters is investigated. The controller consists of four major components arranged in two loops: an inner or control loop and an outer or gain update loop. The inner loop consists of a Kalman state estimator and an optimal stochastic control law which would provide effective control when subjected to disturbances and measurement noise. The outer loop estimates the parameters of the system equations of motion to enable the controller to adapt itself for the changes in ship characteristics which take place due to changes in the ship operating condition and environment. The Brownian motion process is shown to be an effective model for bias disturbances in the design of the Kalman filter. A design criterion is proposed for the selection of the appropriate value of the diffusion coefficient to achieve the desired character of the disturbance model. A control loop designed using this approach is shown to perform very effectively with typical disturbances. The transient response of the control loop is, however, sensitive to variations in two of the coefficients in the equations of motion. Weighted Least-Squares (WLS) and Minimum Variance (MVE) parameter estimation algorithms, which might be used to estimate these coefficients on-line, are investigated. For effective parameter estimation, the ship must be excited to a sufficient level of motion using an open-loop rudder command. Adaptive path control would, therefore, have to consist of alternate periods of open-loop control and closed-loop path control. The WLS algorithm is shown to be more appropriate for off-line estimation of time-invariant parameters. The MVE algorithm shows promise as an effective on-line ship parameter estimator for use in an adaptive system.



## Table of Content

	<u>page</u>
Abstract	i
List of Figures	iii
List of Tables	v
Nomenclature	vi
1. Introduction	1
2. Problem Formulation	6
2.1 Equations of Motion	6
2.2 Measurement Selection	9
2.3 Process Disturbances	12
3. Control Loop Design	17
3.1 Optimal, Steady-State Controller Design	17
3.2 First-Order Shaping Filter Approach	19
3.3 Random Walk Approach	27
3.4 Necessity for an Adaptive Design	36
4. Weighted Least-Squares Parameter Estimator	45
4.1 Derivation and Development	45
4.2 Time-Invariant Parameters Performance	52
4.2.1 Effect of Data Window Length and Dither Period	55
4.2.2 Performance with Bias Disturbances	59
4.3 Time-Varying Parameters Performance	62
4.3.1 Time-Varying Ship Coefficients	63
4.3.2 Time-Varying Disturbances	65
4.4 Computational Requirements	67
5. Minimum Variance Parameter Estimator	69
5.1 Derivation and Development	69
5.2 Algorithm Summary	81
5.3 Time-Invariant Parameters Performance	82
5.4 Time-Varying Parameters Performance	90
5.5 Parameter Identifiability and Measurement Importance	98
5.6 Computational Requirements	101
6. Conclusions	102
7. References	108





## List of Figures

<u>Figure</u>	<u>page</u>
1. Overall Schematic of Adaptive Path Controller	2
2. Coordinate System for Path Control	6
3. Design Passing Ship Disturbance	13
4. Design Lateral Current Disturbance	14
5. Lateral Current Disturbance at ABC Harbor Entrance	16
6. Lateral Offset Response to B/2 Initial Offset and Passing Ship - First-Order Shaping Filter Disturbance Model Design	24
7. Rudder Angle Response to B/2 Initial Offset and Passing Ship - First-Order Shaping Filter Disturbance Model Design	24
8. Lateral Offset Response to Design Lateral Current-- First-Order Shaping Filter Disturbance Model Design	25
9. Rudder Angle Response to Design Lateral Current-- First-Order Shaping Filter Disturbance Model Design	26
10. Yawing Moment Estimate with Design Lateral Current-- First-Order Shaping Filter Disturbance Model Design	26
11. Lateral Offset Response to B/2 Initial Offset and Passing Ship - Random Walk Disturbance Model Design	32
12. Rudder Angle Response to B/2 Initial Offset and Passing Ship - Random Walk Disturbance Model Design	32
13. Lateral Offset Response to Design Lateral Current-- Random Walk Disturbance Model Design	33
14. Rudder Angle Response to Design Lateral Current-- Random Walk Disturbance Model Design	33
15. Yawing Moment Estimate with Design Lateral Current-- Random Walk Disturbance Model Design	34
16. Lateral Offset Response at ABC Harbor Entrance-- Random Walk Disturbance Model Design	35
17. Rudder Angle Response at ABC Harbor Entrance-- Random Walk Disturbance Model Design	35
18. Lateral Offset Response to Design Lateral Current-- Designs for $H/T=1.89$ and $H/T=\infty$ Operating at $H/T=\infty$	37
19. Rudder Angle Response to Design Lateral Current-- Design for $H/T=1.89$ Operating at $H/T=\infty$	38
20. Yawing Moment Estimate with Design Lateral Current-- Design for $H/T=1.89$ Operating at $H/T=\infty$	38
21. Lateral Offset Response to Design Lateral Current-- Partially-Adapted Design and Design for $H/T=\infty$ Operating at $H/T=\infty$	42

<u>Figure</u>	<u>page</u>
22. Rudder Angle Response to Design Lateral Current-- Partially-Adapted Design Operating at $H/T=\infty$	43
23. Yawing Moment Estimate with Design Lateral Current-- Partially-Adapted Design Operating at $H/T=\infty$	43
24. Timing Sequence for Weighted Least-Squares Parameter Estimator	46
25. Stepped Bottom Profile	53
26. Lateral Offset Response to Constant Disturbances -- WLS Parameter Estimator	61
27. Timing Sequence for Minimum Variance Parameter Estimator	70
28. Simulation Conditions and Approximate Ship Path -- Con- stant Bottom Example	86
29. Estimate of $f_{23}$ by MVE Parameter Estimator -- Constant Bottom with Passing Ship Example	88
30. Estimate of $f_{25}$ by MVE Parameter Estimator -- Constant Bottom with Passing Ship Example	89
31. Estimate of $f_{32}$ by MVE Parameter Estimator -- Constant Bottom with Passing Ship Example	89
32. Simulation Conditions and Approximate Ship Path -- Rising Bottom Example	93
33. Estimate of $f_{23}$ by MVE Parameter Estimator -- Rising Bottom with Passing Ship Example	95
34. Estimate of $f_{25}$ by MVE Parameter Estimator -- Rising Bottom with Passing Ship Example	96
35. Simulation Conditions and Approximate Ship Path -- Falling Bottom Example	97
36. Estimate of $f_{23}$ by MVE Parameter Estimator -- Falling Bottom with Passing Ship Example	99
37. Estimate of $f_{25}$ by MVE Parameter Estimator -- Falling Bottom with Passing Ship Example	99

## List of Tables

<u>Table</u>	<u>page</u>
1. Characteristics of <i>Tokyo Maru</i> Model and Prototype	8
2. Coefficients of <i>Tokyo Maru</i> versus H/T at $F_n=0.116$	9
3. Reference Measurement Noise Characteristics	12
4. Optimal Gains for <i>Tokyo Maru</i> at H/T=1.89 and $F_n=0.116$ -- First-Order Shaping Filter Disturbance Model	23
5. Optimal Gains for <i>Tokyo Maru</i> at H/T=1.89 and $F_n=0.116$ -- Random Walk Disturbance Model	31
6. Optimal Gains for <i>Tokyo Maru</i> at H/T= $\infty$ and $F_n=0.116$ -- Random Walk Disturbance Model	39
7. RMS Cost $\bar{J}$ for <i>Tokyo Maru</i> with Various Controllers at H/T= $\infty$ - First-Order Shaping Filter Disturbance Model	40
8. Gains for Partially-Adapted Design for <i>Tokyo Maru</i> at $F_n=0.116$ - Random Walk Disturbance Model	41
9. Reference Measurement Noise for Parameter Estimator $\underline{y}'$	47
10. Permissible Ranges of Parameter Estimates for the <i>Tokyo Maru</i>	51
11. Effect of Data Window Length and Dither Period on WLS Parameter Estimates without Disturbances	57
12. Effect of Data Window Length and Dither Period on WLS Parameter Estimates with Constant Disturbances	60
13. Parameter Estimates from Constant Disturbance Simula- tion	62
14. Parameter Estimates from WLS Parameter Estimator with Sloping Bottom	64
15. Parameter Estimates from Passing Ship Simulation	66
16. Parameter Estimates from MVE Parameter Estimates -- Con- stant Bottom Examples	87
17. Design Diffusion Coefficient Matrix	91
18. Parameter Estimates from MVE Parameter Estimator -- Sloping Bottom Examples	94
19. Typical "Normalized" Optimal Parameter Estimator Gain Matrix	100



## Nomenclature

A	state weighting matrix
a	coefficient in Bech's equation, eq. (1)
$a_{ij}$	elements of state weighting matrix
B	control weighting matrix, ship beam [m], or generalized noise covariance matrix eq. (101)
b	coefficient in Bech's equation, eq. (1)
$b_{ij}$	elements of control weighting matrix
C	optimal control gain matrix
$C_k$	defined by eq. (84)
$\hat{C}_k$	defined by eq. (85)
$\check{C}_k$	defined by eq. (86)
$\hat{D}_k$	defined by eq. (84)
$\hat{D}_k$	defined by eq. (87)
$\check{D}_k$	defined by eq. (88)
E	Balchen's disturbance environment matrix, eq. (58)
$E[\dots]$	expectation operation
$E_z[\dots]$	conditional expectation operation w.r.t. $Z_{k-1}$
F	4-state system open-loop dynamics matrix
$F' = I + \Delta t F$	discrete form of F
$F_e$	estimator open-loop dynamics matrix
$F_n = U/\sqrt{gL}$	Froude number based on ship length
$F_s$	system open-loop dynamics matrix
$f_{ij}$	element i, j of F, $F_e$ , or $F_s$
G	4-state system estimator control distribution matrix
$G' = \Delta t G$	discrete form of G
$G_{k-1}$ or G	generalized measure of noise power, eq. (112)
$G_e$	estimator control distribution matrix
$G_s$	system control distribution matrix
g	acceleration of gravity [ $m/s^2$ ]
H	water depth [m]
$H_e$	estimator measurement scaling matrix
$H_s$	system measurement scaling matrix
I	Identity matrix
$\underline{I}_k$	innovation vector

$I_{zz}$	ship yaw mass moment of inertia [ $\text{kgm}^2$ ]
$I'_{zz} = 2I_{zz}/\rho L^5$	nondimensional yaw mass moment of inertia
J	optimal control or Weighted Least-Squares cost function
$\tilde{J}$	RMS cost, eq. (70)
$J_{zz}$	yaw added mass moment of inertia [ $\text{kgm}^2$ ]
$J'_{zz} = 2J_{zz}/\rho L^5$	nondimensional yaw added mass moment of inertia
K	Kalman-Bucy state estimator gain matrix
$K_k$	MVE parameter estimator gain matrix
k or k'	discrete time index
L	ship length between perpendiculars [m]
LB	length of batch update calculation period
LU	length of the update cycle
LW	length of the data window
$\ell$	identification frequency
M	coefficient matrix of Euler-Lagrange equations, eq. (36)
M'	coefficient matrix of Euler-Lagrange equations, eq. (50)
m	control vector dimension or ship mass [kg];
$m' = 2m/\rho L^3$	nondimensional ship mass
$m_y$	sway added mass [kg]
$m'_y = 2m_y/\rho L^3$	nondimensional sway added mass
N	total yaw moment or yaw moment disturbance [Nm]
$N' = 2N/\rho L^3 U^2$	nondimensional N
$N_r$	derivative of yaw moment w.r.t. yaw angular velocity [Nms/rad]
$N'_r = 2N_r/\rho L^4 U$	nondimensional $N_r$
$N_v$	derivative of yaw moment w.r.t. lateral velocity [Ns]
$N^{\circ}_v$	derivative of yaw moment w.r.t. lateral acceleration [ $\text{Ns}^2$ ]
$N_{\beta}$	derivative of yaw moment w.r.t. drift angle [Nm/rad]
$N'_{\beta} = 2N_{\beta}/\rho L^3 U^2$	nondimensional $N_{\beta}$
$N^{\circ}_{\beta}$	derivative of yaw moment w.r.t. drift angle [Nm/rad]
$N^{\circ}_{\beta_1} = 2N^{\circ}_{\beta}/\rho L^4 U$	nondimensional $N^{\circ}_{\beta}$
$N_{\delta}$	derivative of yaw moment w.r.t. rudder angle [Nm/rad]
$N'_{\delta} = 2N_{\delta}/\rho L^3 U^2$	nondimensional $N_{\delta}$
$N^{\circ}_{\delta}$	derivative of yaw moment w.r.t. rudder angle rate [Nms/rad]
n	dimension of state vector
$\underline{n}$	white noise disturbance vector eq. (58)
ne	dimension of augmented state vector

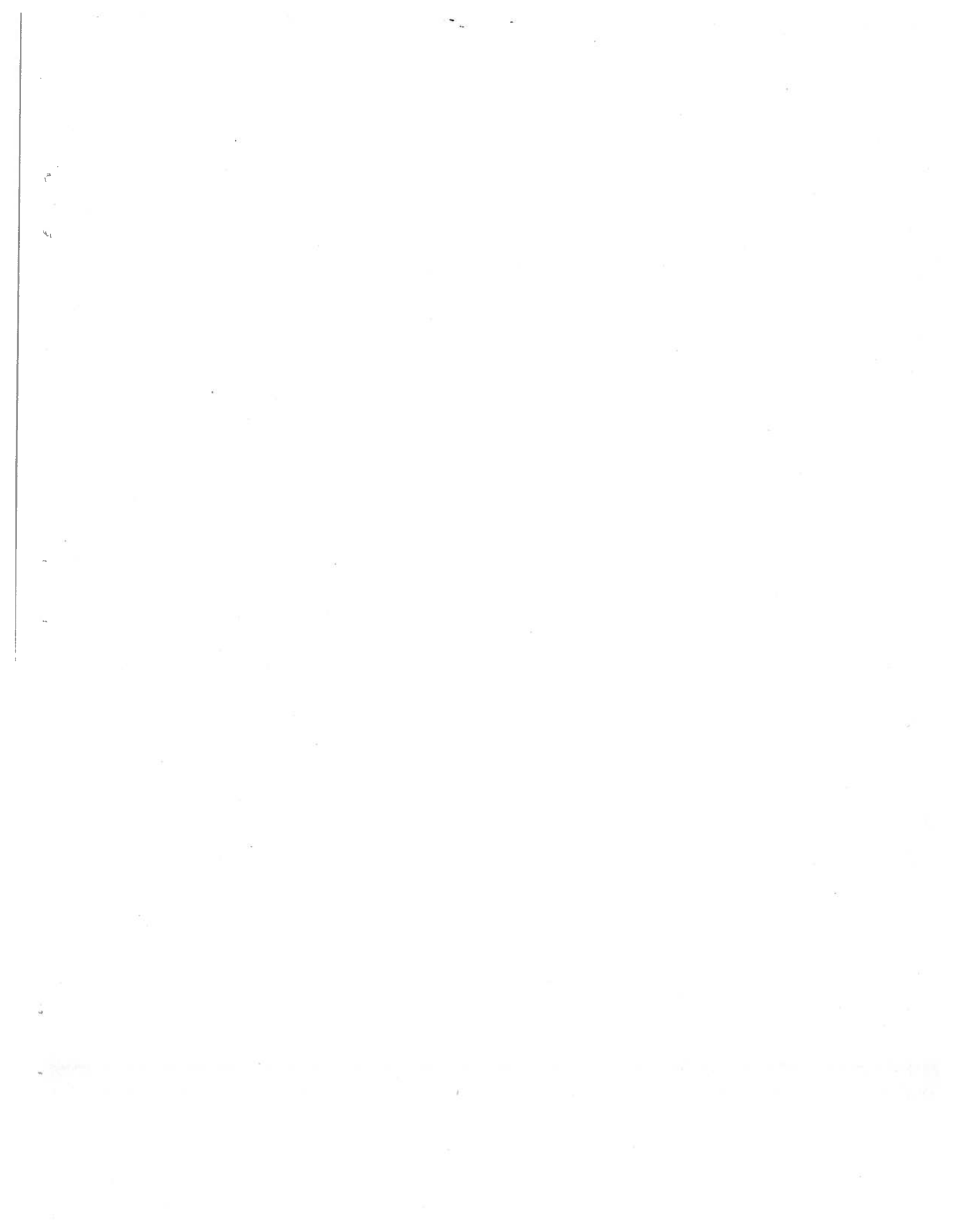
$n_s$	dimension of state vector
$P$	error covariance matrix in estimate of augmented state $\underline{x}'$ or error covariance matrix in estimate of parameter vector
$P_k$	discrete form of $P$
$P_\infty$	steady-state value of $P$
$p$	dimension of measurement vector
$\underline{p}$	parameter vector
$p_i$	component of parameter vector
$p_l$ or $p_u$	limits on parameter estimates, Table 10
$\hat{\underline{p}}$	parameter estimate vector
$\hat{\underline{p}} - \underline{p}$	parameter estimate error vector
$\bar{p}_i$	assumed parameter mean
$Q$	process disturbance power spectral density matrix
$Q_w$	process disturbance covariance matrix
$q$	dimension of disturbance vector or disturbance spectral density
$\bar{q}$	disturbance covariance
$q_{ii}$	diagonal element $i, i$ of $Q$
$R$	measurement noise power spectral density matrix or covariance matrix
$R_{eq, k-1}$ or $R_{eq}$	equivalent noise spectral density matrix eq. (101)
$r = d\psi/dt$	yaw angular velocity [rad/s]
$r' = rL/U$	nondimensional yaw angular velocity
$r'_m$	nondimensional $r$ of model simulation
$\dot{r}$	yaw angular acceleration [rad/s <sup>2</sup> ]
$\dot{r}' = rL^2/U^2$	nondimensional yaw angular acceleration
$r_{ii}$	diagonal element $i, i$ of $R$
$S$	solution to optimal control Riccati equation or slope or maximum rate of change of disturbance
$S_\infty$	steady-state value of $S$
$\underline{s}$	vector of known parameters (here just 1)
$T$	ship draft [m]
$T_N$	nondimensional correlation time of yaw moment disturbance
$T_Y$	nondimensional correlation time of sway force disturbance

$T_r$	nondimensional rudder control time constant
$t$	time [s]
$t'=tU/L$	nondimensional time
$\Delta t$	integration time step, sample time interval
$U$	ship speed [m/s]
$U_{k-1}$ or $U$	weighted covariance matrix, eq. (101)
$u$	longitudinal component of ship speed [m/s]
$\underline{u}$	control vector
$v$	lateral component of ship speed [m/s]
$v'_c$	nondimensional current velocity
$\underline{v}$ or $\underline{v}'$	measurement noise vector
$W_k$	weighting matrix in WLS cost function
$\underline{w}$	process disturbance vector
$w_{ik}$	elements of $W_k$
$w_N$ or $w_Y$	white noise driving disturbance models for N and Y
$X_+, X_-, X'_+, X'_-$	eigenvectors, eq. (37) and (51)
$x$	longitudinal axis of ship
$\underline{x}$	state vector
$\underline{x}'$	augmented state vector
$\hat{\underline{x}}$	estimate of augmented state vector
$\underline{x}_m$	simulated state vector used in the WLS algorithm
$Y$	total sway force or sway force disturbance [N]
$Y'=2Y/\rho L^2 U^2$	nondimensional Y
$Y_r$	derivative of sway force w.r.t. yaw angular velocity [Ns/rad]
$Y'_r=2Y_r/\rho L^3 U$	nondimensional $Y_r$
$Y_{\cdot r}$	derivative of sway force w.r.t. yaw angular acceleration [Ns <sup>2</sup> /rad]
$Y_{\cdot r}'=2Y_{\cdot r}/\rho L^4$	nondimensional $Y_{\cdot r}$
$Y_v$	derivative of sway force w.r.t. lateral velocity [Ns/m]
$Y_{\beta}$	derivative of sway force w.r.t. drift angle [N/rad]
$Y'_{\beta}=2Y_{\beta}/\rho L^2 U^2$	nondimensional $Y_{\beta}$
$Y_{\delta}$	derivative of sway force w.r.t. rudder angle [N/rad]
$Y'_{\delta}=2Y_{\delta}/\rho L^2 U^2$	nondimensional $Y_{\delta}$
$Y_{\dot{\delta}}$	derivative of sway force w.r.t. rudder angle rate [Ns/rad]



$y$	transverse axis of ship
$Z_{k-1}$	whole measurement history to time $k-1$
$\underline{z}$	measurement vector for control loop
$\underline{z}'$	measurement vector for gain update loop
$\tilde{z}_k = z_k - \hat{D}_{k-1} s_{k-1}$	pseudomeasurement vector
$\alpha_i$	assumed parameter standard deviation
$\beta = \beta'$	drift angle [rad] relative to earth
$\beta'_e$	effective drift angle relative to water
$\beta'_m$	nondimensional $\beta$ of model simulation
$\dot{\beta}$	drift angular velocity [rad/s]
$\beta' = \dot{\beta} L / U$	nondimensional drift angular velocity
$\Gamma$	4-state system disturbance distribution matrix
$\Gamma_s$	system disturbance distribution matrix
$\Gamma_e$	estimator disturbance distribution matrix
$\Gamma' = \Delta t \Gamma$	discrete form of $\Gamma$
$\gamma_{ij}$	element $i, j$ of $\Gamma$
$\delta = \delta'$	rudder angle [rad]
$\delta_c = \delta'_c$	commanded rudder angle [rad]
$\delta(t-\tau)$	Dirac delta function
$\epsilon$	numerical parameter in eq. (59)
$\eta$	lateral offset from nominal track [m]
$\eta' = \eta / L$	nondimensional $\eta$
$\eta_k$	Gaussian white sequence in parameter model, eq. (83)
$\eta'_m$	nondimensional $\eta$ of model simulation
$\kappa$	coefficient in Bech's equation, eq. (1)
$\Lambda_+, \Lambda_-, \Lambda'_+, \Lambda'_-$	eigenvectors, eq. (37) and (51)
$\lambda_i$	nondimensional eigenvalues
$\xi$	position along nominal track [m]
$\underline{\xi}_i$	Jordan-form eigenvector
$\rho$	water density [ $\text{kg/m}^3$ ]
$\underline{\sigma}'$	measurement noise standard deviation vector used in simulation (element $\sigma'_i$ )
$\tau$	dummy time variable or correlation time
$\tau_i$	time constant in Bech's equation, eq. (1), or correlation time

$\phi$	parameter diffusion coefficient matrix
$\phi_{ii}$	diagonal elements of $\phi$
$\chi$ and $\chi'$	modal matrices eqs. (37) and (51)
$\psi = \psi'$	heading angle [rad]
$\psi'_m$	heading angle of model simulation
$(\underline{\dots})$	vector quantity
$(\dot{\dots})$	derivative w.r.t. time
$(\dots)_\infty$	steady-state value of quantity, $t = \infty$
$(\tilde{\dots})$	root mean square (RMS) value or assumed, constant value of quantity
$(\overline{\dots})$	mean value of quantity
$(\dots)_o$	initial value of quantity, desired value of quantity on prescribed path, or acceptable value of quantity used in forming A and B weighting matrices
$[\dots]^T$	transpose of a matrix
$[\dots]^{-1}$	inverse of a matrix





## 1. Introduction

The problem of controlling surface ships along prescribed paths in maneuvering situations is becoming increasingly important from operational, safety, and environmental viewpoints. In these situations, ships are subjected to short-term, essentially zero-mean disturbances due to passing ships, current and wind variations, waves, and bank and bottom changes. Ships are also subject to more long-term, non-zero-mean disturbances due to current, wind, second-order wave forces, and banks. The dynamic characteristics of the ships also change significantly depending on depth-under-keel, draft, trim, and speed. These maneuvering situations can place severe demands on pilots, conning officers, and helmsmen thus making some form of automated control desirable or perhaps even necessary in the future.

In this report, we investigate the use of two types of adaptive controllers for the path control of surface ships in restricted waters. In this context, restricted waters include straits, channels, harbors, canals, rivers, and harbors where the ship must steer a prescribed path and not just maintain a prescribed heading. In our earlier work,<sup>1</sup> we investigated the use of non-adaptive, optimal stochastic controllers for this purpose. These control systems consisted of a steady-state Kalman filter and a steady-state optimal state feedback controller. The Kalman filter uses noisy measurements to generate an unbiased estimate of the state which is then used by the controller to generate the rudder command. These controllers were shown to provide effective control when a ship is subjected to short-term, essentially zero-mean disturbances. Our earlier work did not produce controllers which could accommodate more long-term disturbances without a mean offset from the desired path. We also showed the desirability of an adaptive system which could automatically account for changes in the dynamic characteristics of the ship due to changes in depth-under-keel or other operating conditions.

In this work, we develop surface ship path controllers which can accommodate long-term disturbances with a zero-mean offset from the path and which can adapt for changes in the dynamic characteristics of the ship. Our overall approach is shown schematically in Fig. 1. The control system consists of four major components which are arranged into two loops. The inner or control loop consists of a steady-state Kalman filter or state estimator and a steady-state optimal state feedback controller. This inner loop is similar to the

control systems used in our earlier work<sup>1</sup> except that the design used here can accommodate long-term disturbances. The outer or gain update loop consists of an on-line parameter estimator and a second function which recalculates the steady-state filter and controller gains using the latest estimates of the ship parameters. The gain update loop would be implemented batch-wise or at a slower rate than the control loop. Thus, the control loop uses piecewise constant gains. The control and gain update loops would both be implemented in an onboard digital computer.

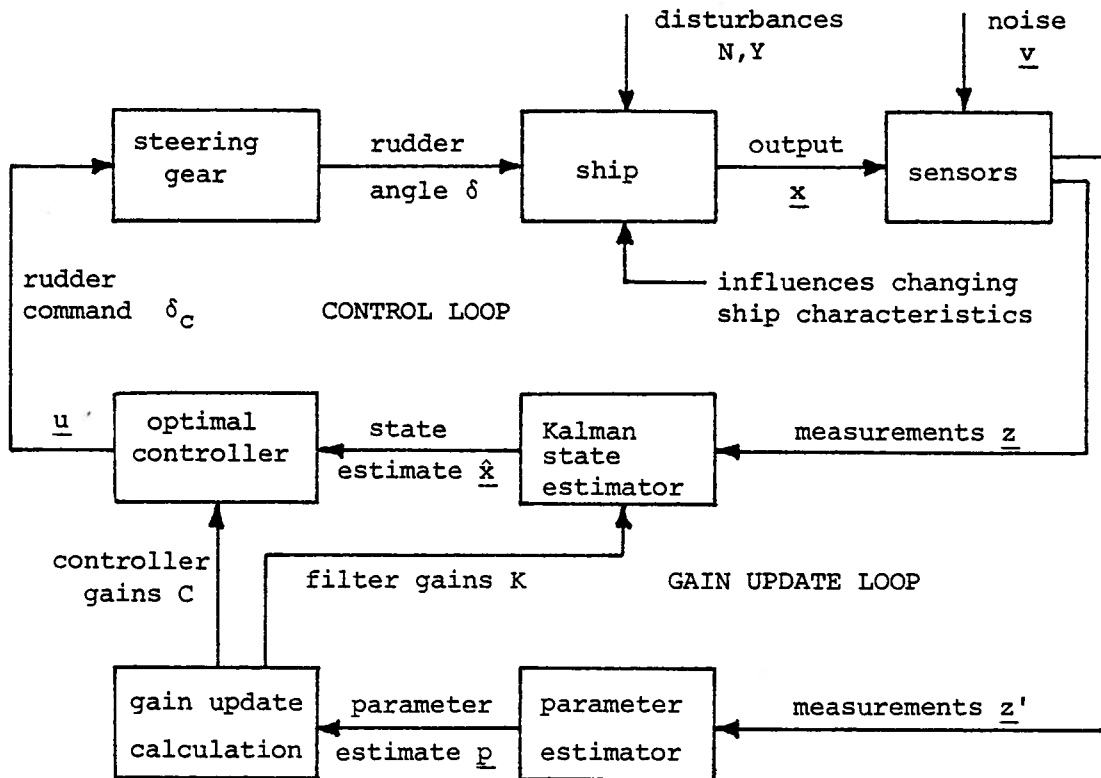


Figure 1. Overall Schematic of Adaptive Path Controller

A number of approaches can be taken to develop an adaptive ship path controller. The preferred approach would be a design which would be robust enough to provide effective control under all ship operating conditions without adjustment. In general, this is not feasible. For years, ship heading autopilots have included manual deadband and gain adjustments to accommodate changing sea states. This approach can provide only limited adaptation and requires proper operator action. An alternative approach would be to have

controller gains preprogrammed as functions of a few operating conditions such as depth-to-draft ratio H/T and draft. This approach would be feasible but could not cover all variables and would require more extensive knowledge of ship characteristics than is usually available. The final approach, which we use here, is to have the controller automatically establish the predominant part of the ship dynamics on-line thus permitting adaptation to changing conditions.

Work has been underway in recent years on the development of adaptive ship heading autopilots. Development in The Netherlands began with simplified versions of Bech's second-order turning rate ( $\dot{\psi}$ ) equation; i.e.,

$$\ddot{\psi} + \left[ \frac{1}{\tau_1} + \frac{1}{\tau_2} \right] \dot{\psi} + \frac{\kappa}{\tau_1 \tau_2} (a\dot{\psi}^3 + b\dot{\psi}) = \frac{\kappa}{\tau_1 \tau_2} (\tau_3 \dot{\delta} + \delta) . \quad (1)$$

Honderd and Winkelman<sup>2</sup> assumed that  $\tau_3=0$  and that only  $b$  varies with water depth. They designed a simple model reference adaptive controller for heading control using a sensitivity model approach. van Amerongen and Udink ten Cate<sup>3,4</sup> developed a second model reference adaptive controller using a stability (Liapunov) approach. van Amerongen, Nieuwenhuis, and Udink ten Cate<sup>5</sup> also reported the development of a model reference adaptive controller using a gradient based method. In this latter work, the  $\dot{\delta}$  term in eq. (1) was retained and both  $a$  and  $b$  were assumed to vary with depth. Some of these heading autopilots have been successfully tested at sea. van Amerongen and van Nauta Lemke<sup>6</sup> reported the most recent Dutch work on model reference type adaptive heading autopilots in 1978.

In contrast to the Dutch work, a number of recent heading autopilot designs include adaptive features which are preprogrammed; i.e., open-loop schedules which are prescribed in advance. Oldenburg<sup>7</sup> describes an autopilot which adapts for speed, depth-under-keel and sea state in this manner. Ware, Fields, and Bozzi<sup>8</sup> describe an autopilot which includes a pair of parallel notch filters in which the notch frequencies are scheduled as a function of vessel speed in order to provide adaptation to changes in wave encounter frequency. Sugimoto and Kojima<sup>9</sup> report another example of a recent autopilot design with preprogrammed gain adjustment. Their autopilot is designed to adapt for loading condition, speed, and sea-state.

A third direction in adaptive heading autopilot development has evolved from the work of Åström in Sweden. Åström<sup>10</sup> recently demonstrated the need for adaptive ship heading controllers and noted that Källström had used the approach presented by Åström, et al<sup>11,12</sup> to design adaptive heading autopilots for a number of large tankers. He noted that these have been tested successfully and that one had been operating for more than one year at sea (1976). Källström and his colleagues<sup>13</sup> reported on this work in 1977. In this approach, the system is modeled as a discrete, single-input, single-output system (auto regressive moving average formulation) disturbed by white noise. The unknown system parameters are then estimated by recursive least-squares, extended least-squares or maximum likelihood schemes. A minimum output variance control law is used. Volta and Tiano<sup>14</sup> have also developed adaptive heading controllers based on the work of Åström and Wittenmark.<sup>11</sup> Simulation of these controllers was reported by Brink, Baas, Tiano, and Volta<sup>15</sup> in 1978.

In this work, we are concerned with path control instead of heading control of the ship. Our approach also uses multi-variable instead of single-input, single-output methods. In restricted waters where path control is of interest, the conditions which alter the characteristics of the ship, such as water depth, can change fairly rapidly compared to the dynamics of the ship. This creates a difficult on-line parameter estimation problem. Off-line system identification methods have been applied to marine vehicles with success in recent years. Abkowitz<sup>16</sup> has used an extended Kalman filter approach. Work in Sweden at Lund Institute of Technology and the Swedish State Tank<sup>17,18,19</sup> has used output error, prediction error, and maximum likelihood methods to estimate linear and more recently non-linear surface ship steering dynamics. The maximum likelihood method is also being applied to submarine systems identification in this country.<sup>20,21</sup> Work in Japan<sup>22,23</sup> has utilized Akaike's Information Criterion for the identification of ship steering dynamics. In general, these techniques utilize ship motion histories which are minutes long during which the ship travels many ship lengths. The ship parameters to be estimated must be constant during this period for successful identification. It is usually considered necessary for the record length to be at least a few times the longest time constant of the system for success using noisy measurements. In restricted waters, the ship characteristics may not be even reasonably constant over a length of time equal to the longest time constant of the system



which might be 50 to 100 s. and a ship length or two. This makes practical on-line parameter estimation from noisy measurements very difficult in restricted waters.

This report is presented in four principal parts. In Section 2, we formulate the ship path control problem including a development of the linear equations of motion, a discussion of measurement selection, and a development of the design process disturbances which are used in the evaluation of system performance using digital simulation. In Section 3, we present the development and evaluation of the inner or control loop part of the path controller. This presentation also includes the optimal state feedback controller and Kalman filter gain calculation methods used in the gain update calculation function of the outer loop in Fig. 1. This section includes a review of the shaping filter approach for process disturbance modeling which we used in our earlier work<sup>1</sup> and which cannot accommodate more long-term process disturbances without a non-zero mean offset from the path. We then present an alternative approach using a random-walk process disturbance model which can accommodate the more long-term disturbances. This section closes with a demonstration of the need for adaptation in a surface ship controller used in restricted waters. Sections 4 and 5 present the development and evaluation of two separate approaches for the parameter estimation function of the outer or gain update loop. Section 4 presents a batch type, weighted-least-squares parameter estimation scheme using a moving window of ship motion data. This is a statistical approach which makes no use of the probable measurement noise levels. Section 5 presents a recursive type, minimum variance scheme. This is a probabilistic approach which utilizes probabilistic estimates of the measurement noise levels. The final section, Section 6, presents our conclusions based upon this work.

## 2. Problem Formulation

In this section, we formulate the surface ship path control problem as a linear, state-variable control problem. The selection of measurements and typical process disturbances are also discussed.

### 2.1 Equations of Motion.

The development of the linearized, state-variable equations of motion for a surface ship moving in the horizontal plane presented here is based on the formulation by Fujino<sup>24</sup> and is presented in more detail in our earlier work.<sup>1</sup> The coordinate system for the problem is shown in Fig. 2. The  $0-\xi\eta$  system is fixed in space with the desired ship path along the  $\xi$ -axis. We assume here that the desired path is a straight line. This simplification does not alter the essential character of the control problem and is typical in maneuvering situations where the ship is to follow a series of straight path or leading line segments. The CG-xy system is fixed at the center of gravity of the ship. The positive sense of the drift angle  $\beta$ , heading angle  $\psi$ , yaw rate  $r$ , and rudder angle  $\delta$  are shown. Neglecting the effects of pitch and roll, the ship motion can be described by coordinates  $x, y$ , and  $\psi$ .

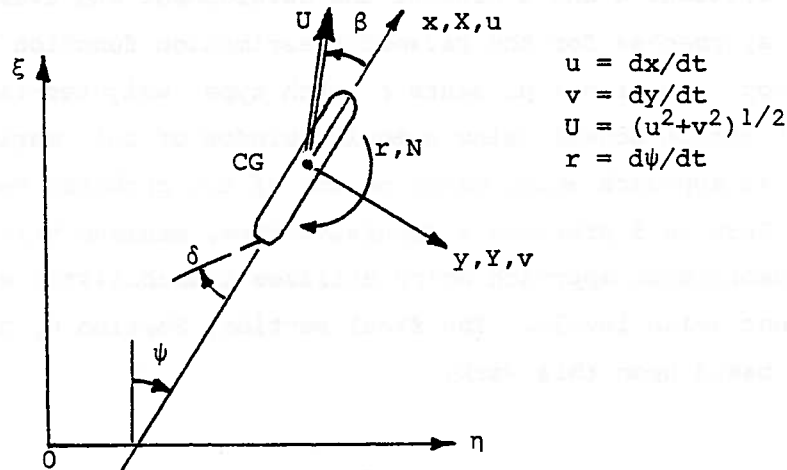


Figure 2. Coordinate System for Path Control

The exact equations of motion of the ship are integro-differential equations in which convolution integrals represent the memory effect of the fluid to previous motion.<sup>25</sup> An alternative formulation yields differential equations with frequency dependent coefficients. Fujino<sup>26</sup> has shown that for the maneuvers

of interest here the frequency dependence is negligible and constant-coefficient differential equations can be utilized. This assumption becomes less and less valid as  $H/T \rightarrow 1$ . When the equations of motion are linearized about the nominal path, the equation in the x-coordinate decouples so that the ship motion can be given by,

$$(m+m_y) \frac{dv}{dt} = Y_v v + (-mU+Y_r)r + Y_r \dot{r} + Y_\delta \delta + Y \quad , \quad (2)$$

$$(I_{zz}+J_{zz}) \frac{dr}{dt} = N_v v + N_r r + N_v \dot{v} + N_\delta \delta + N \quad , \quad (3)$$

$$\frac{d\eta}{dt} = U(\psi-\beta) \quad , \quad (4)$$

which are valid for small deviations from the equilibrium straight-line, constant speed  $U$  condition. An external sway force  $Y$  and an external yawing moment  $N$  are included to account for disturbances which act on the ship. It is common and convenient to utilize drift angle  $\beta$  instead of the lateral velocity  $v$  so we can use,

$$v = -U \sin \beta \approx -U\beta \quad , \quad (5)$$

to express eq. (2) and (3) in terms of the drift angle. These equations can then be nondimensionalized as shown in the Nomenclature to yield,

$$\frac{d\psi'}{dt'} = r' \quad , \quad (6)$$

$$-(m'+m_{y'}) \frac{d\beta'}{dt'} = Y_{\beta, \beta'} + (-m'+Y_{r'})r' + Y_{r'} \dot{r}' + Y_{\delta'} \delta' + Y' \quad , \quad (7)$$

$$(I'_{zz}+J'_{zz}) \frac{dr'}{dt'} = N_{\beta, \beta'} + N_{r'} r' + N_{\beta'} \dot{\beta}' + N_{\delta'} \delta' + N' \quad , \quad (8)$$

$$\frac{d\eta'}{dt'} = \psi' - \beta' \quad , \quad (9)$$

$$\frac{d\delta'}{dt'} = \frac{1}{T_r} (\delta'_c - \delta') \quad , \quad (10)$$

where we have now included a first-order model for the steering gear dynamics. The control is the commanded rudder angle  $\delta'_c$ . The unit of nondimensional time  $t'$  is the time it takes the ship to travel one ship length.

Equations (6) through (10) can be transformed into state-variable form; i.e.,

$$\frac{d}{dt'} \begin{bmatrix} \psi' \\ r' \\ \beta' \\ \eta' \\ \delta' \end{bmatrix} = \begin{bmatrix} 0 & 1 & 0 & 0 & 0 \\ 0 & f_{22} & f_{23} & 0 & f_{25} \\ 0 & f_{32} & f_{33} & 0 & f_{35} \\ 1 & 0 & -1 & 0 & 0 \\ 0 & 0 & 0 & 0 & -1/T_r \end{bmatrix} \begin{bmatrix} \psi' \\ r' \\ \beta' \\ \eta' \\ \delta' \end{bmatrix} + \begin{bmatrix} 0 \\ 0 \\ 0 \\ 0 \\ 1/T_r \end{bmatrix} \delta'_c + \begin{bmatrix} 0 & 0 \\ Y_{21} & Y_{22} \\ Y_{31} & Y_{32} \\ 0 & 0 \\ 0 & 0 \end{bmatrix} \begin{bmatrix} N' \\ Y' \end{bmatrix}, \quad (11)$$

or,

$$\dot{\underline{x}}' = F_s \underline{x}' + G_s \underline{u} + \Gamma_s \underline{w}. \quad (12)$$

The coefficients of the open loop dynamics matrix  $f_{ij}$  and the disturbance distribution matrix  $Y_{ij}$  are algebraic combinations of the stability derivatives and mass and inertia terms in eq. (7) and (8).<sup>1</sup> For this study, we utilize data obtained by Fujino<sup>24,27,28</sup> for a model of the 290 m. tanker *Tokyo Maru*. Fujino conducted planar motion mechanism (PMM) and oblique tow tests of the model at various water depth-to-draft ratios  $H/T$ . Selected characteristics for this vessel are shown in Table 1. The coefficients  $f_{ij}$  and  $Y_{ij}$  obtained for the *Tokyo Maru* at 12 knots full-scale at  $H/T$  values of 1.30, 1.50, 1.89, 2.50, and  $\infty$  are given in Table 2. As shown by Fujino<sup>24</sup> this vessel is course unstable for the intermediate depth-to-draft ratios from about 3.0 down to 1.75 as is typical of many large tankers.

characteristic	Fujino's model	prototype
linear scale ratio, $\lambda$	145.0	-
length between perpendiculars, m	2.000	290
breadth, m	.3276	47.5
draft, m	.1103	16.0
displacement	58.4 kg	179,100 LT
block coefficient	0.8054	0.8054
rudder area	3,390.0 mm <sup>2</sup>	71.29 m <sup>2</sup>
propeller diameter	53.8 mm	7.80 m
P/D	0.740	0.740
expanded area ratio	0.619	0.619
number of blades	5	5

Table 1. Characteristics of *Tokyo Maru* Model and Prototype.

H/T	1.30	1.50	1.89	2.50	$\infty$
f <sub>22</sub>	-1.6508	-1.7136	-1.7657	-1.8177	-1.9515
f <sub>23</sub>	9.3157	6.6235	5.7359	4.6112	3.1591
f <sub>25</sub>	-0.55543	-0.79235	-0.88074	-1.0416	-1.0410
Y <sub>21</sub> =f <sub>26</sub>	346.69	385.98	477.68	536.00	567.13
Y <sub>22</sub> =f <sub>27</sub>	4.8040	-2.2145	-5.0043	-5.8625	2.3365
f <sub>32</sub>	0.02974	0.13890	0.17199	0.23621	0.31507
f <sub>33</sub>	-1.0388	-0.71895	-0.52766	-0.54560	-0.63651
f <sub>35</sub>	-0.09995	-0.12092	-0.15607	-0.16639	-0.16163
Y <sub>31</sub> =f <sub>36</sub>	11.825	14.230	21.141	21.942	16.844
Y <sub>32</sub> =f <sub>37</sub>	-19.216	-23.123	-28.233	-31.490	-37.384

Table 2. Coefficients of *Tokyo Maru* versus H/T at  $F_n=0.116$   
(12 knots full-scale)

## 2.2 Measurement Selection.

All of the states in the ship path control problem as formulated in eq. (11) are available for measurement. The heading  $\psi'$  can be obtained from a compass; the yaw rate  $r'$  can be obtained from a rate gyro; the drift angle  $\beta'=-v'$  can be obtained from a doppler sonar; the rudder angle  $\delta'$  can be obtained from the rudder stock or less accurately from the steering gear rams. The lateral offset from the desired path  $\eta'$  must be obtained using navigation aids such as DECCA Hi-Fix or radar. Each of these measurements may be subject to bias and zero-mean measurement errors and system transmission noise. In the presence of this measurement "noise" and with the measurement of only selected states, the complete state vector can be estimated using a Kalman filter<sup>1,29,30</sup> provided all of the states are observable with the chosen measurements.

The authors have previously studied the observability of the ship path control problem.<sup>1</sup> It was shown that it is necessary to measure the lateral offset  $\eta'$ . Additional measurements improve the ability of a Kalman filter to estimate all the states and thus improve the effectiveness of an optimal state feedback controller. The yaw rate  $r'$  is the next most effective measurement. The heading  $\psi'$  is readily available and is the next most effective measurement. The drift angle  $\beta'$  measurement was shown to add little to the effectiveness of a ship path controller which already measures  $\eta', r',$  and  $\psi'$ . With the steering gear model used in Section 2.1, there is little need to measure the rudder angle since the state is known exactly given any initial condition  $\delta'(t_0)$  and the subsequent rudder command history  $\delta'_c(t), t \geq t_0$ . In any practical application, the steering gear would have its own, separate feedback system; the first-order model included in eq. (11) is just a means of intro-

ducing a realistic rudder time response into our study. For the purposes of the inner or control loop design, it is reasonable to assume a measurement vector consisting of measurements of  $\psi'$ ,  $r'$ , and  $\eta'$  each contaminated by Gaussian, white noise; i.e.,

$$\underline{z}^{p \times 1} = \begin{bmatrix} 1 & 0 & 0 & 0 & 0 \\ 0 & 1 & 0 & 0 & 0 \\ 0 & 0 & 0 & 1 & 0 \end{bmatrix} \underline{x} + \begin{bmatrix} v_1 \\ v_2 \\ v_3 \end{bmatrix} = H_S \underline{x} + \underline{v} \quad (13)$$

The concept of observability relates to the feasibility of estimating the states of a system from a particular set of measurements. In an adaptive system (or in off-line parameter estimation), a second objective is the estimation of the parameters of the system from a particular set of measurements and the system input history. Identifiability is the dual of observability in this context. Åström and Källström<sup>18</sup> have studied the parameter identifiability of the open-loop dynamics matrix parameters  $f_{ij}$  in the  $\dot{r}'$  and the  $\dot{\beta}'$  equations in eq. (11). They showed that these parameters are identifiable provided both  $\psi'$  and  $v'$  are measured. This conclusion requires that the ship is controllable with the rudder which is known to be generally true and which has been demonstrated theoretically by the authors.<sup>1</sup> In the path control problem,  $\psi'$  and  $\eta'$  can provide the same identifiability as  $\psi'$  and  $v'$  as can be seen from eq. (9). Regardless, it is advisable to use all feasible measurements in the parameter estimation so we assume that all states are measured for use in the outer or gain update loop in Fig. 1. This gives,

$$\underline{z}'^{n \times 1} = \underline{x} + \underline{v}' \quad (14)$$

This full measurement vector is also used in some of the inner or control loop designs which are presented in the following sections.

The final part of measurement definition is to establish reasonable levels for the measurement noise  $\underline{v}$  and  $\underline{v}'$ . The white noise power spectral density needed in our continuous system design approach can be estimated by assuming the noise to be exponentially correlated with an RMS noise level  $\sigma_j$  and a correlation time  $\tau_j$ . The  $\tau_j$  should be much faster than the time constants of the ship and less than the system sampling time for the white noise model to be valid. The power spectral density can then be estimated by,

$$r_{jj} \cong 2(\sigma_j)^2 \tau_j . \quad (15)$$

To evaluate the control system effectiveness in this study, we use digital simulation with a fixed-stepsize Euler integration scheme. This has the effect of approximating the continuous Gauss-Markov process, eq. (11) and eq. (13), by a discrete Gauss-Markov process. In these simulations, the covariance of the computer generated random measurement noise must be selected to be consistent with the design noise power spectral density. To provide equivalent state estimate error covariances, it is necessary that the simulation measurement noise variance given by,

$$\sigma_j'^2 = \frac{r_{jj}}{\Delta t} , \quad (16)$$

where  $\Delta t$  is the integration stepsize.<sup>1,31</sup> This can also be considered from a more direct viewpoint. If the controller is implemented digitally in an onboard computer with the system sampled each  $\Delta t$ , the measurement noise will be a white sequence with variance  $\sigma_j'^2$ .

The reference measurement noise levels used in this work are shown in Table 3. In view of our earlier comments about the rudder model included in eq. (11), we assume exact knowledge of the rudder angle. Åström and Källström<sup>18</sup> note that all sensors have dynamics with time constants less than 1 sec. and that the measurement errors are about 0.1° in  $\psi$ , 0.02°/s in  $r$  and 0.01 m/s in  $v$ . Millers<sup>32</sup> uses RMS errors of 0.2° in  $\psi$ , 0.01°/s in  $r$  and 10 m. in  $\eta$ . Canner<sup>33</sup> states that DECCA Hi-Fix crosstrack errors are as low as 1m. when the baseline is along the desired path as is done at the entrance to Europoort. Åström and Källström<sup>18</sup> and Byström and Källström<sup>19</sup> have found errors in  $r$  of less than 0.002 °/s in systems identification of full-scale experiments. In view of this data, the reference levels assumed in Table 3 seem reasonable. The values for  $r_{jj}$  and  $\sigma_j'$  are nondimensional. The  $\sigma_j'$  are calculated by eq. (16) assuming  $\Delta t'=0.005$  ( $\Delta t \cong .24$  s) which we use in our simulations. A noise correlation time of 0.1 s. and a sampling time of .24 s. imply some correlation but the resulting values for  $\sigma_j'$  yield reasonable covariances for a white measurement noise sequence. Dimensionally, the  $\sigma_j'$  are about 93 percent of the assumed values for  $\sigma_j$ .

measurement	source	$\sigma_j$	$\tau_j$	$r_{jj}$	$\sigma_{j'}$
$\psi'$	compass	0.1°	0.1s	$1.298 \times 10^{-8}$	$1.611 \times 10^{-3}$
$r'$	rate gyro	0.01°/s	0.1s	$2.860 \times 10^{-7}$	$7.563 \times 10^{-3}$
$\beta'(v')$	doppler sonar	0.01 m/s	0.1s	$1.118 \times 10^{-8}$	$1.459 \times 10^{-3}$
$\eta'$	DECCA Hi-Fix	3m	0.1s	$4.559 \times 10^{-7}$	$9.549 \times 10^{-3}$

Table 3. Reference Measurement Noise Characteristics

### 2.3 Process Disturbances.

While operating in restricted waters, a ship can be subjected to a wide range of disturbances. Many of these can be characterized as being short-term relative to the time constants of the ship and as having essentially a zero mean value. First-order wave forces, wind gusts, bottom ripples as observed outside Europoort,<sup>34</sup> and passing ships can be included in this category. Other disturbances remain long enough relative to the time constants of the ship that they must be considered to have non-zero mean value. Second-order wave forces and the effect of a lateral current, bank, or steady wind are included in this category. For the purposes of this study, we define a number of typical or design process disturbances which are used in simulations to evaluate the performance of the various path controllers. These design disturbances are defined briefly here.

Passing Ship. The lateral force  $Y'$  and yawing moment  $N'$  due to a passing ship was selected as a typical short-term, essentially zero-mean disturbance. The assumed design disturbance is shown in Fig. 3. This disturbance is based on results originally presented by Newton<sup>35</sup> for two *Mariner* vessels passing in deep water. These results are considered to be representative forces and moment histories and thus are reasonable for use in comparisons here. Yung<sup>36</sup> and Abkowitz, Ashe, and Fortson<sup>37</sup> show that the magnitude of the disturbances increase in shallow water as  $H/T > 1$  so the magnitudes in Fig. 3 are known to be low at the shallower depths. In Fig. 3, the nondimensional time scale is in ship lengths and the ships are beam-to-beam at  $t'=0$ . These lateral force and yawing moment histories are assumed to be independent of depth under keel in our simulations.



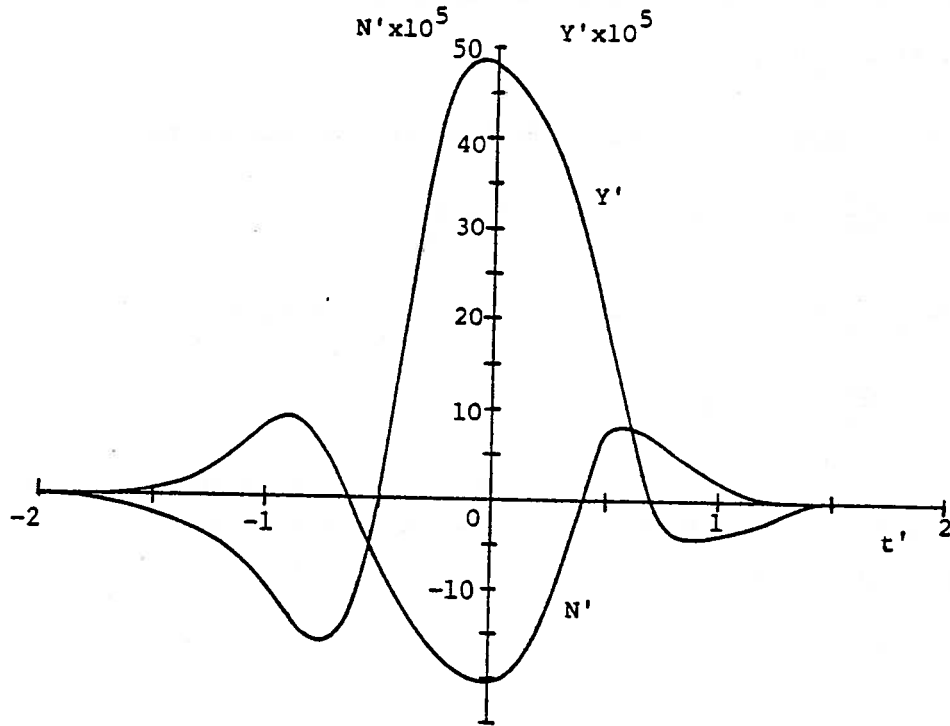


Figure 3. Design Passing Ship Disturbance.

Lateral Current. The effect of a lateral current was selected as a typical long-term, nonzero-mean disturbance for use in our ship path controller simulations. In a steady current, the ship assumes an equilibrium condition with  $\delta'=0$  and  $\psi'=\beta'$  so that the effective drift angle relative to the water  $\beta_e'$  is zero. In this condition, there is no external hydrodynamic lateral force or yawing moment on the ship. In our ship maneuvering equations, we have assumed to this point that the drift angle  $\beta'$  is with respect to the earth. In shallow water, a doppler sonar would actually measure lateral velocity relative to the bottom. In a lateral current  $v_c'$  without an additional disturbance, eq. (7), (8), and (9) should properly be written,

$$-(m'+m_y') \frac{d\beta_e'}{dt'} = Y_\beta \beta_e' + (-m'+Y_r) r' + Y_r \dot{r}' + Y_\delta \delta' \quad , \quad (17)$$

$$(I'_{zz} + J'_{zz}) \frac{dr'}{dt'} = N_\beta \beta_e' + N_r r' + N_\beta \dot{\beta}_e' + N_\delta \delta' \quad , \quad (18)$$

$$\frac{d\eta'}{dt'} = \psi' - \beta_e' + v_c' \quad . \quad (19)$$

Now if the drift angle relative to the earth  $\beta'$  is introduced,

$$\beta_e' = \beta' + v_C' \quad , \quad (20)$$

eq. (17), (18), and (19) become as follows in a steady current:

$$-(m' + m_y') \frac{d\beta'}{dt} = Y_{\beta} \beta' + (-m' + Y_r) r' + Y_r \dot{r}' + Y_{\delta} \delta' + Y_{\beta} v_C' \quad , \quad (21)$$

$$(I'_{zz} + J'_{zz}) \frac{dr'}{dt} = N_{\beta} \beta' + N_r r' + N_{\beta} \dot{\beta}' + N_{\delta} \delta' + N_{\beta} v_C' \quad , \quad (22)$$

$$\frac{dn'}{dt} = \psi' - \beta' \quad . \quad (23)$$

Thus when using the drift angle with respect to the earth in eq. (11), a steady current has the effect of applying an external lateral force and yawing moment given by,

$$Y' = Y_{\beta} v_C' \quad , \quad (24)$$

and,

$$N' = N_{\beta} v_C' \quad . \quad (25)$$

For design evaluation purposes, we have used eq. (24) and (25) to establish the lateral force and yawing moment produced by a 1 knot lateral current on the *Tokyo Maru* moving at 12 knots in an intermediate water depth  $H/T=1.89$ . This disturbance was assumed to be constant for 15 ship lengths and then to reduce linearly to one half this value at 20 ship lengths. This design disturbance is shown in Fig. 4. These lateral force and yawing moment histories are assumed to be independent of depth under keel in our simulations.

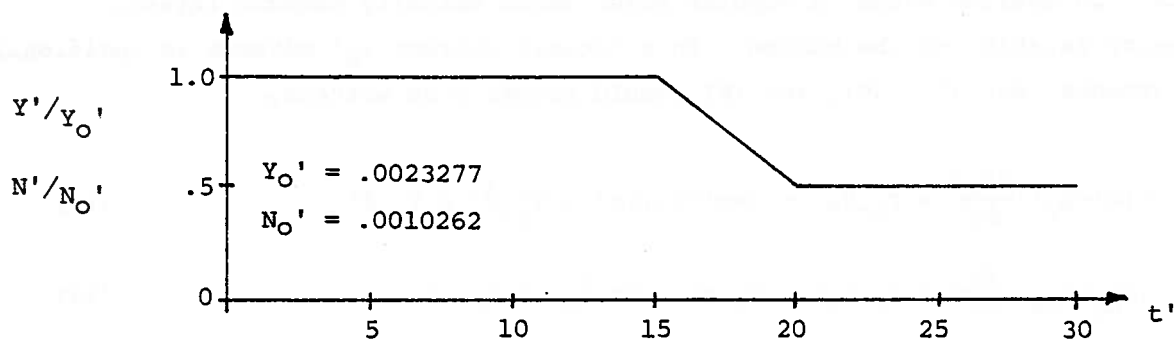


Figure 4. Design Lateral Current Disturbance

ABC Harbor Entrance. As a final design evaluation disturbance we selected an approximation to the lateral current disturbance experienced at the entrance to Europoort (Rotterdam). This lateral current was included in the ABC harbor definition recommended by the SNAME H-10 Controllability panel for use in ship controllability studies.<sup>38</sup> This proves to be a very demanding test for a path controller. There is about a 1 knot lateral current outside the entrance which increases up to about 2 knots at about 0.4 km from the harbor entrance. The lateral current then reduces to zero at the harbor entrance. In this situation, the lateral current produces two types of forces and moments on the ship in addition to those resulting from the use of the drift angle with respect to the earth in eq. (11). First, the changing current will cause the ship to accelerate with respect to the earth so additional inertial forces and moments will appear in eq. (7) and (8). Second, the spatial current change over the length of the ship will produce a changing lateral force along the hull which can be integrated stripwise similar to the approach used by Newman<sup>39</sup> to yield a total lateral force and yawing moment on the ship.

All of the effects of the steady and changing lateral current at the entrance to the ABC harbor can be moved to the right side of eq. (7) and (8) and combined as net lateral force and yawing moment terms. With  $\beta'$  assumed to be with respect to the earth, this net result is a disturbance history similar to that shown in Fig. 5. This disturbance history is based on similar results presented by van Oortmerssen<sup>40</sup> and has been verified by the authors using a simplified strip theory approach. In Fig. 5, the ship's bow reaches the harbor entrance ( $v_c'=0$ ) at  $t'=11.0$ ; the stern thus reaches the entrance at  $t'=12.0$ . The steady values for  $t' \leq 6$  in Fig. 5 have approximately the same magnitude (1 knot lateral current) as those in Fig. 4 for  $t \leq 15$ .

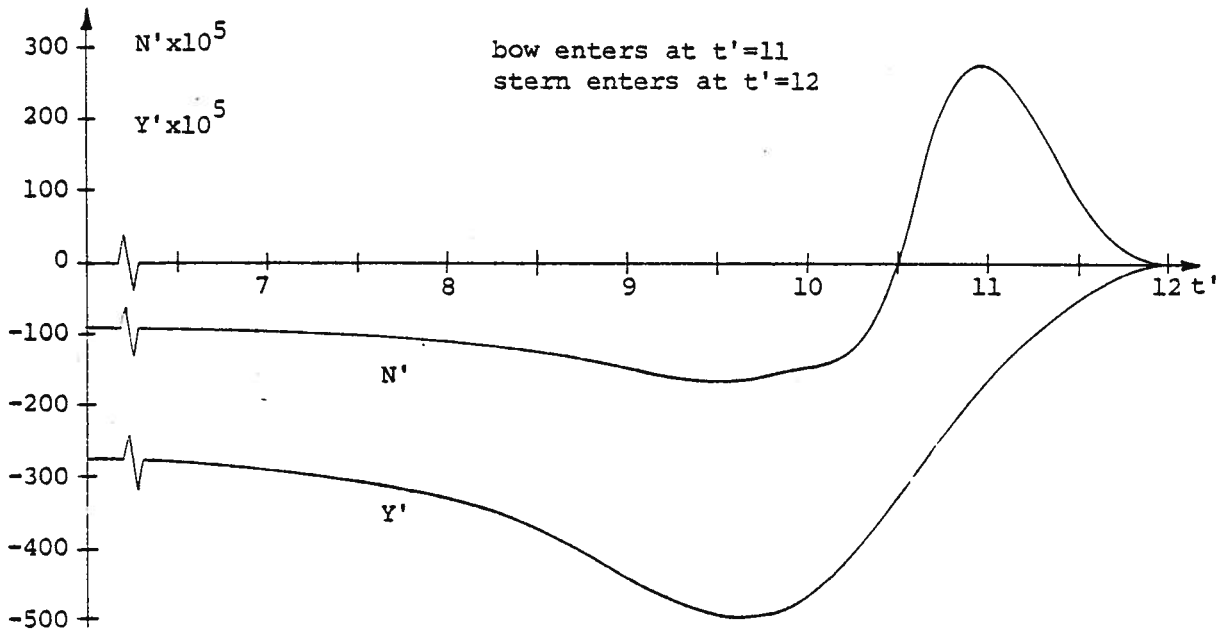


Figure 5. Lateral Current Disturbance at ABC Harbor Entrance

### 3. Control Loop Design

In this section, we discuss the design of the inner or control loop in Fig. 1. This naturally includes the methods used for the calculation of controller gains  $C$  and the Kalman filter gains  $K$  performed in the outer or gain update loop. This section involves an extension of our earlier work<sup>1</sup> and some of the introductory discussion included there and elsewhere<sup>29,30,41</sup> will not be repeated here. We begin with a discussion of the optimal, steady-state controller design and then proceed with development of the Kalman filter which generates the state estimate used by the controller. The section closes with a look at the need and requirements for an adaptive feature in a path controller used in restricted waters.

#### 3.1 Optimal, Steady-State Controller Design.

The control problem is to keep the ship along the desired track using acceptable levels of rudder in the presence of disturbances while using noisy measurements. The ship model is given by eq. (12) where in this subsection we will assume the disturbance vector  $\underline{w}$  consists of a Gaussian white noise lateral force and yawing moment. Equation (12) describes a Gauss-Markov process in which the state of the ship is completely described by its mean value state vector  $\bar{\underline{x}}$  which follows eq. (12) with  $\underline{w}=0$  and by its covariance matrix  $X$  where,

$$\bar{\underline{x}}(t) = E[\underline{x}(t)] \quad , \quad (26)$$

$$X(t) = E[(\underline{x}(t) - \bar{\underline{x}}(t))(\underline{x}(t) - \bar{\underline{x}}(t))^T] \quad , \quad (27)$$

and  $E[\dots]$  is the expected value or ensemble average over the many possible observations at time  $t$ . We will assume that the white noise disturbance has zero mean and covariance given by,

$$E[\underline{w}(t)\underline{w}(\tau)^T] = Q(t)\delta(t-\tau) \quad , \quad (28)$$

where  $Q$  is the power spectral density matrix and  $\delta(t-\tau)$  is the Dirac delta function. We also assume there is no correlation between the initial condition of the system  $\underline{x}(t_0)$  and the disturbances  $\underline{w}$ .

An optimal control design problem can be stated as establishing the linear state feedback control law,

$$\underline{u} = C\underline{x} \quad , \quad (29)$$

which minimizes the linear quadratic cost function,

$$J = \frac{1}{2} \int_{t_0}^{t_f} (\underline{x}^T \underline{A} \underline{x} + \underline{u}^T \underline{B} \underline{u}) dt \quad , \quad (30)$$

where A and B are weighting matrices at the designer's disposal. In this problem, we wish to minimize  $\eta'$  while using acceptable levels of rudder  $\delta'$  and  $\delta_c'$ . We can therefore assume all terms in the A matrix to be zero except the  $a_{44}$  weighting on  $\eta'^2$  and the  $a_{55}$  weighting on  $\delta'^2$  and assume a nonzero  $B=b_{11}$  weighting of  $\delta_c'^2$ . To yield a reasonable weighting among these terms and to accomplish the needed scaling of terms in eq. (30) we assume,

$$a_{44} = (\eta'_0)^{-2} = 772.463 \quad , \quad (31)$$

$$a_{55} = (\delta'_0)^{-2} = 131.332 \quad , \quad (32)$$

$$b_{11} = (\delta_{c0}')^{-2} = 131.332 \quad , \quad (33)$$

based on a dimensional  $\eta_0 = 10.43$  m. (slightly less than one-quarter beam) and a dimensional  $\delta_0 = \delta_{c0} = 5^\circ$ . This indicates that we are willing to commit approximately  $5^\circ$  rudder to path control when the ship deviates  $\eta_0$  from the desired path.

The Separation Theorem<sup>29</sup> states that the optimal control desired here is obtained by assuming exact knowledge of the state for use in eq. (29) and by neglecting the disturbance  $\underline{w}$  in eq. (12). When the matrices  $F_S$ ,  $G_S$ , A, and B are constant, the control which minimizes eq. (30) is given by,

$$\underline{C} = -B^{-1} G_S^T S_\infty \quad , \quad (34)$$

where  $S_\infty$  is the steady-state ( $\dot{S}=0$ ) solution of the matrix Riccati equation,

$$\dot{S} = -SF_S - F_S^T S + S G_S B^{-1} G_S^T S - A \quad . \quad (35)$$

An efficient way to obtain  $S_\infty$  is by Potter's algorithm which utilizes the technique of eigenvector decomposition to obtain a closed-form solution for  $S_\infty$ . MacFarlane<sup>42</sup> and Potter<sup>43</sup> first proposed this solution technique. It was developed into a practical design tool by Bryson and Hall<sup>44</sup> who utilized the QR algorithm to obtain the eigensystem in their OPTSYS computer program. Potter<sup>43</sup> proved that  $S_\infty$  can be expressed in terms of the eigenvectors of the  $2n \times 2n$  partitioned matrix,

$$M = \left[ \begin{array}{c|c} F_S & -G_S B^{-1} G_S^T \\ \hline -A & -F_S \end{array} \right], \quad (36)$$

which can be shown to be the coefficient matrix of the  $2n$  Euler-Lagrange equations for minimizing eq. (30) subject to eq. (12). The eigenvalues of  $M$  are in pairs which are symmetric about the imaginary axis in the complex plane. If the eigenvectors associated with the eigenvalues with positive real parts are designated with the subscript  $+$  and those associated with the eigenvalues with negative real parts are designated with the subscript  $-$ , the eigenvectors can be arranged as follows:

$$X = \left[ \begin{array}{c|c} X_+ & X_- \\ \hline \Lambda_+ & \Lambda_- \end{array} \right]. \quad (37)$$

The steady-state solution of eq. (35) is then given by,

$$S_\infty = \Lambda_- (X_-)^{-1}. \quad (38)$$

Equations (34) and (38) are used to calculate the controller gain matrices in this work. The QR algorithm is used to obtain the eigensystem of  $M$  as defined by eq. (36).

### 3.2 First-Order Shaping Filter Approach.

In Section 3.1, we assumed that the disturbance vector  $w$  in eq. (12) was composed of Gaussian white noise. In our earlier work<sup>1</sup>, we developed path controllers capable of handling short-term, essentially zero-mean disturbances such as the passing ship disturbance shown in Fig. 3. This disturbance acts in a correlated manner over about three ship lengths so the assumption of Gaussian white noise disturbances is poor for this problem. The usual approach when a disturbance is correlated with characteristic times comparable to those of the system under consideration is to model the disturbance as the output of a shaping filter which is driven by Gaussian white noise. The passing ship disturbance in Fig. 3 can be reasonably modeled as exponentially correlated processes with zero means. These can be produced by first-order shaping filters. We therefore introduced the external yawing moment  $N'$  and the external lateral force  $Y'$  as additional states defined by:

$$T_N \frac{dN'}{dt'} = -N' + w_1, \quad (39)$$

and,

$$T_Y \frac{dY'}{dt'} = -Y' + w_2 \quad , \quad (40)$$

where correlation times  $T_N = T_Y = 1$  ship length are reasonable assumptions based on Fig. 3. These shaping filter equations are driven by Gaussian white noise  $\underline{w} = (w_1, w_2)^T$  which has power spectral density  $Q$ . This model is equally valid for the disturbance produced as the ship passes localized fixed objects and other short-term disturbances.

To incorporate the disturbance model eq. (39) and (40) into the controller design, the state vector  $\underline{x}$  is augmented by the addition of states  $N'$  and  $Y'$  to yield an augmented state vector  $\underline{x}'$ . Equation (11) then becomes,

$$\frac{d}{dt'} \begin{bmatrix} \psi' \\ r' \\ \beta' \\ \eta' \\ \delta' \\ N' \\ Y' \end{bmatrix} = \begin{bmatrix} 0 & 1 & 0 & 0 & 0 & 0 & 0 \\ 0 & f_{22} & f_{23} & 0 & f_{25} & f_{26} & f_{27} \\ 0 & f_{32} & f_{33} & 0 & f_{35} & f_{36} & f_{37} \\ 1 & 0 & -1 & 0 & 0 & 0 & 0 \\ 0 & 0 & 0 & 0 & -1/T_r & 0 & 0 \\ 0 & 0 & 0 & 0 & 0 & -1/T_N & 0 \\ 0 & 0 & 0 & 0 & 0 & 0 & -1/T_Y \end{bmatrix} \begin{bmatrix} \psi' \\ r' \\ \beta' \\ \eta' \\ \delta' \\ N' \\ Y' \end{bmatrix} + \begin{bmatrix} 0 \\ 0 \\ 0 \\ 0 \\ 1/T_r \\ 0 \\ 0 \end{bmatrix} \delta_c' + \begin{bmatrix} 0 & 0 \\ 0 & 0 \\ 0 & 0 \\ 0 & 0 \\ 0 & 0 \\ 1/T_N & 0 \\ 0 & 1/T_Y \end{bmatrix} \begin{bmatrix} w_1 \\ w_2 \end{bmatrix} \quad , \quad (41)$$

or,

$$\dot{\underline{x}}' = F_e \underline{x}' + G_e \underline{u} + \Gamma_e \underline{w} \quad . \quad (42)$$

The upper right (5x2) partition of  $F_e$  in eq. (41) is  $\Gamma_s$  in eq. (11); i.e.,  $f_{26} = \gamma_{21}$ , etc. The measurement eq. (13) now becomes,

$$\underline{z} = H_e \underline{x}' + \underline{v} \quad , \quad (43)$$

where  $H_e$  is just  $H_s$  in eq. (13) with a (3x2) block of zeros added at the right. The optimal control law is now given by,

$$\underline{u} = C \underline{x}' \quad , \quad (44)$$

where the control gain matrix is obtained as described above except the  $A$  matrix must be extended to (7x7) with additional rows and columns of zeros for use with  $\underline{x}'$  in lieu of  $\underline{x}$  in eq. 30 and  $F_e$  and  $G_e$  must be used in eq. (34), (35), and (36) in lieu of  $F_s$  and  $G_s$ . The optimal control gains are then given by,



$$C = -B^{-1}G_e^T S_\infty \quad . \quad (45)$$

Having only the noisy measurements of three states included in  $\underline{z}$ , the state vector  $\underline{x}'$  needed in eq. (44) is not directly available. The Separation Theorem states that it is optimal to use the control gains produced by eq. (45) with a maximum likelihood estimate of the augmented state vector  $\hat{\underline{x}}'$  produced by an optimal stochastic state estimator or Kalman-Bucy filter. The control law then becomes,

$$\underline{u} = C\hat{\underline{x}}' \quad , \quad (46)$$

where the state estimate is produced by the Kalman-Bucy filter given by,

$$\dot{\hat{\underline{x}}}' = F_e \hat{\underline{x}}' + G_e \underline{u} + K(\underline{z} - H_e \hat{\underline{x}}') \quad . \quad (47)$$

When the system is stationary; i.e., a statistical steady-state with  $F_e$ ,  $G_e$ ,  $\Gamma_e$ ,  $Q$ , and  $R$  constant, the steady-state filter gain matrix  $K$  is given by,

$$K = P_\infty H_e^T R^{-1} \quad , \quad (48)$$

where  $P_\infty$  is the steady-state ( $\dot{P}=0$ ) solution of the matrix Riccati equation,

$$\dot{P} = F_e P + P F_e^T + \Gamma_e Q \Gamma_e^T - P H_e^T R^{-1} H_e P \quad , \quad (49)$$

and  $Q$  is the power spectral density of the white noise process disturbance  $\underline{w}$  in eq. (42) and  $R$  is the power spectral density of the white measurement noise  $\underline{v}$  in eq. (43).

An efficient way to obtain  $P_\infty$  is again by Potter's algorithm which utilizes eigenvector decomposition. In this case,  $P_\infty$  can be expressed in terms of the eigenvectors of the  $2n' \times 2n'$  partitioned matrix,

$$M' = \left[ \begin{array}{c|c} F_e & -\Gamma_e Q \Gamma_e^T \\ \hline -H_e^T R^{-1} H_e & -F_e^T \end{array} \right] \quad . \quad (50)$$

If the eigenvectors associated with the eigenvalues of  $M'$  with positive real parts are designated with the subscript  $+$  and those associated with the eigenvalues with negative real parts are designated with the subscript  $-$ , the eigenvectors can be arranged as follows:

$$\chi' = \left[ \begin{array}{c|c} \underline{x}'_+ & \underline{x}'_- \\ \hline \underline{\Lambda}'_+ & \underline{\Lambda}'_- \end{array} \right] \quad . \quad (51)$$

The steady-state solution of eq. (49) is then given by,

$$P_{\infty} = -X_{+}' (\Lambda_{+}')^{-1} . \quad (52)$$

Equations (48) and (52) are used to calculate the Kalman filter gain matrices in this work. The QR algorithm is used to obtain the eigensystem of  $M'$  as defined by eq. (50).

At this point, we will present typical results for a path controller designed using the first-order shaping filter disturbance models eq. (39) and (40). These results illustrate the effectiveness and the limitations of this type of design. The authors have previously shown<sup>1</sup> that if a non-adaptive path controller is designed assuming constant ship characteristics, the best overall performance is achieved with a controller designed for the least course stable ship characteristics. For the *Tokyo Maru* this condition is at about  $H/T=1.89$  so the characteristics for this depth-to-draft ratio in Table 2 are used in this example. The measurement noise power spectral density  $R$  is taken from Table 3 assuming measurements of  $\psi'$ ,  $r'$ , and  $\eta'$  in eq. (43). The nonzero terms in the controller cost function weighting matrices are defined by eq. (31), (32), and (33). The remaining definition needed is the process disturbance power spectral density  $Q$ . Using the passing ship disturbance in Fig. 3 as the design disturbance, the RMS values of  $N'$  and  $Y'$  between  $t'=-2$  and  $t'=1.4$  are  $\sigma_N=8.798 \times 10^{-5}$  and  $\sigma_Y=21.178 \times 10^{-5}$ , respectively. Assuming correlation times  $T_N=T_Y=1$  as noted above, the nonzero terms in the power spectral density matrix can be taken as,

$$q_{11} = 2T_N \sigma_N^2 = 1.548 \times 10^{-8} \quad , \quad (53)$$

and,

$$q_{22} = 2T_Y \sigma_Y^2 = 8.970 \times 10^{-8} \quad . \quad (54)$$

The control loop was designed for the *Tokyo Maru* with the above assumptions using the Michigan Terminal System (MTS) version of Bryson and Hall's OPTSYS program.<sup>31,44</sup> The resulting controller gains and Kalman-Bucy filter gains are shown in Table 4. These results are different from those reported earlier by the authors<sup>1</sup> due to the use of a corrected Froude number of 0.116, the use of a zero weighting  $a_{11}$  on  $\psi'^2$  in eq. (30), and

the use of lower assumed measurement noise levels. The zero row in the K matrix results because with our steering gear model the control history produces exact knowledge of the rudder angle. Therefore, the measurements provide no additional information. All the nonzero gains in Table 4 must vary with water depth if they are to remain optimal except  $c_{14}=2.4252$  which the authors have shown to be vessel, speed, and water depth independent.

controller gains $C^T$	Kalman-Bucy filter gains K		
5.5421	4.6335	0.8400	-0.0021
2.6601	18.5075	12.2263	-0.3278
6.3895	3.3586	2.6208	-4.2929
2.4252	-0.0753	-0.5225	2.9000
-0.8499	0.0000	0.0000	0.0000
679.68	0.1164	0.1850	0.0440
-52.776	-0.0982	-0.1604	0.1654

Table 4. Optimal Gains for *Tokyo Maru* at  $H/T=1.89$  and  $F_n=0.116$ -  
First-Order Shaping Filter Disturbance Model

To illustrate the effectiveness of the design given in Table 4, we simulated the *Tokyo Maru* under the control of this controller using the SHIPSIM/OPTSIM computer program.<sup>31</sup> Figures 6 and 7 show the results of a simulation which begins with the ship one half beam ( $B/2=23.75$  m.) off the desired track with all other states zero. The filter is assumed to have been operating for some time and is given exact knowledge of the state  $\hat{x}=x$  at  $t'=0$ . In this simulation, the ship also passes another ship beam-to-beam at  $t'=20$ . The magnitude of this passing ship disturbance is arbitrarily taken as four times that shown in Fig. 3. Figure 6 shows the resulting lateral offset response. The maximum overshoot at  $t'=5.3$  is 1.6 m.; the maximum deviation due to the passing ship is 6.2 m. Figure 7 shows the corresponding rudder angle response. The controller provides effective control under these conditions. It provides effective control when the ship is subjected to the short-term, essentially zero mean disturbances for which the controller was designed.

The weakness of the ship path controller designed using first-order shaping filters, as defined above, to model the process disturbances is that the controller cannot accommodate more long-term disturbances without a non-zero offset from the desired path. Normal state-variable feedback controllers,

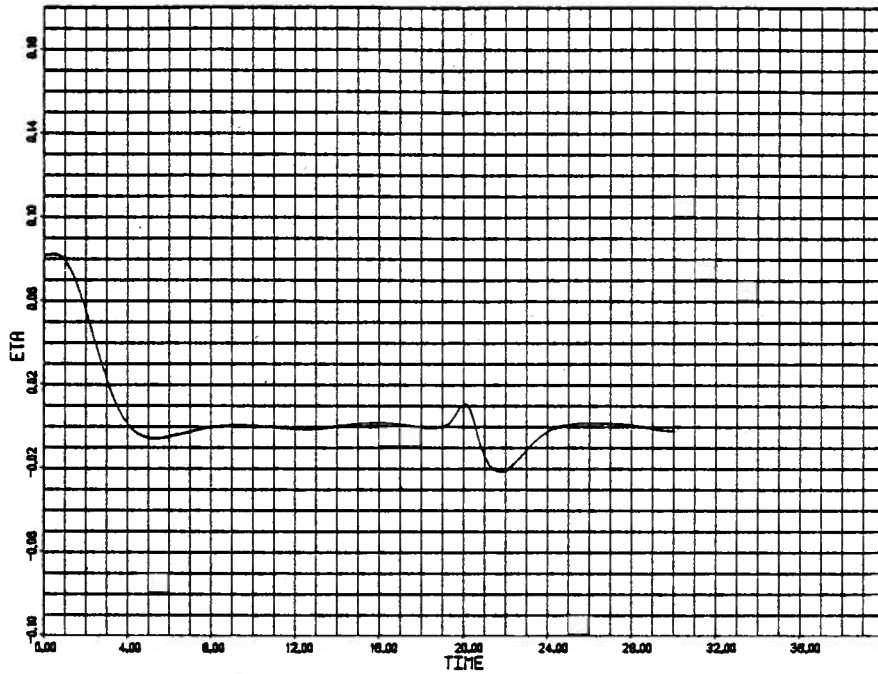


Figure 6. Lateral Offset Response to B/2 Initial Offset and Passing Ship - First-Order Shaping Filter Disturbance Model Design

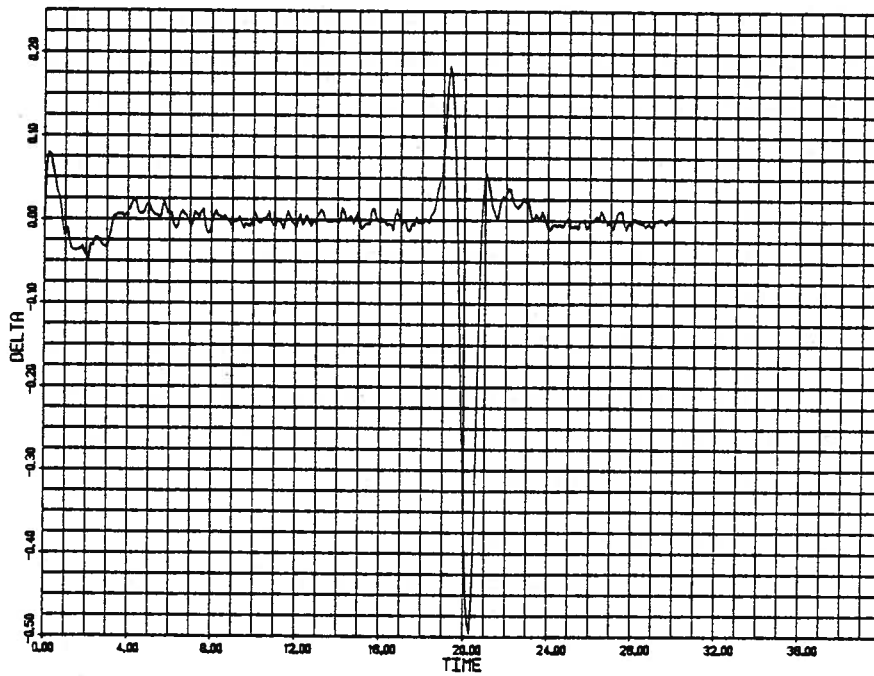


Figure 7. Rudder Angle Response to B/2 Initial Offset and Passing Ship - First-Order Shaping Filter Disturbance Model Design

as this approach produces, yield a proportional plus derivative (P-D) type control law. To produce zero steady-state errors with a constant disturbance some type of integral action is needed; i.e. a (P-I-D) type control law is needed. To show the performance of the controller given in Table 4 with constant disturbances, the *Tokyo Maru* was simulated under control of this controller while being subjected to the design lateral current disturbance shown in Fig. 4. The initial condition is  $\underline{x}=\hat{x}=0$  in this simulation. The lateral offset response is shown in Fig. 8. Steady offsets of about 54 m. and 27 m. occur during the two periods of constant disturbance. A 1 knot lateral current produces a steady offset of over one ship beam. The corresponding rudder angle response is shown in Fig. 9. The yawing moment estimate  $\hat{N}'$  produced by the Kalman-Bucy filter is shown in Fig. 10. The filter produces approximately constant but biased estimates of  $N'$  and  $Y'$  during the periods of constant disturbance. The state estimates have much smaller or no apparent bias errors. Comparing Fig. 10 with Fig. 4, the filter estimates the 0.00103 yawing moment during the first 15 ship lengths to be about 0.00072. The equilibrium rudder angles in Fig. 9 are zero and the equilibrium heading and drift angles are equal. Thus, from eq. (46) it can be seen that a steady offset  $\eta'$  develops to "counteract" the steady errors in the disturbance estimates  $\hat{N}'$  and  $\hat{Y}'$ .

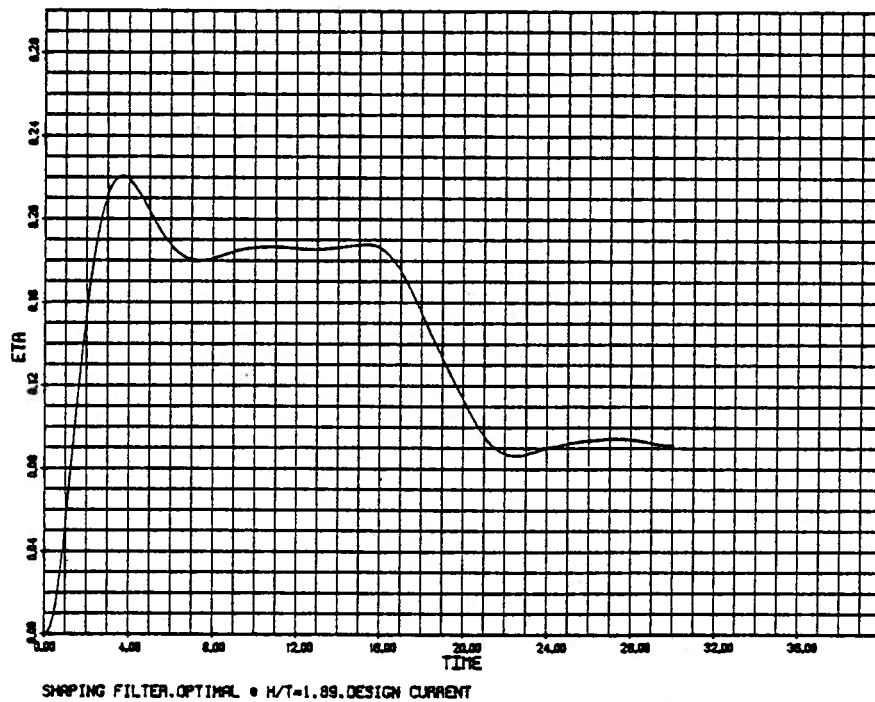


Figure 8. Lateral Offset Response to Design Lateral Current - First-Order Shaping Filter Disturbance Model Design

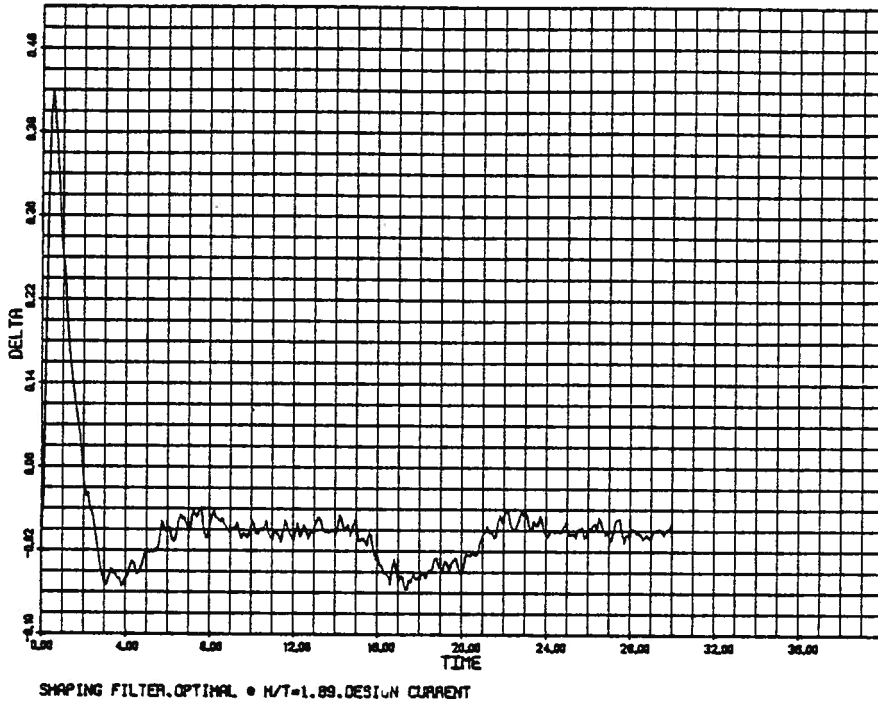


Figure 9. Rudder Angle Response to Design Lateral Current - First-Order Shaping Filter Disturbance Model Design

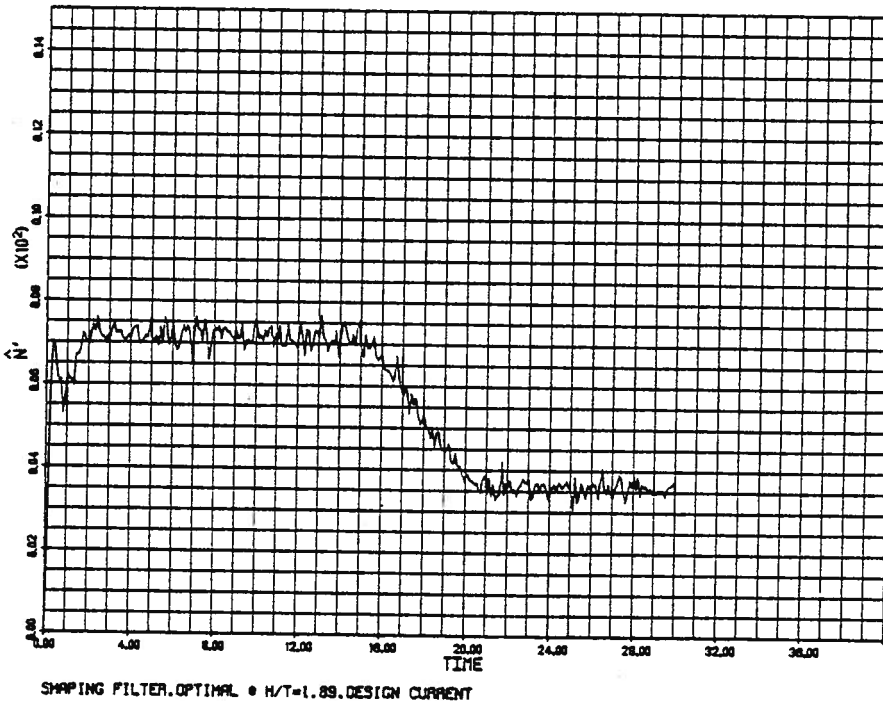


Figure 10. Yawing Moment Estimate with Design Lateral Current - First-Order Shaping Filter Disturbance Model Design

### 3.3 Random Walk Approach.

As noted in the previous section, some type of integral control action is needed to produce a zero offset of the ship from the desired path with a constant disturbance. Attention has been directed recently toward the development of stochastic state variable controllers with integral control properties when using only incomplete, noisy state measurements. Among this work is that of Holley and Bryson<sup>45</sup> in which they applied a number of approaches to the control of an aircraft landing in a crosswind. Alternative approaches which are similar to that which we present here have been presented by Kwatny<sup>46</sup> and by Balchen, et al.<sup>47</sup>

A reasonable first attempt at the treatment of a constant disturbance might be to model the disturbance as a random bias; i.e.,

$$\frac{dN'}{dt'} = 0 \quad , \quad N'(0) = N_0' \quad , \quad (55)$$

where  $N_0'$  is an unknown, random quantity. In this problem, models of this type could be assumed for  $N'$  and  $Y'$  and the state vector could be augmented to become  $\underline{x}' = [\underline{x}^T, N', Y']^T$  as done above with the first-order shaping filters. Holley and Bryson<sup>45</sup> have shown, however, that the steady-state Kalman filter, as used here, does not exist for this problem. This results because a time-varying Kalman filter would yield statistically exact estimates of the random biases so that in the steady-state the measurements will contain no additional information on these disturbances.

A number of successful approaches do, however, exist for this control problem. First, it is feasible to model the disturbances as first-order shaping filters as in the previous section but with the assumption that the correlation times are very long compared with the dynamics of the ship. Disturbance models eq. (39) and (40) would be used with the assumption that  $T_N$  and  $T_Y$  are perhaps 100 ship lengths. It would be necessary to assume RMS values of the disturbances  $\sigma_N$  and  $\sigma_Y$  for use in eq. (53) and (54) and the design could then proceed as in the previous section. This approach would continue to produce biased estimates of constant disturbances but these estimates approach the correct values as the correlation times are increased.<sup>45</sup> Note that in this approach it is necessary to make assumptions of both the correlation times and the RMS disturbance values.

A second approach was presented recently by Holley and Bryson.<sup>45</sup> They develop a state variable generalization of integral control in which a Kalman filter is used to estimate the state vector  $\underline{x}$  ignoring the disturbances and then an integral of the output deviations is added separately to the control law. They note that this approach produces a degraded transient response compared with the use of first-order shaping filters with long correlation times but that the controller is less sensitive to modeling errors. The authors will be undertaking an investigation of this type of controller for ship path control during the coming year and these results will be reported separately later.

A third approach to the development of a state variable controller with integral control properties is to model the constant or nearly constant disturbances as a random walk. More precisely this model is an independent-increment, continuous process and should therefore be called a Wiener-Lévy process or Brownian motion. In this approach the disturbances are assumed to be the integral of white noise; i.e., for this problem,

$$\frac{dN'}{dt'} = w_N \quad , \quad (56)$$

and

$$\frac{dY'}{dt'} = w_Y \quad . \quad (57)$$

Note that now it is only necessary to estimate the power spectral density  $Q$  of the disturbance white noise  $\underline{w} = [w_N, w_Y]^T$ . Kwatny<sup>46</sup> has used this modeling approach to develop state variable controllers with integral control properties. Balchen, et al<sup>47</sup> have used a more general "environment" disturbance model,

$$\dot{\underline{w}} = E\underline{w} + \underline{n} \quad , \quad (58)$$

where  $\underline{n}$  is white noise. They then consider the random walk model as a special case of this approach; i.e.  $E=0$ . We have chosen to investigate the effectiveness of this disturbance modeling approach in this work.

Using eq. (56) and (57), the state vector  $\underline{x}$  can be augmented with  $N'$  and  $Y'$  so that eq. (11) now becomes,



$$\frac{d}{dt'} \begin{bmatrix} \psi' \\ r' \\ \beta' \\ \eta' \\ \delta' \\ N' \\ Y' \end{bmatrix} = \begin{bmatrix} 0 & 1 & 0 & 0 & 0 & 0 & 0 \\ 0 & f_{22} & f_{23} & 0 & f_{25} & f_{26} & f_{27} \\ 0 & f_{23} & f_{33} & 0 & f_{35} & f_{36} & f_{37} \\ 1 & 0 & -1 & 0 & 0 & 0 & 0 \\ 0 & 0 & 0 & 0 & -1/T_R & 0 & 0 \\ 0 & 0 & 0 & 0 & 0 & -\epsilon & 0 \\ 0 & 0 & 0 & 0 & 0 & 0 & -\epsilon \end{bmatrix} \begin{bmatrix} \psi' \\ r' \\ \beta' \\ \eta' \\ \delta' \\ N' \\ Y' \end{bmatrix} + \begin{bmatrix} 0 \\ 0 \\ 0 \\ 0 \\ 1/T_R \\ 0 \\ 0 \end{bmatrix} \delta_c' + \begin{bmatrix} 0 & 0 \\ 0 & 0 \\ 0 & 0 \\ 0 & 0 \\ 0 & 0 \\ 1 & 0 \\ 0 & 1 \end{bmatrix} \begin{bmatrix} w_N \\ w_Y \end{bmatrix}, \quad (59)$$

or,

$$\dot{\underline{x}}' = F_e \underline{x}' + G_e \underline{u} + \Gamma_e \underline{w}. \quad (60)$$

In this formulation,  $\epsilon$  is a small quantity introduced so that Potter's algorithm can be used to design the steady-state controller and the steady-state filter which estimates  $\underline{x}'$ . With  $\epsilon=0$ , matrix  $M$  defined by eq. (36) with  $F_e$  and  $G_e$  used in lieu of  $F_S$  and  $G_S$ , respectively, has four zero eigenvalues; matrix  $M'$  defined by eq. (50) has two zero eigenvalues. MacFarlane<sup>42</sup> has shown that under these conditions general solutions for  $S_\infty$  and  $P_\infty$  in terms of the eigenvectors of  $M$  and  $M'$ , respectively, do not exist. As  $\epsilon \rightarrow 0$ , however, the steady-state controller gain matrix  $C$  and the steady-state filter gain matrix  $K$  approach limits. As an example, in the design presented in detail below the gain  $C_{16}=995.32$  when  $\epsilon=10^{-2}$ , 998.50 when  $\epsilon=10^{-4}$ , and 998.54 when  $\epsilon=10^{-6}$ . We have, therefore, used  $\epsilon=10^{-4}$  here. It is not necessary to include  $\epsilon \neq 0$  in the implementation of the filter once the gains have been obtained.

The remaining definition needed to specify the control loop design is the white noise  $\underline{w}$  power spectral density matrix  $Q$ . General results for Brownian motion can be used to obtain a direct, physical way to establish  $Q$ . If we have a continuous, Brownian motion process  $y(t)$ , it has a zero mean and the following properties,<sup>48</sup>

$$E[y(t)^2] = \sigma^2 t, \quad (61)$$

where  $\sigma^2$  is the diffusion coefficient or variance parameter and,

$$E[(y(t_2)-y(t_1))^2] = \sigma^2(t_2-t_1), \quad (62)$$

provided  $t_2 > t_1$ . The formal derivative of the Brownian motion is white noise where the noise spectral density is given by,

$$q = \sigma^2. \quad (63)$$

Now if a white noise process is approximated by an equivalent white noise sequence with time step  $\Delta t$ , Jazwinski<sup>48</sup> shows that it must have a covariance  $\bar{q}$  which is related to the process spectral density  $q$  by,

$$\bar{q} = \frac{q}{\Delta t} , \quad (64)$$

in order to provide a constant noise "power" level; i.e., constant area under the autocorrelation curve. If  $\Delta t$  is taken as  $t_2 - t_1$ , eqs(62), (63), and (64) yield,

$$\bar{q} = E \left[ \left[ \frac{y(t_2) - y(t_1)}{t_2 - t_1} \right]^2 \right] , \quad (65)$$

Further, if  $\Delta t$  is viewed as the integration stepsize used in the Euler integration discretization of the continuous process we can use eq. (64) and (65) to approximate the white noise power spectral density as,

$$q = \Delta t S^2 , \quad (66)$$

where  $S$  is the maximum expected rate of change or slope of the continuous process being modeled by the Brownian motion.

For the design presented here, eq. (66) was used to establish the disturbance model power spectral densities. Assuming that the yawing moment and lateral force disturbances could change by approximately twice the values produced by a steady one knot lateral current in one ship length we have  $S_N = 0.002$  and  $S_Y = 0.005$ . With our  $\Delta t = 0.005$ , eq. (66) then yields,

$$q_{11} = \Delta t S_N^2 = 2.000 \times 10^{-8} , \quad (67)$$

and,

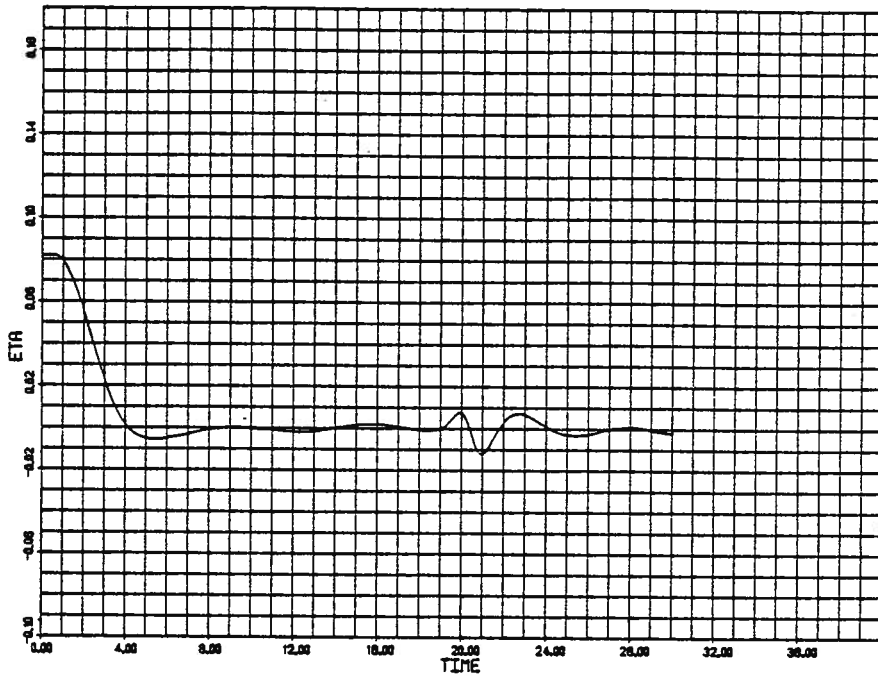
$$q_{22} = \Delta t S_Y^2 = 1.250 \times 10^{-7} . \quad (68)$$

The measurement noise power spectral density and remaining assumptions are the same as in the previous section. With these assumptions, the control loop was designed for the *Tokyo Maru* using the OPTSYS program. The resulting controller gains and Kalman-Bucy filter gains are shown in Table 5. These results can be compared with those shown in Table 4 for the design using the first-order shaping filter disturbance models. The state feedback gains  $C_{11}$  through  $C_{15}$  are the same in both approaches.

controller gains $C^T$	Kalman-Bucy filter gains K		
5.5421	4.6600	0.8798	-0.0019
2.6601	19.3843	14.1945	-0.3561
6.3895	3.7193	3.4862	-8.1031
2.4252	-0.0651	-0.5677	4.0000
-0.8499	0.0000	0.0000	0.0000
998.50	0.1358	0.2366	0.0907
-12.571	-0.1551	-0.2844	0.4719

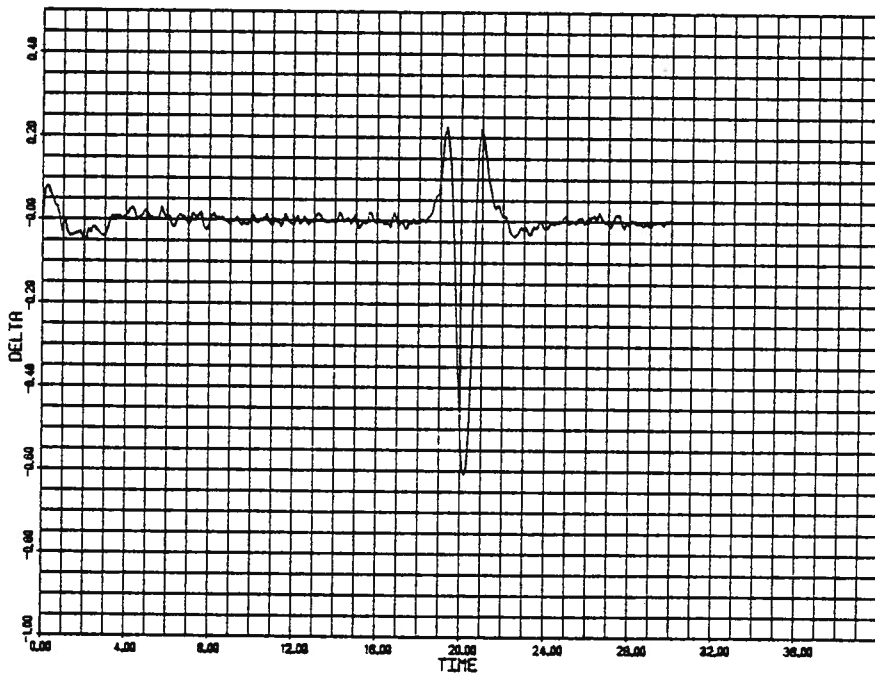
Table 5. Optimal Gains for *Tokyo Maru* at  $H/T=1.89$  and  $F_n=0.116$  - Random Walk Disturbance Model

To illustrate the effectiveness of the design given in Table 5, we simulated the *Tokyo Maru* under the control of this controller using a one-half beam initial offset with all other states zero and  $\hat{x}(0)=x(0)$ . This simulation also includes a ship passing at  $t'=20$  producing a disturbance four times that shown in Fig. 3. Figure 11 shows the resulting lateral offset response and is directly comparable with Fig. 6. The overshoot at  $t'=5.6$  is 1.7 m.; the maximum deviation due to the passing ship is 3.5 m. Figure 12 shows the corresponding rudder angle response and is directly comparable with Fig. 7. The controller provides control comparable to that provided by the first-order shaping filter design shown in Fig. 6 and 7. The maximum rudder angle in Fig. 12 of  $35^\circ$  shows that the assumed disturbance of four times the values shown in Fig. 3 actually violates the validity of the linear model. To illustrate the integral control properties of this design, we simulated the *Tokyo Maru* under the control of this controller while being subjected to the design lateral current disturbance shown in Fig. 4. The initial condition is  $\underline{x}=\hat{x}=0$  in this simulation. The lateral offset response is shown in Fig. 13 which is directly comparable with Fig. 8. The maximum lateral offset during the startup of the system is 34.5 m.; the controller then returns the ship to the desired track in the presence of the constant one knot lateral current. The maximum offset during the ramp current change is about 9 m. The corresponding rudder angle response is shown in Fig. 14; the Kalman filter estimate of the yawing moment disturbance  $\hat{N}'$  is shown in Fig. 15. Comparing Fig. 10 with Fig. 4, the filter produces essentially exact estimates of the constant disturbance levels of 0.00103 and 0.000515. As desired, this design provides effective control in the presence of constant external disturbances without a steady offset from the desired path.



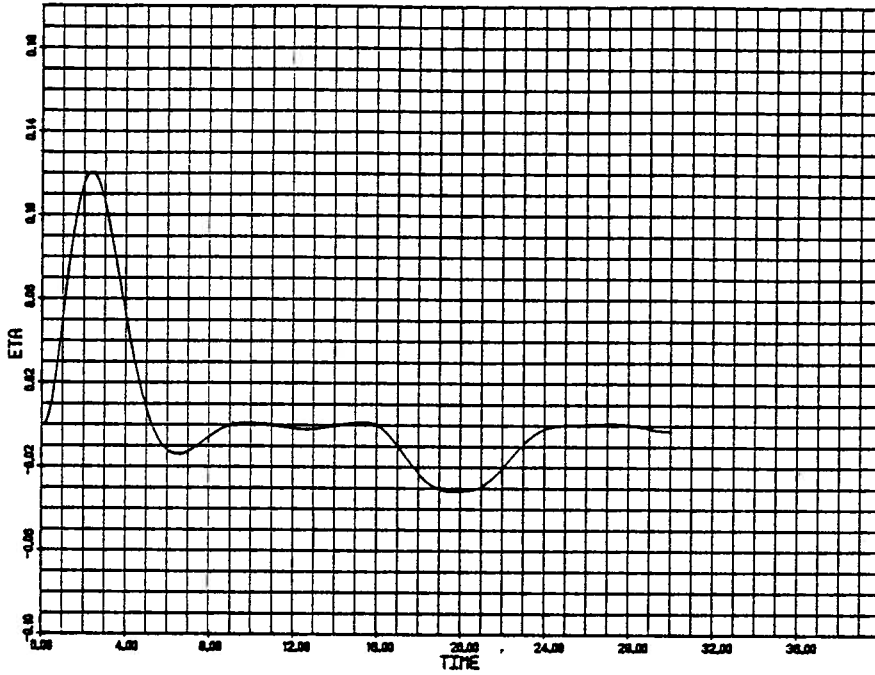
RANDOM WALK MODEL. OPTIMAL AT H/T=1.89. LARGE PASSING SHIP DISTAB

Figure 11. Lateral Offset Response to B/2 Initial Offset and Passing Ship - Random Walk Disturbance Model Design



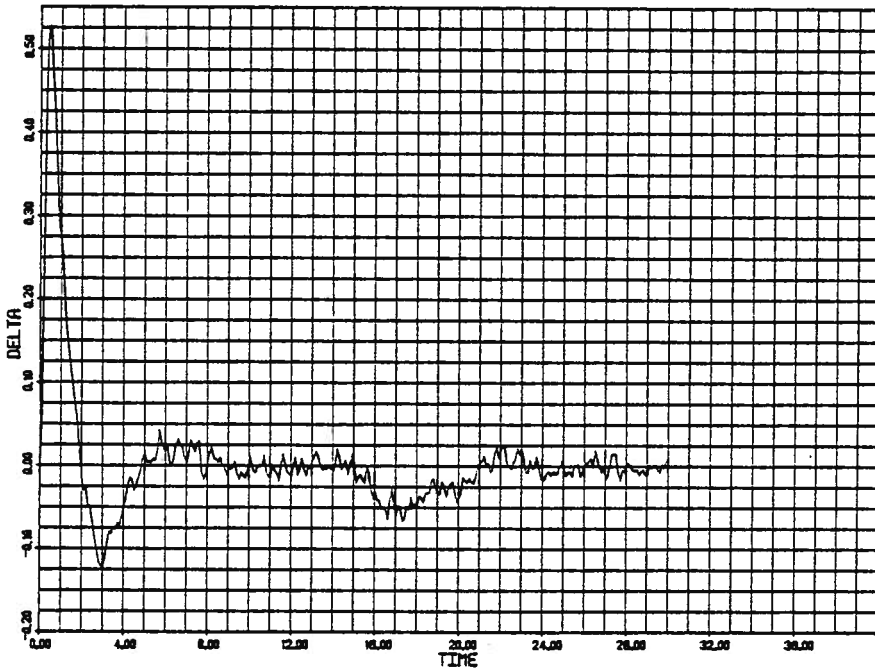
RANDOM WALK MODEL. OPTIMAL AT H/T=1.89. LARGE PASSING SHIP DISTAB

Figure 12. Rudder Angle Response to B/2 Initial Offset and Passing Ship - Random Walk Disturbance Model Design



RANDOM WALK MODEL.OPTIMAL AT H/T=1.89.DESIGN CURRENT .

Figure 13. Lateral Offset Response to Design Lateral Current - Random Walk Disturbance Model Design



RANDOM WALK MODEL.OPTIMAL AT H/T=1.89.DESIGN CURRENT .

Figure 14. Rudder Angle Response to Design Lateral Current - Random Walk Disturbance Model Design

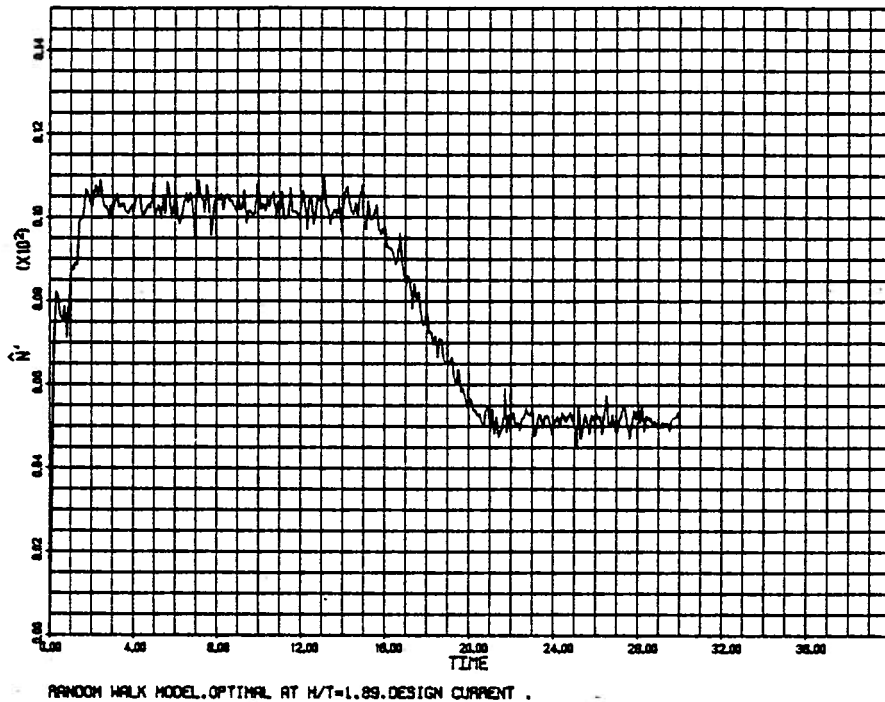


Figure 15. Yawing Moment Estimate with Design Lateral Current -  
Random Walk Disturbance Model Design

As a final illustration of the effectiveness and limitations of the controller given in Table 5, we simulated the *Tokyo Maru* entering the ABC harbor defined in Fig. 5 while under control of this controller. The resulting lateral offset response is shown in Fig. 16. The maximum deviation of 72.5 m. is not excessive but the corresponding rudder angle response shown in Fig. 17 is physically impossible. The controllers developed here just cannot accommodate this extreme a disturbance. With the lateral current decreasing from 2 knots to zero in just over one ship length an extremely large yawing moment is placed on the ship. This is very difficult for a nonanticipatory (causal) control system, as used here, to handle. A pilot would most likely create a yawing rate just prior to the harbor entrance in anticipation of the large yawing moment which he knows will be experienced at the channel mouth. A control system could be created in a similar manner using a preprogrammed rudder control based on time-to-go to the channel mouth. This "local" control feature could be superposed upon a general control law of the type studied here.

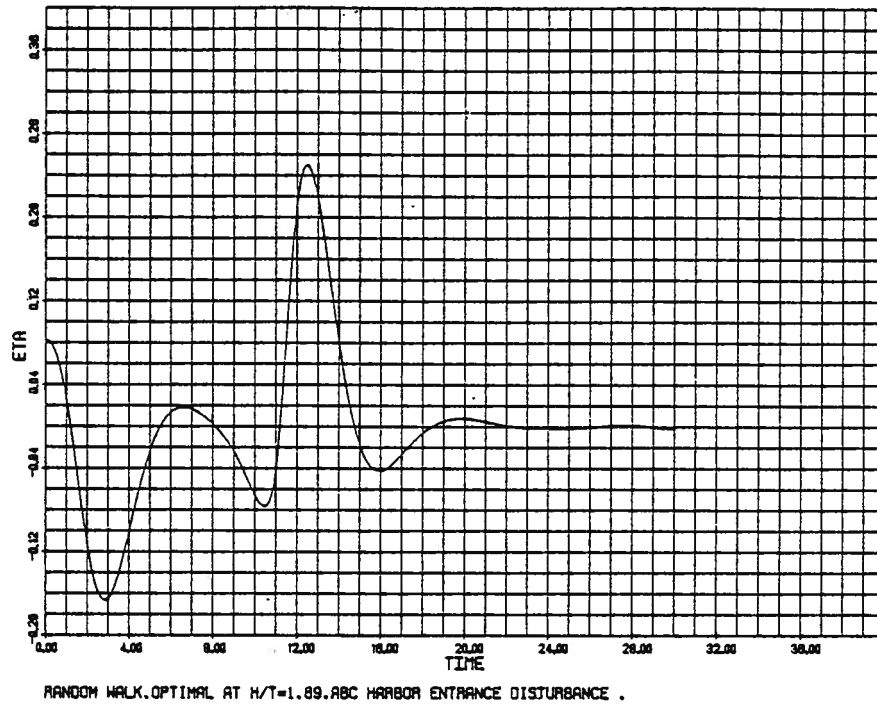


Figure 16. Lateral Offset Response at ABC Harbor Entrance - Random Walk Disturbance Model Design

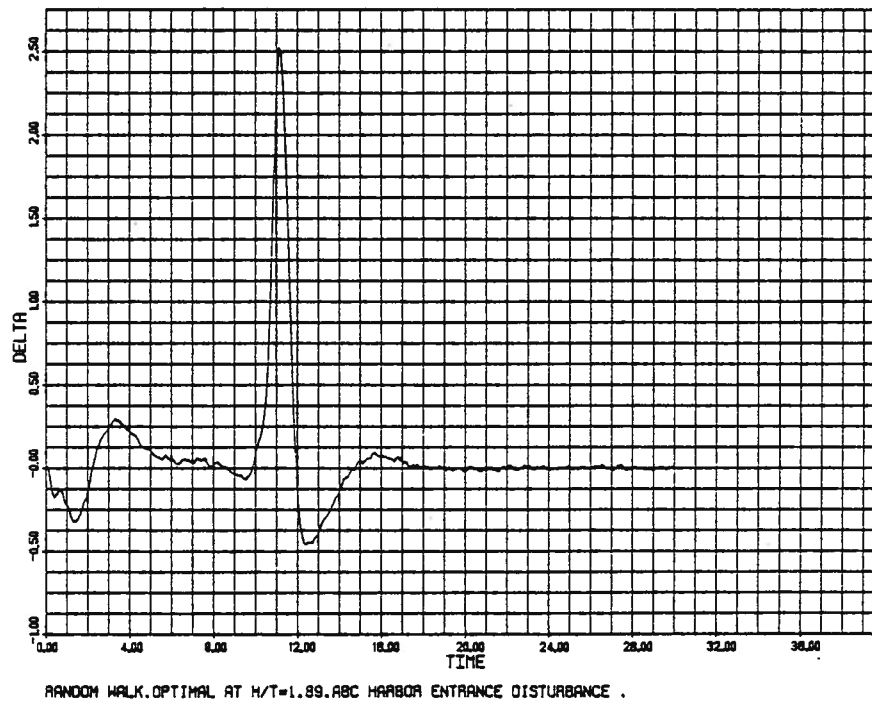


Figure 17. Rudder Angle Response at ABC Harbor Entrance - Random Walk Disturbance Model Design

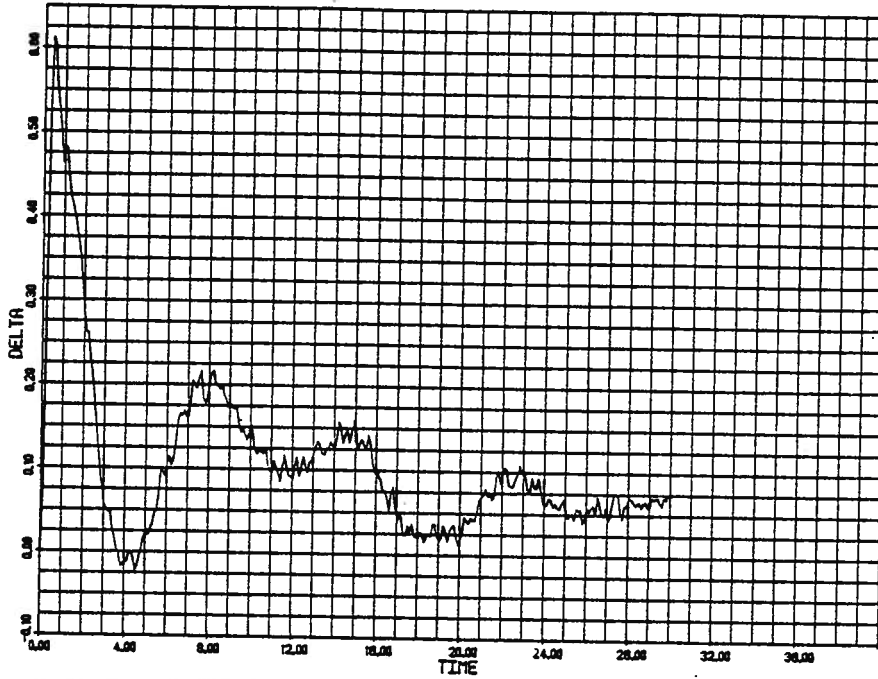
### 3.4 Necessity for an Adaptive Design.

In the previous section we showed that the path controller designed using random walk disturbance models provided effective control with essentially zero mean disturbances as shown in Figure 11 and with the design lateral current disturbance as shown in Fig. 13. In these examples, the controller was designed for the ship characteristics at its least course stable depth-to-draft ratio,  $H/T=1.89$ , and then the ship was simulated to operate at this same depth-to-draft ratio. The characteristics of the ship are, however, known to change considerably with water depth as shown in Table 2. They will also change with ship operating condition such as draft and trim. We have previously shown that if a constant gain design is to be used, the best overall performance is achieved by using the design developed for the ship's least course stable depth-to-draft ratio.<sup>1</sup> With this design approach, the question remains as to how much performance is lost by not adjusting the gains to be optimal at each ship operating condition. Notice also that the model of the ship ( $F_e$ ) included in the Kalman filter implementation in accordance with eq. (47) should be updated to reflect the ship characteristics in each operating condition if these are known. An adaptive path controller is one which can detect the existing ship characteristics and automatically adjust the controller and filter gains and the Kalman filter model of the ship accordingly.

To illustrate the effect of an "incorrect" water depth, we simulated the *Tokyo Maru* under the control of the controller defined in Table 5 while being subjected to the design lateral current disturbance shown in Fig. 4 in deep water ( $H/T=\infty$ ). The resulting lateral offset response is shown in Fig. 18 as the solid line. This response is comparable with that shown in Fig. 13 for the same disturbance in the "design" water depth  $H/T=1.89$ . Also shown in Fig. 18 as the dashed line is the response which would result if the controller had been redesigned (or adapted) to be optimal at  $H/T=\infty$  in lieu of  $H/T=1.89$ . The loss in performance due to the use of a nonadaptive, constant-gain and constant filter ship model design can be seen by comparing the two responses in Fig. 18. The maximum lateral offset during the *startup* of the system increases from 50.2 m. to 63.5 m.; the maximum offset during the ramp change in disturbance level increases from 13.8 m. to 18.5 m. While the transient response is degraded, the controller does retain the desired integral control property and returns the ship to the desired path in the presence of a constant disturbance.

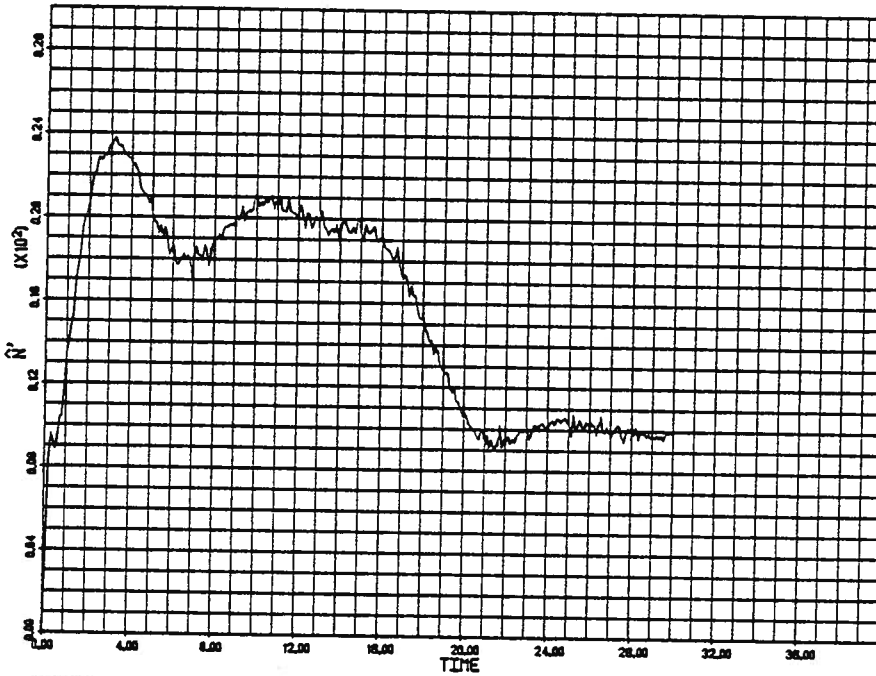






RANDOM WALK MODEL, DESIGNED FOR H/T=1.89 RUNS DEEP, DESIGN CURRENT .

Figure 19. Rudder Angle Response to Design Lateral Current - Design for H/T=1.89 Operating at H/T= $\infty$ .



RANDOM WALK MODEL, DESIGNED FOR H/T=1.89 RUNS DEEP, DESIGN CURRENT .

Figure 20. Yawing Moment Estimate with Design Lateral Current - Design for H/T=1.89 Operating at H/T= $\infty$ .

when the ship is subjected to the yawing moment and lateral force shown in Fig. 4 for  $t' \leq 15$  while in deep water ( $H/T = \infty$ ). The equilibrium rudder angle is nonzero here because the "design" disturbance in Fig. 4 is not exactly equivalent to a lateral current when applied to the ship in any water depth other than the  $H/T = 1.89$  for which it was derived.

For a path controller to remain optimal at each operating condition, the controller gains  $C$ , the Kalman-Bucy filter gains  $K$ , and the ship model  $F_e$  used in the filter eq. (47) must be adjusted. The change of the ship characteristics  $F_s$  or  $F_e$  with water depth is shown in Table 2. To illustrate the effect of water depth on the gains, Table 6 shows the optimal gains for the *Tokyo Maru* at  $H/T = \infty$ . These gains produce the lateral offset response shown by the dashed line in Fig. 18. The gains in Table 6 for  $H/T = \infty$  can be compared with those in Table 5 for  $H/T = 1.89$ . The controller feedback gains on  $\beta'$  and  $Y'$  show the greatest variations.

controller gains $C^T$	Kalman-Bucy filter gains $K$		
5.8752	4.6624	0.8842	0.0001
2.4635	19.4819	15.1516	-0.2571
1.9204	3.5844	2.8169	-10.9043
2.4252	0.0034	-0.4099	4.6587
-0.7955	0.0000	0.0000	0.0000
1126.44	0.1394	0.2548	0.0509
82.614	-0.0878	-0.1596	0.5079

Table 6. Optimal Gains for *Tokyo Maru* at  $H/T = \infty$  and  $F_n = 0.116$  - Random Walk Disturbance Model

In Table 2, it can be seen that ten parameters in the linear state variable equations of motion of the ship eq. (11) vary with water depth. These same parameters will also vary with draft, trim, etc. In considering the use of an adaptive control system it is useful to establish how important the variation in each of these parameters is to the response of the system. If the variation of a parameter has little influence on or correlation with the response, it will be difficult to establish that parameter from the response. Fortunately, if a parameter has little influence on the response it may not be necessary to estimate the parameter accurately or it may not be necessary to adapt for the changes in that parameter at all. In our previous work,<sup>1</sup> we studied the sensitivity of the ship path control response to the ten

parameters which vary with depth. This study was for somewhat different path controller designs for the *Tokyo Maru* utilizing first-order shaping filter disturbance models. These results are still useful, however, in this context and are summarized in Table 7. In this computer experiment, a number of controllers were designed and then their root mean square (RMS) responses to the design disturbance and noise levels were established using the OPTSYS computer program. These results were then combined into a single RMS cost  $\tilde{J}$  which is proportional to the cost function used in the optimal control system design; i.e.,

$$\tilde{J} = \tilde{\psi}^2 + 5.8818 \tilde{\eta}^2 + \tilde{\delta}^2 + \tilde{\delta}_c^2, \quad (70)$$

where ( $\tilde{\cdot}$ ) signifies the RMS value of each quantity. This RMS cost provides an appropriate single measurement of the effectiveness of each controller.

case	cost $\tilde{J}$
1. all parameters adapted; optimal at $H/T=\infty$	0.00681
2. all parameters adapted except $\gamma_{31}, f_{35}, \gamma_{22}$ , or $f_{33}$	0.00681
3. all parameters adapted except $f_{22}$ or $\gamma_{32}$	0.00682
4. all parameters adapted except $f_{32}$	0.00683
5. all parameters adapted except $\gamma_{21}$	0.00689
6. all parameters adapted except $f_{25}$	0.00693
7. all parameters adapted except $f_{23}$	0.00746
8. no parameters adapted; optimal for $H/T=1.89$	0.00783
9. only parameters $f_{23}, f_{25}$ , and $\gamma_{21}$ adapted	0.00683

all nonadapted parameters for  $H/T=1.89$

Table 7. RMS Cost  $\tilde{J}$  for *Tokyo Maru* with Various Controllers at  $H/T=\infty$  - First-Order Shaping Filter Disturbance Model<sup>1</sup>

Shown in lines 1 and 8 of Table 7 are the RMS cost  $\tilde{J}$  for the controllers designed to be optimal at  $H/T=\infty$  and  $H/T=1.89$ , respectively, when both are operated at  $H/T=\infty$ . The RMS cost can be seen to degrade from the optimal 0.00681 to 0.00783 (+15%) if a nonadaptive design were used in deep water with the design developed for the ship's least-course-stable depth of  $H/T=1.89$ . To show the importance of each individual parameter we also designed a series of controllers using all characteristics for  $H/T=\infty$  except a single parameter which was set at its value for  $H/T=1.89$ . This produces the response of a controller which could adapt for all parameters except the one held at its

H/T=1.89 value and shows the sensitivity of the response to that parameter. In lines 2 through 7 of Table 7, it can be seen that only  $f_{23}$ ,  $f_{25}$ , and  $\gamma_{21}$  have a significant effect on the RMS response. Coefficient  $f_{23}$  of  $\beta'$  in the  $\dot{r}'$  equation is by far the most significant parameter. In line 9 of Table 7 we show the RMS cost produced by a design which would adapt only for changes in  $f_{23}$ ,  $f_{25}$ , and  $\gamma_{21}$  while keeping the remaining seven parameters fixed at their value at H/T=1.89. This RMS cost is within 0.3% of that achieved with the optimal design shown in line 1. These results are very significant and show that it is not essential that the adaptive path control systems to be studied in the following chapters adapt for all ten of the parameters which vary with water depth, draft, trim, etc.

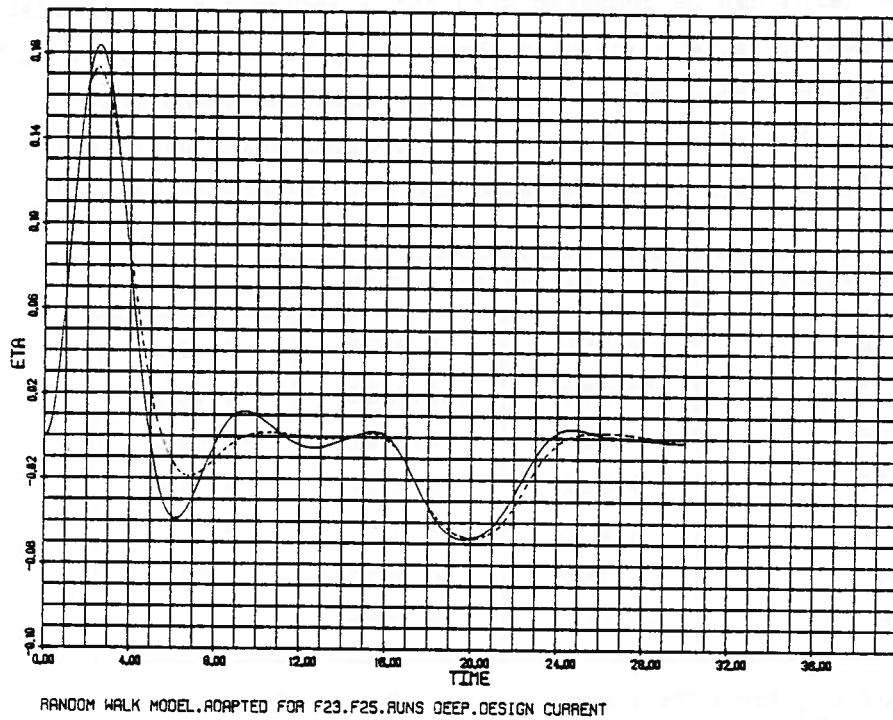
To further investigate the point made in the previous paragraph, we designed a "partially-adapted" controller using all the assumptions of Section 3.3 except that the parameters  $f_{23}$  and  $f_{25}$  were taken for H/T= $\infty$  from Table 2 while the remaining eight parameters were given their values at H/T=1.89. We chose not to include  $\gamma_{21}=f_{26}$  with  $f_{23}$  and  $f_{25}$  because this parameter appears as a product with N' in eq. (59) and is thus very difficult to establish on-line. The resulting controller and Kalman-Bucy filter gains are shown in Table 8. These gains can be compared with those designed to be optimal at H/T=1.89 and shown in Table 5 and with those designed to be optimal at H/T= $\infty$  and shown in Table 6. They can be seen to approach the gains shown in Table 6. The gains in Table 8 represent those of a controller which would adapt only for changes in  $f_{23}$  and  $f_{25}$  at a time when the ship is operating in deep water.

controller gains $C^T$	Kalman-Bucy filter gains K		
5.5438	4.6552	0.8716	0.0010
2.4237	19.2058	13.8893	-0.2338
1.8986	3.2965	2.5069	-8.9281
2.4252	0.0343	-0.3727	4.2156
-0.7889	0.0000	0.0000	0.0000
922.36	0.1529	0.2524	0.0568
46.656	-0.1116	-0.1777	0.5040

$f_{23}$  and  $f_{25}$  for H/T= $\infty$ ; other  $f_{ij}$  for H/T=1.89

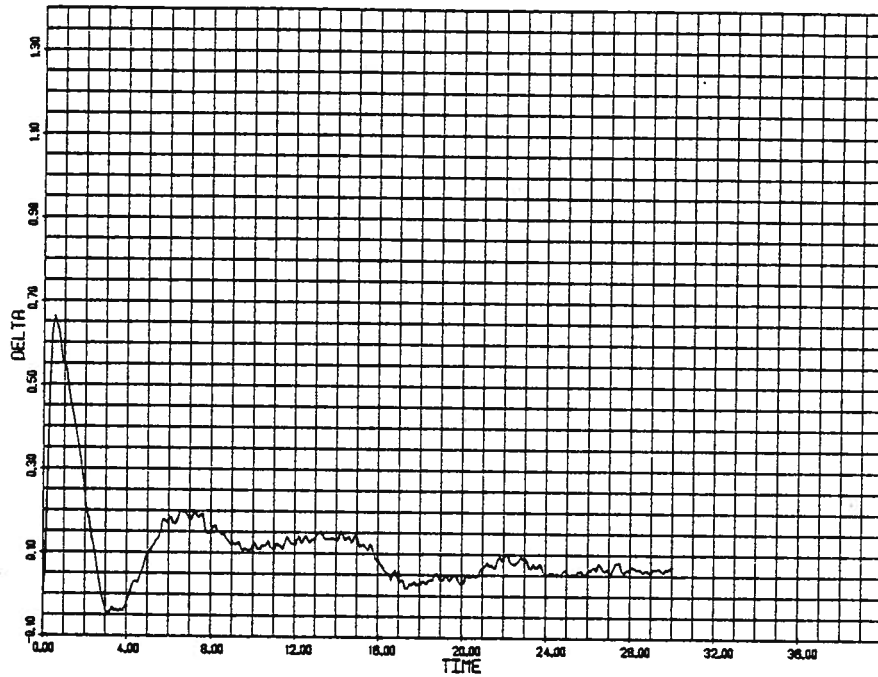
Table 8. Gains for Partially-Adapted Design for *Tokyo Maru* at  $F_n=0.116$  - Random Walk Disturbance Model

To illustrate the effectiveness of the partially-adapted design given in Table 8, we simulated the *Tokyo Maru* under the control of this controller while being subjected to the design lateral current disturbance shown in Fig. 4 in deep water ( $H/T=\infty$ ). The resulting lateral offset response is shown in Fig. 21 as the solid line; this is directly comparable to the response shown for the nonadapted design in Fig. 18. The response with the optimal design for  $H/T=\infty$ , the fully-adapted design, is shown in Fig. 21 as the dashed line for comparison. The maximum lateral offset during the startup of the system is 53.2 m. compared to 50.2 m. with full adaptation and 63.5 m. with no adaptation. The maximum offset during the ramp change in disturbance level is 13.9 m. compared to 13.8 m. with full adaptation and 18.5 m. with no adaptation. Adapting only for changes in  $f_{23}$  and  $f_{25}$  thus provides transient response very close to that provided by the fully-adapted, optimal design. The rudder angle response corresponding to Fig. 21 is shown in Fig. 22; the yawing moment estimate  $\hat{N}'$  is shown in Fig. 23. Notice that the equilibrium, mean yawing moment estimate during the first 15 ship lengths is about 0.00126 compared with 0.00199 with the nonadapted design in Fig. 20 and the exact value of 0.00103 which would be produced by the fully-adapted, optimal design.



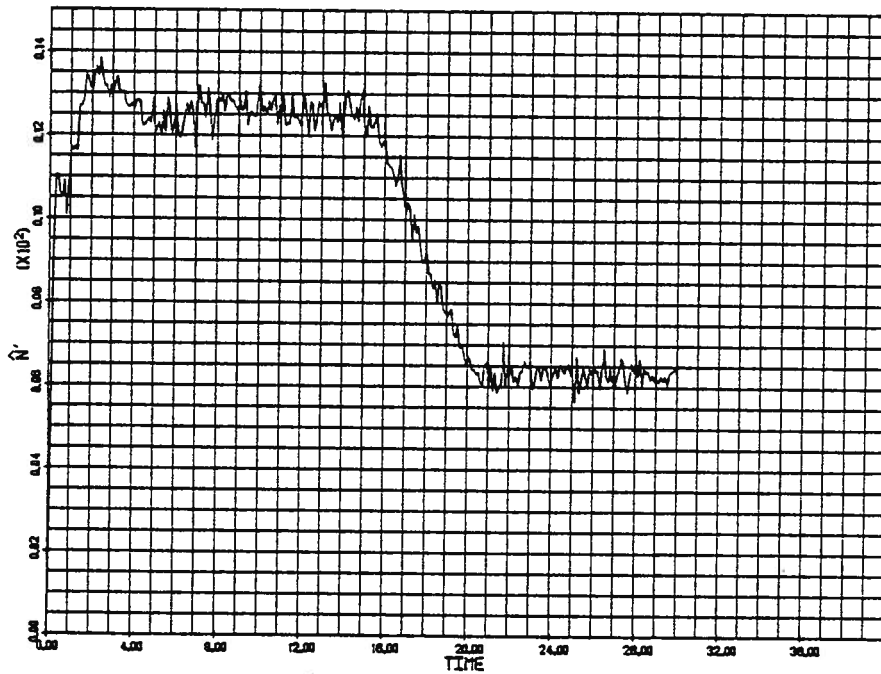
———— adapted only for  $f_{23}$  and  $f_{25}$       - - - - - optimal at  $H/T=\infty$

Figure 21. Lateral Offset Response to Design Lateral Current - Partially-Adapted Design and Design for  $H/T=\infty$  Operating at  $H/T=\infty$ .



RANDOM WALK MODEL, ADAPTED FOR F23.F25.RUNS DEEP.DESIGN CURRENT

Figure 22. Rudder Angle Response to Design Lateral Current - Partially-Adapted Design Operating at  $H/T=\infty$ .



RANDOM WALK MODEL, ADAPTED FOR F23.F25.RUNS DEEP.DESIGN CURRENT

Figure 23. Yawing Moment Estimate with Design Lateral Current - Partially-Adapted Design Operating at  $H/T=\infty$ .

Summarizing this chapter, we have shown that effective ship path controllers can be developed using a random walk model for the yawing moment and lateral force disturbances. This controller provides effective control with short-term, essentially zero-mean disturbances as shown in Fig. 11 and with more long-term, nonzero-mean disturbances as shown in Fig. 13. We then showed that this controller experiences a degradation in transient response when used at an "incorrect depth" or in any other condition causing the ship characteristics to change from the values used in the controller design. At an "incorrect depth" this controller is, however, capable of producing the same equilibrium, mean response as would the optimal design. Finally, we showed that adapting for changes in as few as two parameters in the equations of motion can eliminate almost all of the degradation in transient response experienced with changing ship characteristics. In the following two chapters, we investigate two different approaches for the design of such adaptive ship path controllers and evaluate their performance capabilities and limitations.



#### 4. Weighted Least-Squares Parameter Estimator

In this section, we present the derivation and evaluation of a Weighted Least-Squares (WLS) parameter estimator which could be used in the gain update loop of an adaptive ship path control system. This section is based upon Cuong's Ph.D. Dissertation.<sup>49</sup> The WLS approach requires no probabilistic assumptions about the uncertainties of the measurements and the process disturbances. It treats the observed measurement data in a deterministic rather than probabilistic sense. The unknown system parameters are chosen so that the response of a model of the ship dynamics provides a "best fit" to a finite record of sensor measurements. This treatment of measurement data is called "limited memory" or "moving window". The moving window concept was originally proposed by Jazwinski<sup>48</sup> to handle the divergence problem of Kalman filters. Dunn and Montgomery<sup>50</sup> utilized Jazwinski's concept in a batch processing manner to do the on-line parameter identification for the NASA F8-DFBW aircraft. This approach is conceptually simple which made it a logical first choice in our parameter identification investigation.

##### 4.1 Derivation and Development.

The source of information for the parameter estimation algorithm is the measurement vector  $\underline{z}'$ . Sensor outputs are sampled and the results are buffered in the memory of a control computer. After LW samples have been collected, the parameter estimation algorithm starts processing this information. Meanwhile, additional measurement data can be ignored until it is time to buffer another window of data. The timing sequence is illustrated in Fig. 24 where each graduated mark on the time axis represents a sampling instant and:

- LU is the length of the parameter estimation cycle,
- LW is the length of the data window,
- LB is the length of the batch update calculation period.

A cycle of a typical parameter estimation process starts with a stabilization period during which the ship is run under the control of recently acquired parameter estimates and gain matrices C and K. This period allows transients caused by the abrupt changes in the parameter estimates and gain matrices to die out. This period is followed by the data window loading

period in which LW samples of the measurement vector  $\underline{z}'$  are collected and stored in the estimator memory. The cycle is completed by the batch update calculation period in which the parameter estimation and gain updates are performed. This period produces a new set of parameter estimates and new values for the control gain C and the Kalman filter gain K if the parameter estimates are judged to be physically reasonable.

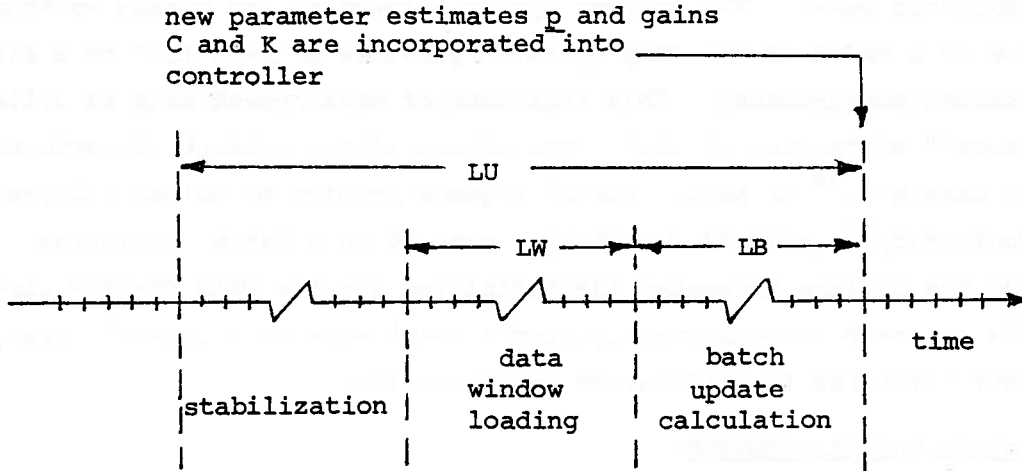


Figure 24. Timing Sequence for Weighted Least-Squares Parameter Estimator.

After another stabilization period, a new data batch is buffered and then processed by the algorithm. In this manner LW memory locations per measurement channel are needed for the moving window. When the states change very slowly or the time constants of the system are long, the window has to be very long. This can represent a large memory requirement. The parameter estimation task can, however, be processed on a time-available basis.

In the control loop development, the equations of motion of the ship were expressed by the 5-state system eq. (11). The rudder angle  $\delta$  was included as a state in order to introduce a realistic time response for the steering system. We noted in Section 3.2 that the rudder angle time response is known exactly if the rudder time constant, the initial condition  $\delta_0$ , and the rudder command history are known. Therefore,  $\delta(t)$  will be considered a known function in this development. The system equations then become,

$$\frac{d}{dt'} \begin{bmatrix} \psi' \\ r' \\ \beta' \\ \eta' \end{bmatrix} = \begin{bmatrix} 0 & 1 & 0 & 0 \\ 0 & f_{22} & f_{23} & 0 \\ 0 & f_{32} & f_{33} & 0 \\ 1 & 0 & -1 & 0 \end{bmatrix} \begin{bmatrix} \psi' \\ r' \\ \beta' \\ \eta' \end{bmatrix} + \begin{bmatrix} 0 \\ f_{25} \\ f_{35} \\ 0 \end{bmatrix} \delta' + \begin{bmatrix} 0 & 0 \\ \gamma_{21} & \gamma_{22} \\ \gamma_{31} & \gamma_{32} \\ 0 & 0 \end{bmatrix} \begin{bmatrix} N' \\ Y' \end{bmatrix}, \quad (71)$$

or,

$$\dot{\underline{x}} = F \underline{x} + G \delta' + \Gamma \underline{w}. \quad (72)$$

The disturbances  $N'$  and  $Y'$  are considered to be stochastic processes in eq. (71) but this assumption has no effect on the WLS development.

Cuong<sup>49</sup> has shown that for a WLS parameter estimation algorithm to be effective in estimating ship parameters all states must be available for measurement. The measurement vector to be used in the gain update loop is therefore taken as,

$$\underline{z}' = \underline{x} + \underline{v}', \quad (73)$$

where  $\underline{v}'$  is a Gaussian white measurement noise vector which is ignored within the WLS algorithm. In general, the parameter estimation loop requires a more accurate level of measurements than does the control loop. In the simulations presented later in this section, the reference level of the measurement noise vector  $\underline{v}'$  is as shown in Table 9. This represents a very small level of noise but is not necessarily the highest level which could be tolerated.

measurement	$\sigma_i$	$\tau_j$	$r_{jj}$	$\sigma_j'$
$\psi'$	$0.1^\circ$	0.01s	$1.2976 \times 10^{-9}$	$5.0943 \times 10^{-4}$
$r'$	$0.0016^\circ/s$	0.01s	$7.7215 \times 10^{-10}$	$3.9298 \times 10^{-4}$
$\beta'$	$0.08^\circ$	0.01s	$8.2777 \times 10^{-10}$	$4.0688 \times 10^{-4}$
$\eta'$	1m	0.01	$5.0651 \times 10^{-9}$	$1.0065 \times 10^{-3}$

Table 9. Reference Measurement Noise for Parameter Estimator  $\underline{v}'$

It was demonstrated in Section 3.4, that accurate estimates of only two of the 10 coefficients in eq. (71),  $f_{23}$  and  $f_{25}$ , are essential to an effective adaptive control loop. Our first approach was therefore to select a parameter vector of minimum dimension, i.e.,

$$\underline{p} = [p_1, p_2, p_3, p_4]^T = [f_{23}, f_{25}, N', Y']^T,$$

in order to minimize the computational load. Cuong<sup>49</sup> has shown that this parameter choice is a condition of underparameterization in which the WLS algorithm converges to an estimate of  $\underline{p}$  which is completely impossible physically. Even though accurate estimates of the other coefficients in the open-loop dynamics matrix  $f_{ij}$  are not really needed by the control loop, these coefficients must be included in the parameter set to be estimated by the parameter estimator. If they are not, the effects of errors in these coefficients are interpreted as changes in  $f_{23}$  and  $f_{25}$ . The parameter vector to be estimated by the parameter estimator must therefore be taken as,

$$\underline{p} = [p_1, \dots, p_8]^T = [f_{22}, f_{23}, f_{25}, f_{32}, f_{33}, f_{35}, N', Y']^T. \quad (74)$$

Recall that the disturbances  $N'$  and  $Y'$  are estimated by the control loop Kalman filter and these estimates are actively used for control purposes. The unknown disturbances must also be included in the parameter set. If they are not, the effect of the disturbances is interpreted as changes in the system parameters. The disturbance estimates produced by the parameter estimator are only a by-product of the estimation process and are not used further.

For use in the WLS parameter estimator, the ship is modeled by the state vector  $\underline{x}_m = [\psi'_m, r'_m, \beta'_m, \eta'_m]^T$  and the following equations:

$$\frac{d}{dt'} \begin{bmatrix} \psi'_m \\ r'_m \\ \beta'_m \\ \eta'_m \end{bmatrix} = \begin{bmatrix} 0 & 1 & 0 & 0 \\ 0 & p_1 & p_2 & 0 \\ 0 & p_4 & p_5 & 0 \\ 1 & 0 & -1 & 0 \end{bmatrix} \begin{bmatrix} \psi'_m \\ r'_m \\ \beta'_m \\ \eta'_m \end{bmatrix} + \begin{bmatrix} 0 \\ p_3 \\ p_6 \\ 0 \end{bmatrix} \delta' + \begin{bmatrix} 0 & 0 \\ \tilde{\gamma}_{21} & \tilde{\gamma}_{22} \\ \tilde{\gamma}_{31} & \tilde{\gamma}_{32} \\ 0 & 0 \end{bmatrix} \begin{bmatrix} p_7 \\ p_8 \end{bmatrix},$$

(75)

where the values of the coefficients in the  $\Gamma$  matrix are assigned constant assumed values indicated by ( $\dots$ ). These "known" coefficients are assigned their value at the ship's least-course-stable depth-to-draft ratio  $H/T=1.89$ . With  $p_7 = N'$  and  $p_8 = Y'$ , the parameter estimator estimates the average values of  $N'$  and  $Y'$ . These estimates, however, are not very accurate because the  $\gamma_{ij}$  coefficients are kept constant at assumed values. The estimates of  $N'$  and  $Y'$  include the effects of these errors. Since we are not interested in the values of the disturbances, per se, this arrangement is clearly acceptable.

At the beginning of the parameter estimation, the computer memory holds the system states at the start of the data window and the rudder angle  $\delta'$  and measurement  $\underline{z}'$  histories during the data window. Using any set of the parameters  $\underline{p}$ , the buffered state at the start of the window, and the buffered rudder angle history, the ship model eq. (75) is simulated through the same time period as the window to produce  $\underline{x}_{m,k}$  where  $k$  is the sample time index. This yields a set of model measurements  $H\underline{x}_{m,k}$  which fill the data window and a Weighted Least-Squares cost function or fit error  $J$  can be defined as:

$$J = \frac{1}{2} \sum_{k=1}^{LW} (\underline{z}'_k - H\underline{x}_{m,k})^T W_k (\underline{z}'_k - H\underline{x}_{m,k}) \quad (76)$$

The weighting matrices  $W_k$  can be used to adjust for dimensional differences among the measurements or can be used to place more emphasis on matching selected measurements or on matching the most recent measurements. The weighting matrix is assumed to be diagonal so the cost function  $J$  can be expanded to give,

$$J = \frac{1}{2} \sum_{k=1}^{LW} \left[ (z'_1 - \psi'_m)_k^2 w_{1k} + (z'_2 - r'_m)_k^2 w_{2k} + (z'_3 - \beta'_m)_k^2 w_{3k} + (z'_4 - \eta'_m)_k^2 w_{4k} \right] \quad (77)$$

The WLS parameter estimation problem is then to vary the parameter estimate  $\underline{p}$  to produce the parameter estimate vector  $\underline{p}^*$  which yields a minimum of this cost function. This causes the response of the ship model as represented by the model measurements to be a least-squares fit to the measured response.

The minimization of the Weighted Least-Squares cost function, eq. (77),

can be accomplished iteratively using any of a number of numerical algorithms. Dunn and Montgomery<sup>50</sup> used a modified Newton-Raphson algorithm. It is difficult and expensive in this problem, however, to numerically estimate the gradient of J needed by this algorithm. This is especially true if an on-line application is desired. In this situation, a derivative-free algorithm is very attractive. It is also desirable to make efficient use of previously computed function values. After preliminary work with a number of alternative methods, the DUD (Doesn't Use Derivatives) algorithm was selected for use here. This algorithm was developed by Ralston<sup>51</sup> and was presented by Ralston and Jennrich<sup>52</sup> in 1978. Cuong<sup>49</sup> extended the DUD algorithm to the Weighted Least-Squares problem and added additional search stopping conditions needed for its application to the ship parameter estimation problem. The DUD algorithm does not require the gradient of J as the name implies. Once the algorithm is started, only one evaluation of J is needed in each optimization cycle performed under normal conditions. DUD has proven to be an effective and efficient search algorithm for this problem.

As noted above the diagonal weighting matrices  $W_k$  in eq. (77) can be used to assign different levels of importance to the various measurements. They can be varied with the time index k to account for a lower confidence in old data. They can also be used to achieve a non-dimensionalization of the various errors in fitting the model response to the data. In our work, the  $W_k$  were chosen to be constant with time. Recall that in the solution of the Linear-Quadratic-Gaussian state estimation problem, the innovation is "weighted" by  $R^{-1}$ , where R is the spectral density of measurement noise. It is reasonable to use a parallel approach here and select  $W_k = W = R^{-1}$ . This accomplishes a desirable non-dimensionalization and reflects the relative noise levels in each measurement. Using this approach, the DUD algorithm was found to require about 17% fewer evaluations of J to converge compared with runs using an equal weighting; i.e.,  $W_k = I$  where I is the identity matrix.

The simulation of the ship model, eq. (75), begins from the buffered state of the system at the start of the data window loading period. We have found that when realistic noise exists in the system, it is preferable to use the estimate of the state at this point produced by the control loop Kalman filter rather than the noisy measured states. The state estimate

is an expected value of the state at the start of the window loading period and is not strongly affected by the noise at that time which probabilistically might be large. It is undesirable in general, however, to use filtered data in parameter estimation so all of the data in the moving window, except the initial values, are taken directly from sensor measurements. This ensures the maximum information content in the data base.

We noted above that the parameter estimates  $\underline{p}^*$  or  $\hat{\underline{p}}$  produced by the DUD algorithm in the WLS parameter estimator are only used to calculate updated controller gains C and Kalman filter gains K if the estimates are judged to be physically reasonable. In our work, we performed this validity check by noting the expected range of each parameter given in Table 2 and the sensitivity study results discussed in Section 3.4 which showed that the control loop needs accurate estimates of only the two parameters,  $f_{23}$  and  $f_{25}$ . The validity check, therefore, utilizes the following logic:

- if either  $\hat{f}_{23}$  or  $\hat{f}_{25}$  is beyond the permissible range, as given in Table 10, no update is made; i.e., the controller remains unchanged;
- if  $\hat{f}_{23}$  and  $\hat{f}_{25}$  are within the permissible ranges but some of the remaining estimates are beyond the permissible ranges, only  $\hat{f}_{23}$  and  $\hat{f}_{25}$  are updated in eq. (59);
- if all estimates are within the permissible ranges, all the  $f_{ij}$  are updated in eq. (59).

If an update is to be made, the new feedback gains C and filter gains K are calculated as described in Section 3.3. The results are then incorporated into the controller.

Parameter	Lower limit $\underline{p}_l$	Upper limit $\underline{p}_u$
$f_{22}$	-2.50	-1.10
$f_{23}$	2.10	12.00
$f_{25}$	-1.30	-0.30
$f_{32}$	0.0	0.42
$f_{33}$	-1.30	-0.30
$f_{35}$	-0.22	0.0

based upon experimental range  $\pm 30\%$ .

Table 10. Permissible Ranges of Parameter Estimates for the *Tokyo Maru*.

The development of the WLS parameter estimator is complete at this point except for the addition of an open-loop excitation or input dither signal which will be shown to be necessary in the next section. Before proceeding, however, it is appropriate to review some of the alternative parameter set choices which were found to be unsuccessful prior to our choosing eq. (74). Cuong<sup>49</sup> discusses these in detail so only brief comments will be included here. The following parameter choices were considered:

$$\bullet p_7 = \gamma_{21}N', p_8 = \gamma_{22}Y', p_9 = \gamma_{31}N', p_{10} = \gamma_{32}Y';$$

$$\bullet p_7 = \gamma_{21}, p_8 = N', p_9 = \gamma_{32}, p_{10} = Y', \gamma_{22} = \tilde{\gamma}_{22}, \gamma_{31} = \tilde{\gamma}_{31};$$

$$\bullet p_7 = \gamma_{21}, p_8 = \gamma_{32}, N' = \hat{N}', Y' = \hat{Y}', \gamma_{22} = \tilde{\gamma}_{22}, \gamma_{31} = \tilde{\gamma}_{31}.$$

In the first approach, the  $\dot{r}$  and  $\dot{\beta}$  equations included terms  $p_7 + p_8$  and  $p_9 + p_{10}$ , respectively. The WLS algorithm quickly produced physically impossible results with the terms in these sums having very large, equal magnitudes but opposite sign. In the second approach, the  $\dot{r}$  and  $\dot{\beta}$  equations involved products of parameters; i.e.  $p_7p_8$  and  $p_9p_{10}$ , respectively. The coefficients  $\gamma_{22}$  and  $\gamma_{31}$  were given constant, assumed values. The DUD algorithm failed to converge in this problem. The third approach would use the yawing moment and lateral force disturbance estimates from the control loop Kalman filter in the parameter estimator. This approach was not actually tried but was discarded because it would produce a highly undesirable coupling between the state estimation filter and the parameter estimator.

#### 4.2 Time-Invariant Parameters Performance

In this section, we evaluate the performance of a WLS ship parameter estimator when the parameters are time-invariant. With the WLS parameter estimator each parameter estimation cycle is a completely independent process. The only information used from the previous cycle is the old parameter estimate which is used as the initial estimate in the DUD algorithm search. This initial estimate affects the convergence rate of the search but has negligible effect on the resulting parameter estimate. Therefore, time-invariant parameters in this context requires that the



parameters be constant only during each data window loading period. The parameters could vary from one window loading period to the next. The stepped bottom profile shown in Fig. 25 was therefore used in our simulations to evaluate the effectiveness of the WLS parameter estimator with locally time-invariant parameters. The timing sequence was selected so that the window loading period would not overlap one of the discrete changes in water depth. Ship parameters can of course change due to many causes; i.e., draft, trim, water depth, etc. Rather than change the parameters in a completely arbitrary and random manner, however, we chose water depth as the independent variable to use to study the effect of physically possible parameter changes.

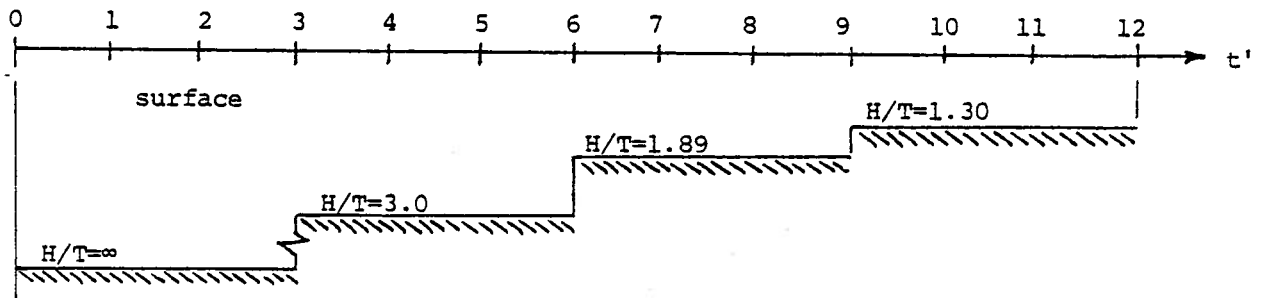


Figure 25. Stepped Bottom Profile

The signal-to-noise ratio is critical to the effectiveness of a WLS ship parameter estimator. The signal here is the measurement vector  $\underline{z}'$  which is contaminated by the noise  $\underline{v}'$  which will be at least as large as shown in Table 9. For the measurements to contain information about the dynamic characteristics of the ship, it is necessary that the ship trajectory include motion which is large compared with the noise level. This requirement is in direct conflict with precise ship path control which seeks to eliminate any motion from the desired track. The information content of the data window can be increased by increasing the amount of ship motion and by lengthening the data window. In off-line systems identification of ship parameters the "data window" is usually many minutes

in which the ship travels many ship lengths. It is usually considered necessary for the record length to be at least a few times the longest time constant of the system for successful identification using noisy measurement. The tests are conducted with constant ship characteristics and in unrestricted waters so that significant ship motion can be used. In path control in restricted waters, ship motion must be restricted, calculations must be performed on-line, and the ship parameters may change significantly over even a ship length. Parameter estimation in this context is very difficult and requires very low levels of acceptable noise and engineering tradeoff in design.

The parameters  $f_{ij}$  which the WLS parameter estimator must estimate are the open-loop parameters of the ship. During path control, however, the dynamics of the ship are governed by the closed-loop properties of the ship and the control loop. Further, Aström and Wittenmark<sup>11</sup> have noted the following conditions as necessary for the convergence of a least-squares parameter estimator:

- the system must be persistently excited by the input signal;
- the input signal must be independent of any disturbances.

The estimation of open-loop ship parameters in the presence of disturbances and the path control are basically incompatible and cannot be undertaken simultaneously. Thus, an adaptive ship path controller must devote itself alternately to parameter estimation using open-loop rudder commands and then to path control. If the rudder commands are generated by the feedback controller during the data window loading period, the input will be correlated with the disturbances and it will not be possible to determine all parameters. Further, the controllers used here will generally not allow the level of ship motion needed for the parameter estimation. Adaptive path control must therefore accept increased ship motion during the window loading period. The improved performance from having better parameter estimates must offset the effects of the periods of open-loop control.

The open-loop input signals used in adaptive controllers are often called *dither* signals. They usually have a zero mean to reduce the long term effect on the system. In highly dynamic systems such as aircraft,

the dither signal could be superposed upon the pilot's input commands and continuous small dither signals have been proposed. In the ship path control problem, the signal-to-noise ratio is such that the dither signal magnitude must be so large that continuous use would be unacceptable. Alternate periods of open-loop control using the dither signal with the control loop turned off followed by closed-loop control without the dither signal are used here. The purpose of the dither signal is to excite all modes of the system and to maintain them at large enough amplitudes for the parameter estimation to be successful. The signal should therefore include all the open-loop natural frequencies of the system.

In this investigation the dither signals were chosen to be square wave rudder commands of various amplitude and period. An alternative might be the Pseudo-Random Binary Sequences (PRBS) used in systems identification of ship parameters.<sup>17</sup> In general, the larger amplitude dither signals excite the ship more and improve the effectiveness of the parameter estimation. With a physical limit on rudder angle of about  $35^\circ$ , we have used a dither rudder command  $\delta_c'$  magnitude of 0.5 rad. in all the simulations presented below. With short dither periods, the rudder does not have time to reach this commanded value before the sign of the command is reversed. A magnitude of 0.5 rad. already stretches the validity of the linear system equations so higher values were not considered. The initial dither signal (at the beginning of the window loading period) was given a sign opposite to the rudder angle existing just prior to that time in order to maximize its effect on the ship. Since the square wave dither signal is used for only the finite window loading period (not continuously), it can excite frequencies below the fundamental frequency of the signal.

#### 4.2.1 Effect of Data Window Length and Dither Period

Various simulations of the *Tokyo Maru* were performed to evaluate the performance of the WLS parameter estimator. In our earliest work, we simulated the *Tokyo Maru* under the control of an adaptive control system

using a WLS parameter estimator when subjected to only 0.001 times the reference noise level given in Table 9 while sailing over the stepped bottom profile shown in Fig. 25. A short data window of only 0.2 ship length was used with this low noise level; the parameter estimation was performed once per ship length. Starting with an initial offset from the desired path of  $\eta' = \hat{\eta}' = 0.1638$  (1 beam) and using no dither signal, the WLS parameter estimator failed to work. Since the simulation started with a reasonably large initial condition, there was large ship motion in the first two ship lengths and the measurements thus contained a reasonable amount of information about the system. The estimator converged in the first cycle and gave poor estimates which were in the permissible ranges given in Table 10. By the second cycle, the ship motion had died out to a large extent and there was much less information contained in the response. As a result, even though the algorithm search converged, the estimates were outside the permissible range. By the third cycle, the path controller had suppressed most of the ship motion and the ship was moving almost in a straight line. The small amount of information which could be extracted from this mild movement was readily masked by the measurement noise (even though only 0.001 of the reference level). The DUD algorithm failed to converge. Without more ship motion a longer data window would be of no value in this case. With the addition of a dither signal with a period of 0.5 ship lengths and an increase in the data window length to 0.5 ship length (100 samples), the WLS parameter estimator quickly converged to estimates which were accurate to three significant figures in all 12 update periods. These results confirmed the necessity of a dither signal and validated the simulation software.

With the use of the reference level of measurement noise given in Table 9, the WLS parameter estimator will only produce acceptable results if the data window loading period is increased and the dither signal is used. The effectiveness is also improved by increasing the length of the dither period. Table 11 summarizes the results of the first update cycle of simulations of the *Tokyo Maru* sailing over the stepped bottom shown in Fig. 25 under the control of an adaptive path controller using the WLS

parameter estimator when subjected to the reference level of noise. Results are shown for various data window lengths and dither signal periods. The initial value of each parameter is only used in the first cycle; in subsequent cycles the most recent valid estimate is used as the starting point for the DUD algorithm search. With a data window length and dither period of 0.5 ship length, the results failed the validity check and the algorithm failed to converge at all after the depth change at  $t'=3$ . Results are also shown for a data window length of 5.0 ship lengths (1000 samples) and dither periods of 0.5, 1.0, and 5.0 ship lengths. In these cases, only one update period of 6.0 ship lengths was simulated. In general, the parameter estimates are reasonably good and improve with the dither signal period.

parameter	initial value H/T=1.89	correct value H/T= $\infty$	WLS parameter estimates using window length (ship lengths)/ dither period(ship lengths)			
			0.5/0.5	5.0/0.5	5.0/1.0	5.0/2.5
$f_{22}$	-1.7657	-1.9515	1.2835*	-1.8179	-1.8323	-1.8582
$f_{23}$	5.7359	3.1591	-9.8155*	2.8715	2.8902	2.9648
$f_{25}$	-0.88074	-1.0410	-0.93100	-1.0146	-1.0229	-1.0216
$f_{32}$	0.17199	0.31507	0.95165*	0.36378	0.32584	0.31693
$f_{33}$	-0.52766	-0.63651	-3.1628*	-0.72829	-0.64829	-0.63519
$f_{35}$	-0.15607	-0.16163	-0.13873	-0.15646	-0.16053	-0.16101
offset $\eta'$ at end of data window			-0.0005	-0.2854	-0.5706	-1.435
number of evaluations of cost J			68	60	107	66

\* estimate outside permissible range in Table 10

Table 11. Effect of Data Window Length and Dither Period on WLS Parameter Estimates Without Disturbances.

The results shown in Table 11 for the 5 ship length data window and 0.5 ship length dither signal probably represent about the best estimates that could be achieved with a WLS parameter estimation in a ship path controller. The offset due to the dither signal at the end of the data window is about 83m or 1.74 times the ship beam. Shorter window lengths and shorter dither periods would reduce this value but produce less accurate parameter

estimates. Simulations results with a 2.5 ship length data window are shown in the next section. Since we showed in Section 3.4 that the control loop only really needs accurate estimates of  $f_{23}$  and  $f_{25}$ , the accuracy of the estimates of only these two parameters should be the basis of judging the effectiveness of a WLS parameter estimator designed for use in an adaptive path controller. A design tradeoff would be necessary to achieve the best overall performance of the path controller. The longer dither periods could not be used in a path controller but are of interest if a WLS parameter estimator were to be used for system identification in unrestricted waters.

It is interesting to note in Table 11 that the short dither period allows good estimates of the parameters in the  $\dot{r}$ -equation ( $f_{22}, f_{23},$  and  $f_{25}$ ) but relatively poorer estimates of the parameters in the  $\dot{\beta}$ -equation ( $f_{32}, f_{33},$  and  $f_{35}$ ). The longer dither periods, however, significantly improve the estimator's ability to estimate the parameters in the  $\dot{\beta}$ -equation. This can be explained by consideration of the system time constants and eigenvectors. The open-loop eigenvalues and eigenvectors of the 5-state model of the *Tokyo Maru* include two zero eigenvalues and a third associated with the rudder time constant. The other two eigenvalues and the associated eigenvectors for deep water are as follows:

$$\lambda_4 = -0.0992, \tau_4 = 10.08 \text{ ship lengths,}$$

$$\xi_4 = [-0.0933, 0.0093, 0.0054, 0.9958, 0.0]^T,$$

$$\lambda_5 = -2.489, \tau_5 = 0.402 \text{ ship length,}$$

$$\xi_5 = [-0.3669, 0.9132, -0.1553, -0.0850, 0]^T.$$

Eigenvector  $\xi_5$  has a time constant of 0.4 ship length and is dominated by the second component ( $r'$ ). A dither period of 0.5 ship length is effective in exciting this mode and thus allows effective estimation of the parameters in the  $\dot{r}$ -equation. Eigenvector  $\xi_4$  is dominated by the fourth component ( $\eta'$ ). Although  $\beta'$  is only a weak component of eigenvector  $\xi_4$

it is directly fed into the  $\dot{\eta}$ -equation and  $\eta$  is the main component of  $\xi_4$ . With a time constant of 10 ship lengths, this mode is more effectively excited by the longer dither periods thus making the parameters in the  $\dot{\beta}$ -equation more identifiable.

#### 4.2.2 Performance with Bias Disturbances

In a ship path controller application, the WLS parameter estimator would also have to estimate the yawing moment and lateral force disturbances acting on the ship as included in eq. (74). To evaluate the performance of the WLS parameter estimator with time-invariant disturbances, we simulated the *Tokyo Maru* under the control of an adaptive ship path controller using this algorithm while being subjected to a constant 1-knot lateral current as defined in Fig. 4 for  $t' < 15$ . This disturbance was held constant for 18 ship lengths; the reference measurement noise level from Table 9 was used. The controller and parameter estimator were initialized with ship parameters for  $H/T=1.89$  but the ship was simulated to be actually operating in deep water ( $H/T=\infty$ ). The initial conditions for these simulations were the steady-state conditions for the control loop; i.e.,

$$\begin{aligned} \psi' = \hat{\psi}' = \beta' = \hat{\beta}' &= -0.1428, \\ r' = \hat{r}' = \eta' = \hat{\eta}' &= 0.0, \\ \delta' = \hat{\delta}' &= 0.1310, \\ \hat{N}' &= 0.001992, \\ \hat{Y}' &= 0.003437. \end{aligned}$$

The disturbance shown in Fig. 4 is not exactly equivalent to a lateral current when the ship is at any depth-to-draft ratio other than  $H/T=1.89$  for which it was derived so the steady-state rudder angle is not zero.

The constant disturbance simulations used a parameter estimation cycle of 6 ship lengths ( $LU=1200$  samples) and three combinations of data window length and dither period. The results of the first parameter estimation cycle of these simulations are shown in Table 12. The results with window

length of 2.5 ship lengths (500 samples) and a 0.5 ship length dither period are excellent. Results with a 5 ship length data window and two dither periods are shown as a reference point for the effectiveness of the WLS parameter estimator. These designs would be impractical in a path control application due to the excessive offset from the desired path. These paths would also clearly violate the validity of the linear ship model. The effects of the assumed constant values for the  $\gamma_{ij}$  coefficients in eq. (75) on the estimates of the disturbances  $N'$  and  $Y'$  can be clearly seen in Table 12. In addition to allowing a more reasonable offset from the path, the reduction of the window length from 5 to 2.5 ship lengths reduces the computation cost of each evaluation of the cost  $J$  by about one-half so the shorter window length results in about half the data storage and computational load with only a small loss in parameter estimate accuracy.

parameter	initial value H/T=1.89	correct value H/T= $\infty$	WLS parameter estimates using window length/dither period (ship lengths)		
			2.5/0.5	5.0/0.5	5.0/2.5
$f_{22}$	-1.7657	-1.9515	-2.0037	-1.9722	-1.9505
$f_{23}$	5.7359	3.1591	3.2540	3.2007	3.1544
$f_{25}$	-0.88074	-1.0410	-1.0424	-1.0415	-1.0406
$f_{32}$	0.17199	0.31507	0.32362	0.33157	0.31412
$f_{33}$	-0.52766	-0.63651	-0.65439	-0.66466	-0.63414
$f_{35}$	-0.15607	-0.16163	-0.16388	-0.16076	-0.16169
$N' \times 10^2$	0.00000	0.10262	0.12987	0.12824	0.12648
$Y' \times 10^2$	0.00000	0.23277	0.35415	0.35960	0.34070
offset $\eta'$ at end of cycle			0.1745	1.273	2.422
number evaluations of cost $J$			113	112	75
final cost $J \times 10^2$			0.1059	0.2092	0.2095

Table 12. Effect of Data Window Length and Dither Period on WLS Parameter Estimates with Constant Disturbances

To further illustrate the performance of the WLS parameter estimator with a 2.5 ship length data window and a 0.5 ship length dither period when subjected to a constant disturbance, the ship trajectory for the simulation shown in Table 12 is shown in Fig. 26. Fig. 26 shows the lateral offset



response of the ship for the first three update periods or 18 ship lengths. The dither signal has a zero mean rather than a mean value corresponding to the equilibrium rudder angle for the constant disturbance when the controller is using the initial parameters. As a result, the first dither period gives the ship a strong motion to the right ( $\eta' > 0$ ). This produces improved estimates in Table 12 compared with the corresponding results in Table 11. As soon as the controller is updated with nearly correct parameters at  $t' = 6.0$ , the equilibrium rudder angle is essentially zero and subsequent dither periods have less of an effect on the ship's offset from the desired track. The maximum offset is almost one-half ship length during the second update cycle. The simulation represents a type of "start-up transient" for the adaptive control system so the lateral offset in the third update period more closely represents the offset which the dither signal would cause in subsequent update cycles.

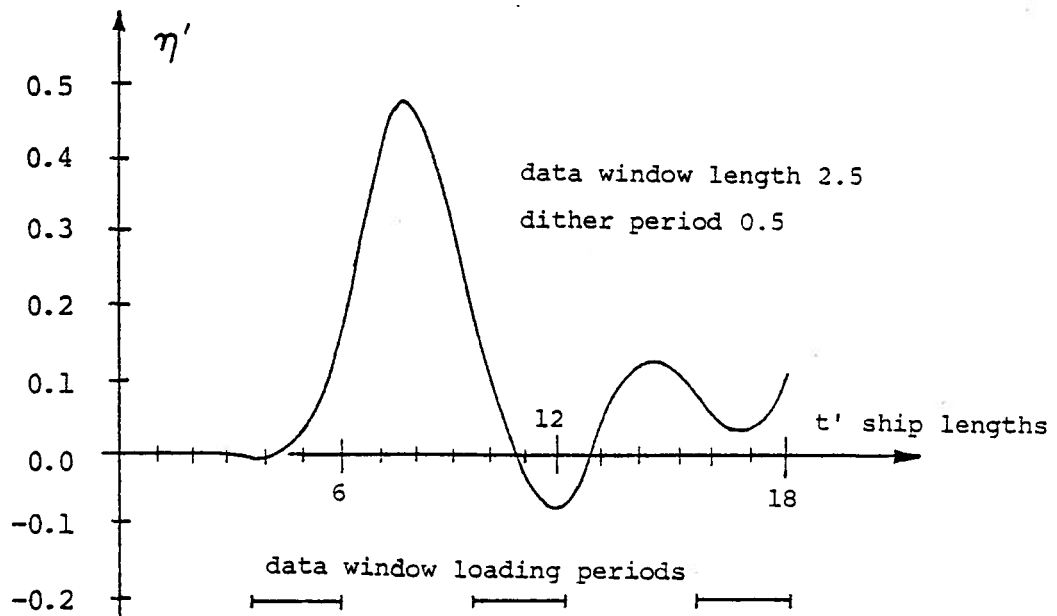


Figure 26. Lateral Offset Response to Constant Disturbance - WLS Parameter Estimator.

The parameter estimate results for the WLS parameter estimator simulation shown in Fig. 26 are shown in Table 13. The estimates were acceptable in each update. The Kalman filter ship equations and the gains C and K were therefore updated at the end of each cycle. Since the initial parameter

estimate for the second and third estimation cycles was the estimate produced by the previous estimation cycle, the number of evaluations of the cost function decreased significantly after the first update. The accuracy of the estimates of the  $\beta$ -equation parameters appears to decrease as the ship motion is reduced. In general, the parameter estimates are very good. Recall that the disturbance estimates are never used. A shorter data window length might continue to produce parameter estimates of acceptable accuracy with a smaller offset from the desired path. Further design tradeoff studies could establish the best compromise.

parameter	initial value H/T=1.89	correct value H/T= $\infty$	WLS parameter estimates using 2.5 window length/0.5 dither period		
			update 1	update 2	update 3
$f_{22}$	-1.7657	-1.9515	-2.0037	-1.9258	-1.9306
$f_{23}$	5.7359	3.1591	3.2540	3.1177	3.1414
$f_{25}$	-0.88074	-1.0410	-1.0424	-1.0414	-1.0405
$f_{32}$	0.17199	0.31507	0.32363	0.36511	0.28817
$f_{33}$	-0.52766	-0.63651	-0.65439	-0.72306	-0.59633
$f_{35}$	-0.15607	-0.16163	-0.16388	-0.16289	-0.16275
$N'x10^2$	0.00000	0.10262	0.12987	0.12561	0.12541
$Y'x10^2$	0.00000	0.23277	0.35415	0.39149	0.31570
maximum offset $\eta'$ in cycle			0.1745	0.4779	0.1257
number of evaluations of cost J			113	22	19
final cost $Jx10^2$			0.1059	0.1012	0.1035
update time			6	12	18

Table 13. Parameter Estimates from Constant Disturbance Simulation

#### 4.3 Time-Varying Parameters Performance

In this section, we evaluate the performance of a WLS ship parameter estimator when the parameters are time-varying. In the previous section, we considered the performance when the parameters were constant during each data window loading period which might have to be as long as 2.5 ship lengths.

The parameters could however, change from one parameter estimation cycle to the next. Here we consider situations in which the parameters change continuously during the data window loading periods. We continue to use the water depth as the independent variable which defines the changing parameters. We consider two cases. First, we consider the situation in which the water depth is changing continuously so that the ship coefficients are changing in a continuous manner. We then consider the situation in which the disturbances in the parameter vector, eq. (74), change continuously during the data window loading period as they would when the passes another ship or fixed obstruction.

#### 4.3.1 Time-Varying Ship Coefficients

To evaluate the performance of the WLS parameter estimator with continuously varying ship coefficients, we simulated the *Tokyo Maru* under the control of an adaptive path controller using the WLS parameter estimator while sailing over a downward sloping bottom. This simulation was performed without any measurement noise using a very short data window loading period of only 0.2 ship length. The update cycle was 0.3 ship length. The bottom profile was constructed to be level at  $H/T=1.89$  during the first data window. The estimator was initialized with parameter values at  $H/T=1.89$  and this startup period was introduced to allow the system to stabilize prior to experiencing a change in parameters. From time  $t' = 0.35$ , which was the beginning of the second update period, the bottom began a downward slope in which the depth-to-draft ratio increased linearly at a rate of 0.105/update or 0.350/ship length. The results of the first 10 updates in this simulation are summarized in Table 14. In many updates, the estimates were far from the true values. In many instances, the algorithm produced parameter values which were beyond the permissible ranges defined in Table 10. The estimates began to improve somewhat after the initial transient caused by the abrupt change in bottom slope at  $t'=0.35$ . Notice that the estimates do not approximate the mean value of each parameter during the data window loading period as would be desired. Considering that the simulation summarized in Table 14 is without measurement noise and used only a 0.2 ship length data window, we conclude that the WLS parameter estimator can not effectively estimate time-varying ship coefficients. With realistic measurement noise, the data loading window period would have to be at least two ship lengths as shown in Section 4.2. The bottom slope used in the simulation summarized in Table 14; i.e. about one draft in three ship lengths, is not unrealistically high.

Time $t'$ at End of Data Window	H/T at End of Data Window	$f_{22}$	$\hat{f}_{22}$	$f_{23}$	$\hat{f}_{23}$	$f_{25}$	$\hat{f}_{25}$
0.30	1.890	-1.7657	-1.7657	5.7359	5.7359	-0.88074	-0.88074
0.60	1.995	-1.7729	-1.1310	5.6156	3.0221	-0.89644	-0.86090
0.90	2.100	-1.7817	-0.69911*	5.4579	1.3944*	-0.91806	-0.81465
1.20	2.205	-1.7906	-0.75665*	5.2836	1.6099*	-0.94285	-0.81888
1.50	2.310	-1.7995	-0.57249*	5.0878	0.89297*	-0.97138	-0.77627
1.80	2.415	-1.8086	-0.57624*	4.8650	0.91717*	-1.0042	-0.77875
2.10	2.520	-1.8177	-0.28755*	4.6121	-0.25888*	-1.0416	-0.69869
2.40	2.625	-1.8189	-1.7178	4.5941	4.2887	-1.0430	-1.0186
2.70	2.730	-1.8202	-1.8720	4.5761	4.7388	-1.0443	-1.0562
3.00	2.835	-1.8214	-1.6427	4.5580	3.9916	-1.0456	-1.0065
Time $t'$ at End of Data Window	No. of Evaluations of J	$f_{32}$	$\hat{f}_{32}$	$f_{33}$	$\hat{f}_{33}$	$f_{35}$	$\hat{f}_{35}$
0.30	8	0.17199	0.17199	-0.52766	-0.52766	-0.15607	-0.15607
0.60	54	0.17791	0.20063	-0.51662	-0.56307	-0.15947	-0.15080
0.90	39	0.18621	0.25741	-0.50889	-0.77190	-0.16288	-0.14367
1.20	37	0.19593	0.25455	-0.50774	-0.76124	-0.16538	-0.14315
1.50	35	0.20734	0.37040	-0.51336	-1.2150	-0.16686	-0.11556
1.80	75	0.22071	-1.4881*	-0.52597	6.4811*	-0.16723	-0.64536*
2.10	38	0.23622	0.02253	-0.54561	0.28318*	-0.16639	-0.22215
2.40	48	0.23724	0.22875	-0.54653	-0.51562	-0.16642	-0.16841
2.70	44	0.23826	0.23961	-0.54748	-0.54750	-0.16644	-0.16576
3.00	37	0.23929	0.23143	-0.54843	-0.52062	-0.16646	-0.16751

\*estimate outside permissible range in Table 10  
Table 14. Parameter Estimates from WLS Parameter Estimator with Sloping Bottom.

The failure of the WLS parameter estimator to effectively estimate time-varying ship coefficients can be explained by considering the formulation of the algorithm. The true ship response can be considered as the response of a system of time-varying linear differential equations. The coefficients in these equations vary continuously during the time period of the data window. The ship model, on the other hand, is the time-variant system, eq. (75), and we seek the parameter vector  $\underline{p}^*$  which minimizes eq. (77). We expect this parameter estimate to be within the permissible ranges defined in Table 10 and further would hope that the estimates are the mean values of each parameter during the data window loading period. There is no guarantee at all that the constant parameter  $\underline{p}^*$  which minimizes eq. (77) will meet these objectives. The results shown in Table 14 show that even without measurement noise and using a unrealistically short data loading window period the estimates do not meet these objectives.

#### 4.3.2. Time-Varying Disturbances

Even when the ship coefficients are essentially constant during the data window loading period, it is possible that the ship will be subjected to external disturbances which vary over this period. To evaluate the performance of the WLS parameter estimator in this type of situation, we simulated the *Tokyo Maru* under the control of an adaptive path controller using the WLS parameter estimator while sailing past another ship. The bottom was assumed to be constant deep water ( $H/T=\infty$ ). The ship was given zero initial conditions  $\underline{x}=\hat{\underline{x}}=0$ ; the controller and parameter estimator were initialized for parameters at  $H/T=1.89$ . The reference measurement noise from Table 9 was utilized. The ship was simulated for 15 ship lengths. It was simulated to pass another ship as defined by Fig. 3 beam-to-beam at  $t'=7$ . The WLS parameter estimation cycle was 5 ship lengths. The data window length was 2.5 ship lengths; the dither period was 0.5 ship length. With an update period of 5 ship lengths, three update cycles were completed during the simulation. The effects of the passing ship were felt from  $t'=5$  through  $t'=8.5$  so the disturbance was present during the first part of the window loading period for the second update.

A summary of the results of the three update cycles of the simulation is presented in Table 15. During the first update, the parameter estimates, particularly  $f_{23}$  and  $f_{25}$  which are needed by the control loop, are close to the

true values. The disturbance estimates  $N'$  and  $Y'$  are within the noise levels corresponding to these quantities. At the end of this update cycle, the parameters in the Kalman filter ship model were updated. New gain matrices  $C$  and  $K$  were calculated and updated in the system. During the second update period the passing ship disturbance starts to act at  $t'=5.0$  when the ship is running under the command of the updated controller. At  $t'=7.0$ , the disturbances reach their maximum values of about:

$$N' \times 10^5 = -20.4,$$

$$Y' \times 10^5 = 48.0.$$

The second data window was loaded from  $t'=7.45$  to  $t'=9.95$ . During this period, the disturbances declined from their peak values to zero at  $t'=8.50$ . The DUD algorithm search was very slow to converge in the second cycle and the results were bad. Three parameters were outside the permissible ranges defined in Table 10. Since the estimate  $\hat{f}_{23}$  was beyond the permissible range, there was no update. During the third update period, the disturbance was gone. The parameter estimates were good and the controller was updated a second time.

parameter	initial value H/T=1.89	correct value H/T= $\infty$	WLS parameter estimates using 2.5 window length/0.5 dither period		
			update 1	update 2	update 3
$f_{22}$	-1.7657	-1.9515	-1.9446	-0.62936*	-1.9247
$f_{23}$	5.7359	3.1591	3.2178	-1.8532*	3.0732
$f_{25}$	-0.88074	-1.0410	-1.0428	-1.0017	-1.0434
$f_{32}$	0.17199	0.31507	0.33260	0.18843	0.30193
$f_{33}$	-0.52766	-0.63651	-0.53544	-1.7884*	-0.70178
$f_{35}$	-0.15607	-0.16163	-0.16275	-0.17338	-0.16349
$N' \times 10^5$	0.00000	varying	-0.17504	-8.2745	0.11698
$Y' \times 10^5$	0.00000	varying	6.6942	67.778	-6.9666
maximum offset $\eta'$ in cycle			0.0698	0.1394	-0.2154
offset $\eta'$ at end of cycle			0.0698	-0.0953	0.1511
number of evaluations of J			65	253	38
final $J \times 10^2$			0.1022	0.3642	0.1031
update time			5	10	15

\*estimate outside permissible range in Table 10

Table 15. Parameter Estimates from Passing Ship Simulation

We conclude from this simulation that the WLS parameter estimator cannot estimate the parameters when there is a significant time-varying disturbance present during the window loading period. During the second update shown in Table 15 the algorithm tried to approximate the time-varying disturbances by constant quantities  $N'$  and  $Y'$ . In the process, it adjusted the other parameter estimates to minimize the cost  $J$ . Since the relative effect of the disturbances on  $J$  is much larger than the changes due to the system parameters, the final estimates of the system parameters were substantially off. The system protected itself, however, through the check on the validity of the parameters. When the parameter estimates in the second update failed the validity check, no update was made and the controller continued to operate with the gains obtained in the first update. The slow rate of convergence in the second update is also an indication that time-varying disturbances were present during the data window loading period. Thus, the estimation process could be stopped without an update after a prescribed number of evaluations of the cost function as further protection against invalid results.

#### 4.4 Computational Requirements

The WLS parameter estimator would place a fairly large dynamic data storage and computational load on an onboard computer. The parameter estimation and gain update calculations could, however, be performed on a batch basis as time is available. In developing the simulation program used in our work, we made no serious effort to conserve storage locations or CPU time. The program was therefore very expensive to run. The Euler integration step-size used in the various simulations presented above was taken as 0.005 ship lengths or about .24s. For convenience, this was also used as the sample time. In a practical application of a WLS parameter estimator on a ship such as the *Tokyo Maru*, the sample time could easily be extended to perhaps 1s. With a data window of 2.5 ship lengths at the 12 knots used in our simulations, the data window would require 120 locations for each of the four measurements and the rudder angle plus an additional 4 locations for the initial state. The DUD algorithm as used here would require another 4057 storage locations. This would give a total number of dynamic storage

locations of 4661 for the implementation of the WLS parameter estimator. A WLS ship parameter estimator would therefore be feasible but it would place fairly heavy storage and CPU time demands on an onboard computer. If dynamic storage were a limiting factor, alternative search algorithms could be considered. For example, the Nelder and Mead SIMPLEX algorithm was used in some of our earlier work. This algorithm generally required more iterations than DUD to converge but would require only 81 additional dynamic storage locations. This would give a total number of dynamic storage locations of only 685. The reduced storage would be offset by a greater CPU time requirement.



## 5. Minimum Variance Parameter Estimator

In this section, we present the derivation and evaluation of a Minimum Variance Parameter Estimator (MVE) which could be used in the gain update loop of an adaptive ship path control system. This section is based upon Cuong's Ph.D. Dissertation.<sup>49</sup> The MVE is a probabilistic digital filtering technique which can be used to determine a set of parameters of the ship equations of motion. The filter gains are chosen to minimize the trace of the estimate error covariance matrix. It is a recursive filtering technique where the new parameter estimate is formed from the previous estimate plus a proportional constant times the innovation. The filter gains and propagation of the error covariance can be calculated recursively based on previous values and recent measurements.

The derivation of this parameter estimator parallels the derivation of the state estimation Kalman filter. It is more complicated, however, because the measurements are contaminated with both additive and multiplicative noise.<sup>54</sup> This method was first proposed by Kotob and Kaufman<sup>54</sup> for a linear system with measurement noise, time-invariant parameters, and no process disturbances. They used this filter to estimate the system parameters of the F-8 DFBW aircraft. They showed it to be more efficient and effective than an Extended Kalman Filter and a Weighted Least-Squares Parameter estimator in three simulated performance tests. They also proposed an extension for time-varying parameters. Here we extend the MVE approach to accommodate zero-mean process disturbances and time-varying parameters.

### 5.1 Derivation and Development

The Minimum Variance Estimator is a linear parameter identification scheme which has three inherent restrictions. First, the equations of motion must be linear in the estimated parameters  $\underline{p}$ . Second, in order to separate the state estimation problem from the parameter identification problem, it is required that all states be available for measurement. Finally, the algorithm as developed here can accommodate only zero-mean process disturbances.

The ship path control problem must be formulated to satisfy the restrictions of the MVE. First, the linearity requires that there be no coupling

among the estimated parameters. This condition is automatically satisfied if we choose the parameter vector to be:

$$\underline{p} = [f_{22}, f_{23}, f_{25}, f_{32}, f_{33}, f_{35}]^T \quad (78)$$

The separation condition demands that we utilize the 4-state system because we can measure only  $\psi', r', \beta'$ , and  $\eta'$ . The external yawing moment  $N'$  and side force  $Y'$  are not available through direct measurement. Any attempt to use their estimates from the Kalman Filter in parameter estimation will represent a coupling between state and parameter estimators which we want to avoid. Fortunately, the precise knowledge of the disturbances is not necessary in this case since we only need the covariances of the disturbances in the calculation of estimator gain.

As mentioned earlier, the MVE is a recursive filtering technique which makes it well suited to real-time operation. A possible timing sequence for this algorithm is shown in Fig. 27. The parameters are not identified at every measurement sample time. In this case, the parameters are estimated at intervals of  $\ell = 10$ . (The derivation of this algorithm requires that  $\ell > 1$ .) A preliminary study was carried out to compare performance of an estimator with  $\ell = 2$  with that of an estimator with  $\ell = 10$ . Although the higher identification frequency estimator increased the computational load five times, it did not present any clear-cut superiority compared with the lower frequency estimator. For  $\ell = 10$  and the sample time assumed in this work, the estimator would have about 2.4 seconds for each update each cycle. This represents a realistic computational time allotment. Being a recursive technique, the MVE has a very small dynamic data storage requirement. At each recursive step, the algorithm needs two consecutive measurements vectors  $\underline{z}'_{k-1}$  and  $\underline{z}'_k$ , the recent rudder angle  $\delta'_{k-1}$ , the last parameter estimate  $\hat{\underline{p}}_{k-\ell}$  and the last estimate error covariance matrix  $P_{k-\ell}$ . This in-

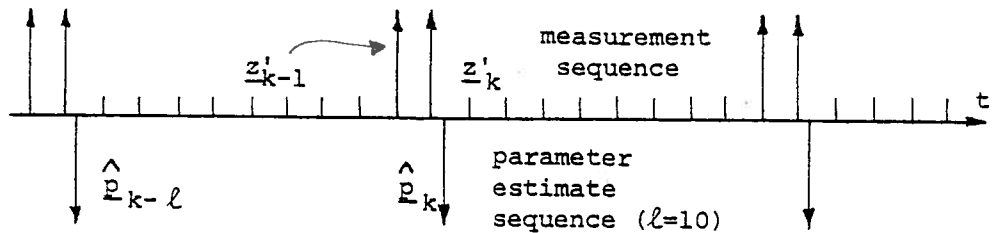


Figure 27. Timing Sequence for Minimum Variance Parameter Estimator

formation requires only 34 storage locations. The entire algorithm could be implemented with less than 100 storage locations.

The Minimum Variance parameter estimation algorithm is derived for a discrete time system of equations. The continuous ship system equations from Section 4.1; i.e.,

$$\dot{\underline{x}} = F\underline{x} + G\delta' + \Gamma\underline{w} , \quad (72)$$

must therefore be transformed into a system of difference equations. These differential equations can be represented by,

$$\frac{\underline{x}_{k+1} - \underline{x}_k}{\Delta t} = F\underline{x}_k + G\delta'_k + \Gamma\underline{w}_k ,$$

or,

$$\underline{x}_{k+1} = [I + \Delta t F]\underline{x}_k + \Delta t G\delta'_k + \Delta t \Gamma \underline{w}_k . \quad (79)$$

If we let  $F' = I + \Delta t F$ ,  $G' = \Delta t G$ , and  $\Gamma' = \Delta t \Gamma$ , the dynamics of the ship can then be represented by the difference equations,

$$\underline{x}_{k+1} = F'\underline{x}_k + G'\delta'_k + \Gamma'\underline{w}_k , \quad (80)$$

or,

$$\begin{bmatrix} \psi' \\ r' \\ \beta' \\ \eta' \end{bmatrix}_{k+1} = \begin{bmatrix} 1 & \Delta t & 0 & 0 \\ 0 & 1 + \Delta t f_{22} & \Delta t f_{23} & 0 \\ 0 & \Delta t f_{32} & 1 + \Delta t f_{33} & 0 \\ \Delta t & 0 & -\Delta t & 1 \end{bmatrix}_k \begin{bmatrix} \psi' \\ r' \\ \beta' \\ \eta' \end{bmatrix}_k + \begin{bmatrix} 0 \\ \Delta t f_{25} \\ \Delta t f_{35} \\ 0 \end{bmatrix} \delta'_k + \begin{bmatrix} 0 & 0 \\ \Delta t \tilde{\gamma}_{21} & \Delta \tilde{\gamma}_{22} \\ \Delta t \tilde{\gamma}_{31} & \Delta \tilde{\gamma}_{32} \\ 0 & 0 \end{bmatrix}_k \begin{bmatrix} N' \\ Y' \end{bmatrix}_k \quad (81)$$

The disturbances are now represented by two discrete stochastic sequences  $\{N'_k\}$  and  $\{Y'_k\}$  which we assume to be independent. The  $\gamma_{ij}$  coefficients are given constant, assumed values  $\tilde{\gamma}_{ij}$  as in Section 4. All four states are assumed to be available for measurement; i.e.,

$$\underline{z}'_k = \underline{x}'_k + \underline{v}'_k , \quad (82)$$

where the noise  $\{\underline{v}'_k\}$  is a Gaussian white sequence with covariance matrix  $R$ .

Following an approach similar to that used in Section 3.3, the parameters can be modeled as Brownian motion processes. In this discrete formulation, the parameter vector, eq. (78), is therefore modeled as,

$$\underline{p}_k = \underline{p}_{k-l} + \underline{n}_{k-l}, \quad (83)$$

where  $\{\underline{n}_k\}$  is a Gaussian white sequence with diffusion coefficient matrix  $\phi$ . The parameter  $l$  defines the frequency of identification. It is required that  $l > 1$  throughout this work. The diffusion coefficients can be selected with ease using the properties of the Brownian motion process as developed in Section 3.3.

In order to estimate the unknown parameters in  $F'$  and  $G'$ , it is necessary to rearrange eq. (81) so that  $\underline{x}_{k+1}$  is expressed explicitly in terms of  $\underline{p}_k$  and  $\underline{s}_k$ , the unknown and known parameter vectors, respectively. In this particular problem, the known parameter vector is simply  $\underline{s}_k = [1]$ . The revised system equations become,

$$\underline{x}_{k+1} = C_k \underline{p}_k + D_k \underline{s}_k + \Gamma' \underline{w}_k,$$

or,

$$\begin{bmatrix} x_{k+1,1} \\ x_{k+1,2} \\ x_{k+1,3} \\ x_{k+1,4} \end{bmatrix} = \begin{bmatrix} 0 & 0 & 0 & 0 & 0 & 0 \\ \Delta t x_{k,2} & \Delta t x_{k,3} & \Delta t \delta'_k & 0 & 0 & 0 \\ 0 & 0 & 0 & \Delta t x_{k,2} & \Delta t x_{k,3} & \Delta t \delta'_k \\ 0 & 0 & 0 & 0 & 0 & 0 \end{bmatrix} \begin{bmatrix} f_{22} \\ f_{23} \\ f_{25} \\ f_{32} \\ f_{33} \\ f_{35} \end{bmatrix}_k$$

$$+ \begin{bmatrix} x_{k,1} + \Delta t x_{k,2} \\ x_{k,2} \\ x_{k,3} \\ x_{k,4} + \Delta t(x_{k,1} - x_{k,3}) \end{bmatrix} + \begin{bmatrix} 0 & 0 \\ \Delta t \tilde{\gamma}_{21} & \Delta t \tilde{\gamma}_{22} \\ \Delta t \tilde{\gamma}_{31} & \Delta t \tilde{\gamma}_{32} \\ 0 & 0 \end{bmatrix} \begin{bmatrix} N'_k \\ Y'_k \end{bmatrix}, \quad (84)$$

where  $\underline{x}_k = [x_{k,1}, x_{k,2}, x_{k,3}, x_{k,4}]^T$ . Note that  $C_k$  and  $D_k$  are matrix functions of  $\underline{x}_k$ . Substituting  $\underline{x}_k = \underline{z}'_k - \underline{v}'_k$  into  $C_k$  and  $D_k$ , these matrices can be decomposed into deterministic and stochastic components which depend on  $\underline{z}'_k$  and  $\underline{v}'_k$  separately; i.e.,

$$C(\underline{x}_k) = C(\underline{z}'_k) - C(\underline{v}'_k) = \hat{C}_k - \check{C}_k,$$

where we define,

$$\hat{C}_k = \Delta t \begin{bmatrix} 0 & 0 & 0 & 0 & 0 & 0 \\ z'_{k,2} & z'_{k,3} & \delta'_k & 0 & 0 & 0 \\ 0 & 0 & 0 & z'_{k,2} & z'_{k,3} & \delta'_k \\ 0 & 0 & 0 & 0 & 0 & 0 \end{bmatrix}, \quad (85)$$

and,

$$\underline{v} = \Delta t \begin{bmatrix} 0 & 0 & 0 & 0 & 0 & 0 \\ v'_{k,2} & v'_{k,3} & 0 & 0 & 0 & 0 \\ 0 & 0 & 0 & v'_{k,2} & v'_{k,3} & 0 \\ 0 & 0 & 0 & 0 & 0 & 0 \end{bmatrix}, \quad (86)$$

and use the same notation for  $\underline{z}'_k$  and  $\underline{v}'_k$  as used for  $\underline{x}_k$  above. Similarly, we can write,

$$D(\underline{x}_k) = D(\underline{z}'_k) - D(\underline{v}'_k) = \hat{D}_k - \underline{v} D_k,$$

where,

$$\hat{D}_k = \begin{bmatrix} z'_{k,1} + \Delta t z'_{k,2} \\ z'_{k,2} \\ z'_{k,3} \\ z'_{k,4} + \Delta t(z'_{k,1} - z'_{k,3}) \end{bmatrix}, \quad (87)$$

and,

$$\underline{v} D_k = \begin{bmatrix} v'_{k,1} + \Delta t v'_{k,2} \\ v'_{k,2} \\ v'_{k,3} \\ v'_{k,4} + \Delta t(v'_{k,1} - v'_{k,3}) \end{bmatrix}. \quad (88)$$

Using these definitions, eq. (84) can be rewritten as,

$$\underline{z}'_{k+1} - \underline{v}'_{k+1} = (\hat{C}_k - \underline{v} C_k) \underline{p}_k + (\hat{D}_k - \underline{v} D_k) \underline{s}_k + \Gamma' \underline{w}_k,$$

or,

$$\underline{z}'_{k+1} - \hat{D}_k \underline{s}_k = \hat{C}_k \underline{p}_k - \underline{v} C_k \underline{p}_k - \underline{v} D_k \underline{s}_k + \underline{v}'_{k+1} + \Gamma' \underline{w}_k. \quad (89)$$

The left-hand side of this equation can be defined as a *pseudo measurement vector*, i.e.,

$$\tilde{\underline{z}}_{k+1} \triangleq \underline{z}'_{k+1} - \hat{D}_k \underline{s}_k. \quad (90)$$

Equation (89) then becomes,

$$\tilde{\underline{z}}_{k+1} = \hat{C}_k \underline{p}_k - \underline{v} C_k \underline{p}_k - \underline{v} D_k \underline{s}_k + \underline{v}'_{k+1} + \Gamma' \underline{w}_k. \quad (91)$$

Notice from its definition that  $\tilde{\underline{z}}_{k+1}$  can be directly calculated from  $\underline{z}'_{k+1}$  and  $\underline{z}'_k$ . Therefore, we can treat the pseudomeasurement as a form of obser-

vation which is corrupted by the multiplicative noise term  $\check{C}_{k-1} p_{k-1}$  and the additive noise terms  $v'_{k-1}$  and  $\check{D}_{k-1} s_{k-1}$ . Shifting the index by one step backward, eq. (91) becomes,

$$\tilde{z}_k = \hat{C}_{k-1} p_{k-1} - \check{C}_{k-1} p_{k-1} - \check{D}_{k-1} s_{k-1} + v'_k + \Gamma' w_{k-1}, \quad (92)$$

where we have used  $p_{k-1} = p_{k-1}$  because eq. (83) approximates the stochastic process  $\{p(t)\}$  by the stochastic step function  $\{p_k\}$ .

We can now define the *innovation vector* at time  $k$  as,

$$\underline{I}_k = \underline{z}'_k - E[\underline{z}'_k | Z_{k-1}], \quad (93)$$

where the second term on the right-hand side is the conditional expectation of  $\underline{z}'_k$  with respect to the whole measurement history; i.e.,

$$Z_{k-1} = \{z'_0, z'_1, z'_2, \dots, z'_{k-1}\}.$$

Noting that,

$$\underline{z}'_k = C_{k-1} p_{k-1} + D_{k-1} s_{k-1} + \Gamma' w_{k-1} + v'_k,$$

then,

$$E[\underline{z}'_k | Z_{k-1}] = \hat{C}_{k-1} \hat{p}_{k-1} + \hat{D}_{k-1} s_{k-1},$$

if the process disturbances  $\{w_k\}$  are restricted to zero-mean processes. Thus

$$\underline{I}_k = \underline{z}'_k - \hat{C}_{k-1} \hat{p}_{k-1} - \hat{D}_{k-1} s_{k-1},$$

or,

$$\underline{I}_k = \tilde{z}_k - \hat{C}_{k-1} \hat{p}_{k-1}. \quad (94)$$

Substituting eq. (92) into eq. (94) yields,

$$\underline{I}_k = \hat{C}_{k-1} p_{k-1} - \hat{C}_{k-1} \hat{p}_{k-1} - \check{C}_{k-1} p_{k-1} - \check{D}_{k-1} s_{k-1} + v'_k + \Gamma' w_{k-1},$$

and if we introduce the error in the parameter estimate; i.e.,

$$\tilde{p}_k \triangleq \hat{p}_k - p_k,$$

this becomes,

$$\underline{I}_k = -\hat{C}_{k-1} \tilde{p}_{k-1} - \check{C}_{k-1} p_{k-1} - \check{D}_{k-1} s_{k-1} + v'_k + \Gamma' w_{k-1}. \quad (95)$$

Using an approach parallel to the Kalman filter derivation, we can assume that the parameter estimate  $\hat{p}_k$  can be given by the following scheme,

$$\hat{p}_k = \hat{p}_{k-l} + K_k \underline{I}_k, \quad (96)$$

where the gain matrix  $K_k$  is to be established. Subtracting eq. (83) from eq. (96), we get,

$$\tilde{p}_k = \tilde{p}_{k-l} + K_k \underline{I}_k - \underline{\eta}_{k-l}. \quad (97)$$

If we multiply eq. (97) by its transpose, we get,

$$\begin{aligned} \tilde{p}_k \tilde{p}_k^T &= \tilde{p}_{k-l} \tilde{p}_{k-l}^T + K_k \underline{I}_k \underline{I}_k^T K_k^T + \underline{\eta}_{k-l} \underline{\eta}_{k-l}^T + \tilde{p}_{k-l} \underline{I}_k^T K_k^T + K_k \underline{I}_k \tilde{p}_{k-l}^T \\ &\quad - \underline{\eta}_{k-l} \underline{I}_k^T K_k^T - K_k \underline{I}_k \underline{\eta}_{k-l}^T - \tilde{p}_{k-l} \underline{\eta}_{k-l}^T - \underline{\eta}_{k-l} \tilde{p}_{k-l}^T. \end{aligned} \quad (98)$$

Defining conditional expectations as follows:

$$E_z[\gamma_k] = E[\gamma_k | Z_{k-1}],$$

$$P_k = E_z[\tilde{p}_k \tilde{p}_k^T],$$

$$\phi = E_z[\underline{\eta}_k \underline{\eta}_k^T],$$

the conditional expectation of both sides of eq. (98) with respect to the whole measurement history  $Z_{k-1}$  yields,

$$\begin{aligned} P_k &= P_{k-l} + K_k E_z[\underline{I}_k \underline{I}_k^T] K_k^T + \phi + E_z[\tilde{p}_{k-l} \underline{I}_k^T] K_k^T + K_k E_z[\underline{I}_k \tilde{p}_{k-l}^T] \\ &\quad - E_z[\underline{\eta}_{k-l} \underline{I}_k^T] K_k^T - K_k E_z[\underline{I}_k \underline{\eta}_{k-l}^T] - E_z[\tilde{p}_{k-l} \underline{\eta}_{k-l}^T] - E_z[\underline{\eta}_{k-l} \tilde{p}_{k-l}^T]. \end{aligned} \quad (99)$$

49

Cuong has evaluated the various conditional expectations on the right-hand side of eq. (99) for the case when  $l > 1$ . If these results are substituted into eq. (99), we arrive at the following expression for the propagation of the estimate error covariance,

$$P_k = P_{k-l} + \phi - K_k \hat{C}_{k-1} P_{k-l} - P_{k-l} \hat{C}_{k-1}^T K_k^T + K_k [\hat{C}_{k-1} P_{k-l} \hat{C}_{k-1}^T + R_{eq, k-1}] K_k^T, \quad (100)$$

where we define an equivalent noise covariance matrix  $R_{eq}$  as,

$$R_{eq, k-1} \triangleq U_{k-1} + B + R + \Gamma' Q_w \Gamma'^T, \quad (101)$$

and where R is the measurement noise covariance matrix and,

$$U_{k-1} \triangleq E_z [\hat{C}_{k-1} \underline{p}_{k-1} \underline{p}_{k-1}^T \hat{C}_{k-1}^T] , \text{ weighted covariance matrix,}$$

$$B \triangleq E_z [\hat{D}_{k-1} \underline{s}_{k-1} \underline{s}_{k-1}^T \hat{D}_{k-1}^T] ,$$

$$Q_w \triangleq E_z [\underline{w}_{k-1} \underline{w}_{k-1}^T] , \text{ disturbance covariance matrix.}$$

Elements of these matrices will be developed further below. Minimization of the trace of the estimate error covariance P, will produce a minimum variance estimate of the parameters  $\underline{p}_k$ . Stationary conditions for the minimization of the trace of  $P_k$  are obtained by setting all derivatives of eq. (100) with respect to the elements of  $K_k$  equal to zero; i.e.,

$$2K_k [\hat{C}_{k-1} \underline{p}_{k-1} \hat{C}_{k-1}^T + R_{eq,k-1}] - 2\underline{p}_{k-1} \hat{C}_{k-1}^T = 0 .$$

Rearranging this, we get the following expression for the filter gain:

$$K_k = \underline{p}_{k-1} \hat{C}_{k-1}^T [\hat{C}_{k-1} \underline{p}_{k-1} \hat{C}_{k-1}^T + R_{eq,k-1}]^{-1} . \quad (102)$$

Using eq. (102) to simplify eq. (100), we arrive at the following form of the error covariance matrix,

$$P_k = \underline{p}_{k-1} + \phi - K_k \hat{C}_{k-1} \underline{p}_{k-1} . \quad (103)$$

If the unknown parameters are time-invariant, the parameter model diffusion coefficient  $\phi$  is zero in this expression.

The B matrix is defined below eq. (101) as a conditional expectation involving the product  $\hat{D}_{k-1} \underline{s}_{k-1}$  which in this case is just  $\hat{D}_{k-1}$  given by eq. (88). Eq. (88) can be used in the definition of B to yield,

$$B = \begin{bmatrix} \sigma_1^2 + (\Delta t)^2 \sigma_2^2 & \Delta t \sigma_2^2 & 0 & 0 \\ \Delta t \sigma_2^2 & \sigma^2 & 0 & 0 \\ 0 & 0 & \sigma_3^2 & -\Delta t \sigma_3^2 \\ 0 & 0 & -\Delta t \sigma_3^2 & \sigma_4^2 + (\Delta t)^2 (\sigma_1^2 + \sigma_3^2) \end{bmatrix} . \quad (104)$$

The matrix B is, therefore, a constant matrix which depends entirely on the



measurement noise variances  $\sigma_i^2$  and sampling time  $\Delta t$ . The disturbance power matrix  $\Gamma' Q_w \Gamma'^T$  can be developed next using the definition of  $Q_w$  below eq. (101). We have assumed that  $\{N'_k\}$  and  $\{Y'_k\}$  are independent stochastic processes with zero means. We can assume that these disturbances can be modeled as white noise sequences. The  $Q_w$  matrix then becomes,

$$Q_w = E_z [w_{k-1} w_{k-1}^T] = \begin{bmatrix} q'_N & 0 \\ \frac{q'_N}{\Delta t} & \frac{q'_Y}{\Delta t} \\ 0 & \frac{q'_Y}{\Delta t} \end{bmatrix},$$

where  $q'_N$  and  $q'_Y$  are the spectral densities of the corresponding continuous white noise disturbances  $N'$  and  $Y'$ . Using this result the disturbance power matrix becomes,

$$\Gamma' Q_w \Gamma'^T = \Delta t \begin{bmatrix} 0 & 0 & 0 & 0 \\ -0 & (q'_N \tilde{\gamma}_{21}^2 + q'_Y \tilde{\gamma}_{22}^2) & (q'_N \tilde{\gamma}_{21} \tilde{\gamma}_{31} + q'_Y \tilde{\gamma}_{22} \tilde{\gamma}_{32}) & 0 \\ 0 & (q'_N \tilde{\gamma}_{21} \tilde{\gamma}_{31} + q'_Y \tilde{\gamma}_{22} \tilde{\gamma}_{32}) & (q'_N \tilde{\gamma}_{31}^2 + q'_Y \tilde{\gamma}_{32}^2) & 0 \\ 0 & 0 & 0 & 0 \end{bmatrix}. \quad (105)$$

The disturbance power matrix is, therefore, also a constant matrix.

The weighted covariance matrix  $U_{k-1}$  is defined below eq. (101) as a conditional expectation involving the vector  $\check{C}_{k-1} p_{k-l}$  which is given by,

$$\check{C}_{k-1} p_{k-l} = \begin{bmatrix} 0 \\ \Delta t (v'_{k-1,2} p_{k-l,1} + v'_{k-1,3} p_{k-l,2}) \\ \Delta t (v'_{k-1,2} p_{k-l,4} + v'_{k-1,3} p_{k-l,5}) \\ 0 \end{bmatrix}.$$

The presence of unknown parameters  $p_{k-l,i}$  within this matrix presents computational difficulties. These parameters are known to be within a known finite range so for the purposes of evaluating  $U_{k-1}$ , it is reasonable to assume that the parameters are Gaussian random variables with known means and variances; i.e.,

$$E[p_i] = \bar{p}_i$$

$$E[(p_i - \bar{p}_i)^2] = \alpha_i^2, \quad i = 1, 2, \dots, 6.$$

The mean  $\bar{p}_i$  can be taken as the mean of the probable range of the parameter and  $\alpha_i$  might be taken as half of the probable range of the parameter. Assuming that the various components of the measurement noise are orthogonal, the weighted covariance matrix then becomes,

$$U_{k-1} = (\Delta t)^2 \begin{bmatrix} 0 & 0 & 0 & 0 \\ 0 & a_{22} & a_{23} & 0 \\ 0 & a_{23} & a_{33} & 0 \\ 0 & 0 & 0 & 0 \end{bmatrix}, \quad (106)$$

where,

$$a_{22} = [\sigma_2^2 (\alpha_1^2 + \bar{p}_1^{-2}) + \sigma_3^2 (\alpha_2^2 + \bar{p}_2^{-2})],$$

$$a_{23} = [\sigma_2^2 \bar{p}_1 \bar{p}_4 + \sigma_3^2 \bar{p}_2 \bar{p}_5],$$

$$a_{33} = [\sigma_2^2 (\alpha_4^2 + \bar{p}_4^{-2}) + \sigma_3^2 (\alpha_5^2 + \bar{p}_5^{-2})].$$

The weighted covariance matrix is, therefore, also a constant matrix  $U_{k-1} = U$  which can be calculated in advance. The entire equivalent measurement noise covariance can therefore, be calculated in advance. If the unknown parameters are time-invariant the variances  $\alpha_i$  are zero in eq. (106). The  $U$  and  $R_{eq}$  matrices might then be updated periodically using the latest estimates  $\hat{p}_i^{eq}$  in lieu of the assumed mean values  $\bar{p}_i$ .

54

Kotob and Kaufman noted that a substantial bias was observed to appear in the parameter estimates using their time-invariant parameters MVE algorithm. These biases were caused by the dependence of the additive and multiplicative noise terms in eq. (91). They developed a "bias reduction" scheme to reduce or eliminate this bias. We will follow their basic approach here to develop an bias error correction procedure for the general time-varying parameters case. Postmultiplying both sides of eq. (102) by the expression inside the bracket, it becomes,

$$K_k \hat{C}_{k-1} P_{k-l} \hat{C}_{k-1}^T + K_k R_{eq,k-1} = P_{k-l} \hat{C}_{k-1}^T.$$

Rearranging this expression, we arrive at:

$$K_k R_{eq,k-1} = [P_{k-l} - K_k \hat{C}_{k-1} P_{k-l}] \hat{C}_{k-1}^T. \quad (107)$$

We can now solve eq. (107) for the term in the brackets, substitute this

result into eq. (103) and then postmultiply by  $\hat{C}_{k-1}^T R_{eq,k-1}^{-1}$  to give,

$$K_k = [P_k - \phi] \hat{C}_{k-1}^T R_{eq,k-1}^{-1} \quad (108)$$

Using eq. (94) and eq. (108) in eq. (96) yields,

$$\hat{p}_k = \hat{p}_{k-l} + [P_k - \phi] \left[ \hat{C}_{k-1}^T R_{eq,k-1}^{-1} \tilde{z}_k - \hat{C}_{k-1}^T R_{eq,k-1}^{-1} \hat{C}_{k-1} \hat{p}_{k-l} \right] \quad (109)$$

In order to reduce the bias in estimating  $p$ , an extra term can be added to the above expression. This term should contain  $P_k - \phi$  and  $\hat{p}_{k-l}$  so we can choose,

$$[P_k - \phi] G_{k-1} \hat{p}_{k-l} \quad ,$$

where the gain matrix  $G_{k-1}$  is yet to be determined. Equation (109) then becomes,

$$\hat{p}_k = \hat{p}_{k-l} + [P_k - \phi] \left[ \hat{C}_{k-1}^T R_{eq,k-1}^{-1} \tilde{z}_k - \hat{C}_{k-1}^T R_{eq,k-1}^{-1} \hat{C}_{k-1} \hat{p}_{k-l} + G_{k-1} \hat{p}_{k-l} \right] \quad (110)$$

We can now take the expectation of both sides of eq. (110) and impose the additional condition that:

$$\lim_{k \rightarrow \infty} E[\hat{p}_k] \cong \lim_{k \rightarrow \infty} E[\hat{p}_{k-l}] \quad .$$

This assumes that after initial transients die out and the estimator is tracking a change in parameters, the parameter change between the parameter estimates is small. If the parameters are time-invariant this condition is exact. With time-varying parameters, the effectiveness of this assumption must be evaluated by simulation. Noting that  $[P_k - \phi]$  is always nonzero, the expectation of quantities inside the bracket in eq. (110) must be zero; i.e.,

$$E \left[ \hat{C}_{k-1}^T R_{eq,k-1}^{-1} \tilde{z}_k - \hat{C}_{k-1}^T R_{eq,k-1}^{-1} \hat{C}_{k-1} \hat{p}_{k-l} + G_{k-1} \hat{p}_{k-l} \right] = 0 \quad (111)$$

Equation (111) can now be used to establish the gain  $G_{k-1}$ . The expression,

$$C_{k-1} = \hat{C}_{k-1} - \check{C}_{k-1} \quad ,$$

can be used in eq. (92) and this can be substituted into eq. (111). Next the expression  $\hat{C}_{k-1} = C_{k-1} + \check{C}_{k-1}$  can be used to eliminate  $\hat{C}_{k-1}$  and its

transpose from the terms involving  $\underline{p}_{k-l}$  and  $\hat{\underline{p}}_{k-l}$ . Utilizing the fact that  $C_{k-1}$  and  $\check{C}_{k-1}$ ,  $\check{D}_{k-1}$  and  $\hat{C}_{k-1}$ ,  $v'_k$  and  $\hat{C}_{k-1}$ ,  $\hat{C}_{k-1}$  and  $w_{k-1}$ , and  $\check{C}_{k-1}$  and  $\hat{\underline{p}}_{k-l}$  are orthogonal, the expectation in eq. (111) then reduces to,

$$E[\underline{p}_{k-l}] \cdot E[C_{k-1}^T R_{eq,k-1}^{-1} C_{k-1}] = E[\hat{\underline{p}}_{k-l}] \cdot \{E[C_{k-1}^T R_{eq,k-1}^{-1} C_{k-1}] + E[\check{C}_{k-1}^T R_{eq,k-1}^{-1} \check{C}_{k-1}] - G_{k-1}\}.$$

For an estimate to be unbiased, it is necessary that,

$$\lim_{k \rightarrow \infty} E[\hat{\underline{p}}_{k-l}] = \lim_{k \rightarrow \infty} E[\underline{p}_{k-l}]$$

which will be true if,

$$G_{k-1} = E[\check{C}_{k-1}^T R_{eq,k-1}^{-1} \check{C}_{k-1}] \quad (112)$$

This term is a generalized measure of noise and disturbance power.

The matrix  $G_{k-1}$  can be developed explicitly for this problem using the expressions for  $\check{C}_{k-1}$  and  $R_{eq,k-1}^{-1} = [t_{ij}]$ . The expectation term by term yields,

$$G_{k-1} = (\Delta t)^2 \begin{bmatrix} t_{22}\sigma_2^2 & 0 & 0 & t_{23}\sigma_2^2 & 0 & 0 \\ 0 & t_{22}\sigma_3^2 & 0 & 0 & t_{23}\sigma_3^2 & 0 \\ 0 & 0 & 0 & 0 & 0 & 0 \\ t_{32}\sigma_2^2 & 0 & 0 & t_{33}\sigma_2^2 & 0 & 0 \\ 0 & t_{32}\sigma_3^2 & 0 & 0 & t_{33}\sigma_3^2 & 0 \\ 0 & 0 & 0 & 0 & 0 & 0 \end{bmatrix} \quad (113)$$

The matrix  $G_{k-1}$  is thus a constant matrix which can be calculated in advance knowing the elements of  $R_{eq}^{-1}$  and the measurement noise variances  $\sigma_i^2$ .

The final parameter estimate equation is obtained by adding the bias error correction term to eq. (96) giving,

$$\hat{\underline{p}}_k = \hat{\underline{p}}_{k-l} + K_k \underline{I}_k + [P_k - \Phi] G_{k-1} \hat{\underline{p}}_{k-l} \quad (114)$$

This completes the derivation of the Minimum Variance parameter estimator.

The complete algorithm is summarized below.

## 5.2 Algorithm Summary

Since the derivation of the Minimum Variance parameter estimator has been long and complicated, it is useful at this point to present an algorithmic summary of a typical recursive cycle. The equivalent noise spectral density  $R_{eq}$  can be calculated and stored in advance using eqs. (101), (104), (105), and (106). If the unknown parameters are time-invariant, the variances  $\alpha_i$  are zero in eq. (106). Likewise, the generalized noise power matrix  $G_{k-1}$  can be calculated and stored in advance using eq. (113). Let  $k$  be the value of the time index at the next parameter estimate. The parameter estimation cycle is provided with the previous parameter estimate  $\hat{p}_{k-l}$  and the current estimate error covariance matrix  $P_{k-l}$  which were stored from the previous cycle. The recursive estimation cycle proceeds as follows:

1. At  $t'=k-1$ , a set of measurements  $\underline{z}'_{k-1}$  and the rudder angle  $\delta'_{k-1}$  are sampled;

2. These data are used to calculate  $\hat{C}_{k-1}$  and  $\hat{D}_{k-1}$  using eqs. (85) and (87), respectively;

3. At  $t=k$ , a second set of measurements  $\underline{z}'_k$  is sampled;

4. The pseudomeasurement vector  $\tilde{\underline{z}}_k$  is calculated from its definition;

$$\tilde{\underline{z}}_k = \underline{z}'_k - \hat{D}_{k-1} \underline{s}_{k-1}; \quad (90)$$

5. The filter gain matrix  $K_k$  is calculated using eq. (102); i.e.,

$$K_k = P_{k-l} \hat{C}_{k-1}^T [\hat{C}_{k-1} P_{k-l} \hat{C}_{k-1}^T + R_{eq}]^{-1}; \quad (102)$$

6. The updated error covariance matrix  $P_k$  is calculated using eq. (103); i.e.,

$$P_k = P_{k-l} + \Phi - K_k \hat{C}_{k-1} P_{k-l}, \quad (103)$$

where diffusion coefficient matrix  $\Phi$  is zero in the time-invariant parameters case;

7. The innovation vector is calculated using eq. (94); i.e.,

$$\underline{I}_k = \tilde{\underline{z}}_k - \hat{C}_{k-1} \hat{p}_{k-l}; \quad (94)$$

8. The new parameter estimate  $\hat{p}_k$  is calculated using eq. (114); i.e.,

$$\hat{p}_k = \hat{p}_{k-l} + K_k \underline{I}_k + (P_k - \Phi) G_{k-1} \hat{p}_{k-l}, \quad (114)$$

and again  $\phi$  is zero in the time-invariant parameters case.

This completes one parameter estimation cycle of the Minimum Variance Parameter estimator. Compared with the the Weighted Least-Squares method, it is very elegant and powerful. It is potentially capable of estimating time-varying parameters in real time. Recalling that the computational requirement for the WLS method was quite large, the load imposed by the MVE would be small by comparison. As developed here, the MVE cannot, however, accommodate bias disturbances which can be handled by the WLS approach. We evaluate the performance by the MVE in the next section.

### 5.3. Time-Invariant Parameters Performance

In this section, we evaluate the performance of the MVE ship parameter estimator when the parameters are time-invariant. Simulations were conducted with and without zero mean disturbances. From Section 4.2 we would expect that for the MVE to be effective with disturbances, the system must be persistently excited by an input signal which is independent of the disturbances. Simulations have confirmed this requirement. We therefore continue here to use alternate periods of (1) open-loop control using a dither signal with the controller turned off and (2) closed-loop control using the controller. We continue to use a square wave input rudder command  $\delta'_c$  of 0.5 radian amplitude and 0.5 ship length period for the dither signal in this section.

The need to excite the system can be illustrated further by considering equations (85), (87), (90), (94), (102), and (114). The MVE parameter estimator eq. (114) shows that the estimator improves its estimates primarily through the term  $K_k I_k$ . The estimator gain eq. (102) shows that the gain  $K_k$  is directly proportional to  $\hat{C}_{k-1}^T$ . The innovation vector  $I_k$  is shown in eqs. (94) and (90) to depend upon  $\hat{C}_{k-1}$ ,  $\hat{D}_{k-1}$ , and the measurements  $z'_k$ . From their definitions in eqs. (85) and (87),  $\hat{C}_{k-1}$  and  $\hat{D}_{k-1}$ , respectively, depend directly upon the measurements  $z'_{k-1}$ . As a result, if the ship is closely controlled along the desired path so that the measurements tend to zero both  $K_k$  and  $I_k$  tend to zero and the estimator cannot improve its estimates. For the parameter estimator to be effective, the measurements must contain non-zero states which are large compared to the measurement noise levels. Periods of open-loop control using a dither signal are therefore needed.

To complete the design of the MVE parameter estimator for time-invariant parameters for the *Tokyo Maru* a number of design choices must be made to define the equivalent noise covariance matrix  $R_{eq}$  defined by eq. (101), define the generalized noise power matrix  $G$  defined by eq. (113), and to initialize the error covariance matrix  $P_k$  which is propagated in accordance with eq. (103). Recall that with time-invariant parameters, the diffusion coefficient matrix  $\Phi$  associated with the parameter model eq. (83) is zero. We used the reference measurement noise level from Table 9 to establish the measurement noise covariances needed to calculate the matrices  $R, B, U$ , and  $G$ . The discrete measurement noise standard deviations  $\sigma'_j$  in Table 9 were squared to form the noise variances  $\sigma_j^2$  needed in the diagonal measurement noise covariance matrix  $R$ , the  $B$  matrix defined in eq. (104), the weighted covariance matrix  $U_{k-1} = U$  defined in eq. (106), and the generalized noise power matrix  $G_{k-1} = G$  defined in eq. (113). With time-invariant parameters, the variances  $\alpha_i$  in the weighted covariance matrix  $U$  are zero. To complete the definition of  $U$ , we chose the "mean" values of the parameters needed in eq. (106) to be near the midpoint of the permissible ranges of the parameters defined in Table 10; i.e.,

$$\begin{aligned} f_{22}: \bar{p}_1 &= -1.750, \\ f_{23}: \bar{p}_2 &= 6.250, \\ f_{32}: \bar{p}_4 &= 0.175, \\ f_{33}: \bar{p}_5 &= -0.785. \end{aligned}$$

To complete the definition of the equivalent noise covariance matrix  $R_{eq}$ , the disturbance power matrix  $\Gamma' Q_w \Gamma'^T$  defined by eq. (105) must be established. The  $\tilde{\gamma}_{ij}$  coefficients in eq. (105) were assigned assumed, constant values for  $H/T=1.89$  from Table 2. The remaining required quantities are  $q'_N$  and  $q'_Y$ , the assumed spectral densities for the continuous white noise disturbances  $N'$  and  $Y'$ , respectively. The choice of these quantities has a major impact on the effectiveness of the MVE parameter estimator. If these quantities are selected to be too large, the disturbance power matrix tends to be "large" and the equivalent noise covariance matrix  $R_{eq}$  also tends to be "large". It can be seen in eq. (108) that the parameter estimator gain matrix  $K_k$  is proportional to  $R_{eq}^{-1}$ . If  $R_{eq}$  is "large", the estimator gain matrix is "small" and the parameter estimator will change its estimates very slowly. This is true even when the innovation vector  $I_k$  contains significant

information . The speed of response of the parameter estimator is, therefore, directly controlled by the choice of  $q'_N$  and  $q'_Y$ . We initially assumed these quantities to have the values given in eqs. (67) and (68), respectively. These values are slightly larger than the spectral densities derived from the passing ship disturbance shown in Fig. 3 and given in eqs. (53) and (54). Cuong<sup>49</sup> has shown that using these values the MVE ship parameter estimator response is far too slow to be of any value in an adaptive ship path control application. We therefore chose these quantities to be based upon approximately 0.1 times the passing ship disturbance shown in Fig. 3, i.e.,

$$q'_N = 2.00 \times 10^{-10}, \quad (115)$$

$$q'_Y = 1.25 \times 10^{-9}. \quad (116)$$

These assumed disturbance spectral densities produce a MVE parameter estimator which responds at an acceptable rate. These assumptions complete the definition of the disturbance power matrix and therefore also the equivalent noise covariance matrix  $R_{eq}$  and the generalized noise power matrix  $G$ .

The final quantity to be selected is the initial estimate error covariance  $P_0$ . This assumption is not critical to the effectiveness of the MVE estimator. It affects the initial rate of convergence somewhat but its effect dies out fairly fast. To obtain an initial  $P_0$  it is reasonable to assume that all initial parameter errors are independent Gaussian random variables with zero means. Hence, all off-diagonal elements of  $P_0$  are zero. The diagonal terms, which are the error variances, remain to be chosen. They can be selected based upon the expected range of each parameter. In the simulations, we used the following initial estimate error covariance which assumes that the error covariances are the square of the difference between the respective parameter values at  $H/T=\infty$  and  $H/T=1.89$  shown in Table 2.

$$P_0 = \begin{bmatrix} .03452 & 0 & 0 & 0 & 0 & 0 \\ 0 & 6.640 & 0 & 0 & 0 & 0 \\ 0 & 0 & .02568 & 0 & 0 & 0 \\ 0 & 0 & 0 & .02047 & 0 & 0 \\ 0 & 0 & 0 & 0 & .01185 & 0 \\ 0 & 0 & 0 & 0 & 0 & .00003091 \end{bmatrix}. \quad (117)$$



To evaluate the performance of the MVE parameter estimator with time-invariant parameters, we simulated the *Tokyo Maru* under the control of an adaptive path controller using the MVE parameter estimator defined above. The simulations presented here represent a type of startup condition for the controller. The Kalman filter ship model, path controller gains C, Kalman filter gains K, and the parameter estimator were all initialized for deep water ship characteristics. The ship and Kalman filter were given zero initial conditions  $\underline{x} = \hat{\underline{x}} = 0$ . At the start of the simulations, the depth-to-draft ratio was abruptly changed to  $H/T=1.89$  or viewed differently the adaptive path controller was turned on with the depth-to-draft ratio  $H/T=1.89$ . The depth-to-draft ratio was then held constant to produce time-invariant ship characteristics. The reference measurement noise from Table 9 was utilized. The dither signal was a square wave rudder command  $\delta'_c$  of 0.5 radian amplitude and 0.5 ship length period. The dither signal was utilized only for the first 2.5 ship lengths of each 6.25 ship lengths. This corresponds to an  $LW=2.5$  ship length data window and  $LU=6.25$  ship length update period for the WLS parameter estimator. The MVE parameter estimator frequency was chosen as 10 sample times or about 2.4 seconds.

The *Tokyo Maru* was simulated under the control of the MVE parameter estimator adaptive path controller while being subject to (1) no external disturbances, (2) the passing ship disturbance shown in Fig. 3 with the ship passing beam-to-beam at  $t'=7$ , and (3) fairly small, continuous white noise disturbances with  $\sigma_N = 2 \times 10^{-5}$  and  $\sigma_Y = 5 \times 10^{-5}$ . The simulation conditions and the approximate ship path for the simulation with the passing ship disturbance are summarized in Fig. 28. The ship reached a maximum offset of  $\eta' = 0.01738$  or about one beam at  $t'=3.8$ . Since the simulation represents a startup transient for the controller, the effect of the subsequent dither periods is generally less. The parameter estimate results for the first 10 ship lengths of the three simulations are summarized in Table 16. Since there are 200 estimates for each parameter in the 10 ship lengths, Table 16 presents only the initial guess and the minimum, maximum, mean, and final values of the estimates for each parameter. The RMS error in each estimate,

$$\text{i.e., } \text{RMS}(p_i) = \left[ \sum_{k=1}^{200} (\hat{p}_i - p_i)_k^2 \right]^{1/2}, \quad (118)$$

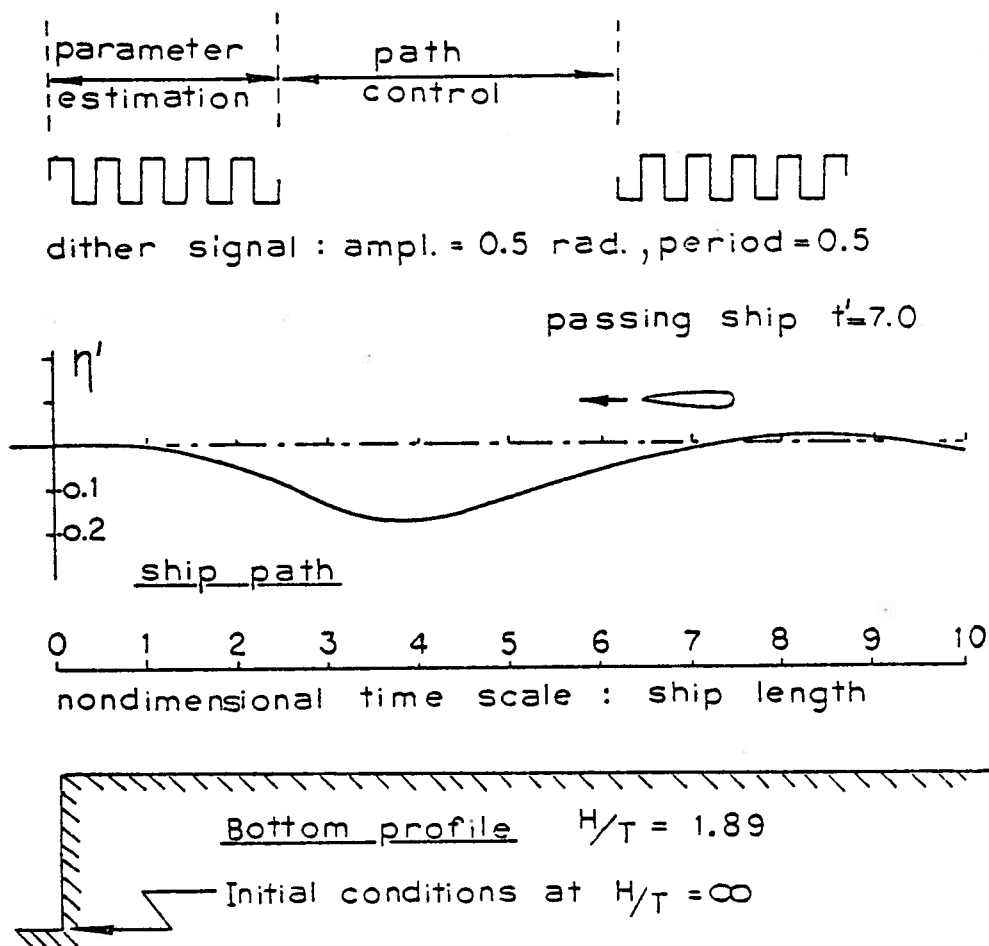


Figure 28. Simulation Conditions and Approximate Ship Path -- Constant Bottom Example.

is also shown as a basis for evaluating the effect of the disturbances on the estimator performance. Recall that the control loop requires effective estimates of only the two most sensitive parameters  $f_{23}$  and  $f_{25}$ . The estimates of these two parameters and  $f_{32}$  are good. The other parameter estimates are slow and generally ineffective. The disturbances do not significantly degrade the performance and in some cases the estimates improve due to the additional ship motion.

Disturbance	Parameter	f <sub>22</sub>	f <sub>23</sub>	f <sub>25</sub>	f <sub>32</sub>	f <sub>33</sub>	f <sub>35</sub>
None	minimum	-1.9685	2.5224	-1.0450	0.16221	-0.66132	-0.16216
	mean	-1.9168	5.2404	-0.89901	0.24378	-0.64976	-0.16170
	maximum	-1.8915	5.8801	-0.84419	0.32722	-0.63519	-0.16147
	final value	-1.9325	5.4886	-0.90793	0.18731	-0.66132	-0.16166
	RMS error	2.1461	12.8305	0.43412	1.17259	1.72961	0.07969
Passing Ship	minimum	-1.9685	2.5227	-1.0450	0.16221	-0.66388	-0.16216
	mean	-1.9127	5.2805	-0.89817	0.23505	-0.65139	-0.16172
	maximum	-1.8915	5.9401	-0.84419	0.32722	-0.63519	-0.16148
	final value	-1.9020	5.9162	-0.92556	0.19843	-0.66257	-0.16176
	RMS error	2.0896	12.8430	0.43989	1.11448	1.75410	-0.07987
White Noise $\sigma_N = 2.0E-5$ $\sigma_Y = 5.0E-5$	minimum	-1.9702	2.4553	-1.04570	0.16100	-0.66127	-0.16216
	mean	-1.9175	5.2358	-0.90398	0.24352	-0.64974	-0.16170
	maximum	-1.8918	5.8529	-0.85260	0.32655	-0.63527	-0.16147
	final value	-1.9320	5.5226	-0.91279	0.18707	-0.66127	-0.16166
	RMS error	2.1570	13.5175	0.47312	1.16839	1.72925	0.07966
Initial value	H/T= $\infty$	-1.9515	3.1591	-1.04100	0.31507	-0.63651	-0.16163
Actual value	H/T=1.89	-1.7657	5.7359	-0.88074	0.17199	-0.52766	-0.15607

Table 16. Parameter Estimates from MVE Parameter Estimator -- Constant Bottom Examples

The estimates of parameters  $f_{23}$ ,  $f_{25}$ , and  $f_{32}$  from the simulation with the passing ship disturbance are shown in Figures 29, 30, and 31, respectively. The true values are shown by constant, dashed lines. The simulation results with the reference noise level from Table 9 are shown as the solid lines. The simulation results with 0.001 times of the reference noise level are sketched approximately as long, broken dashed lines in Figures 29, 30, and 31 for reference. The estimate of parameter  $f_{23}$  shown in Fig. 29 converges to near its true value in about 3 ship lengths. The estimate of parameter  $f_{25}$  shown in Fig. 30 converges to near its true value in only one ship length. After about  $t'=4$  it varies about the low noise estimate which appears to have a small bias error. These estimates appear to be more than acceptable for use by an adaptive path controller. The estimate of parameter  $f_{32}$  shown in Fig. 31 is slower to converge and shows two jumps at the end of each dither period. The effect of the dither signal can be seen fairly clearly in the low noise estimates in Figures 29, 30, and 31. The additional ship motion produced by the passing ship disturbance which acts from about  $6 < t' < 8$  appears to help the parameter estimates move closer to their true value.

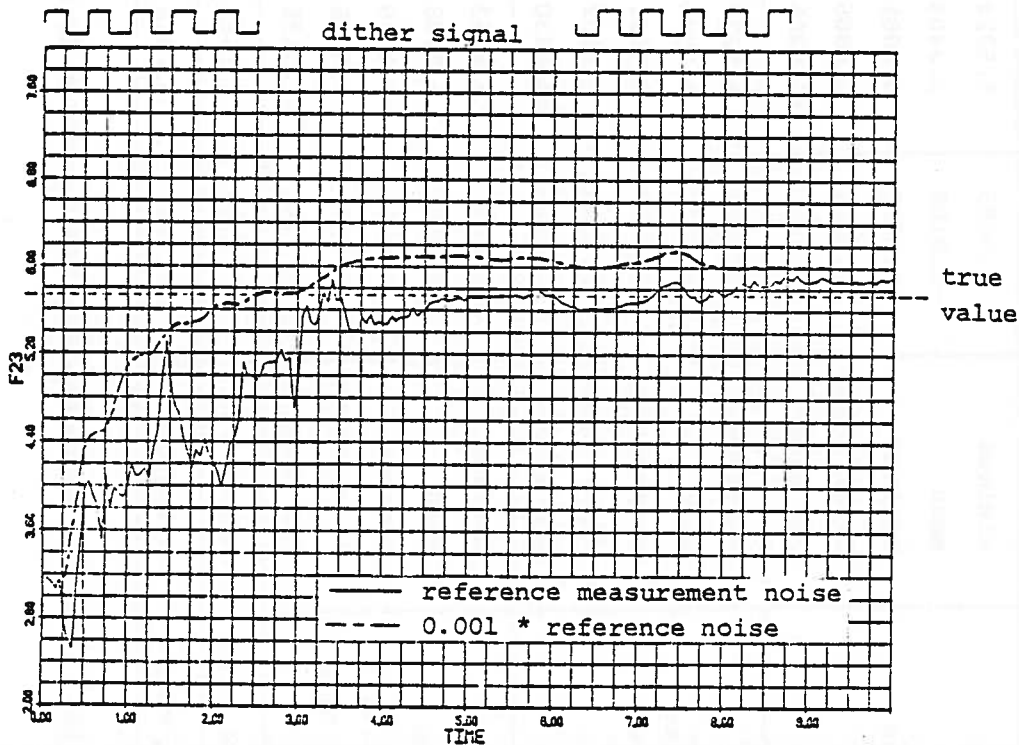


Figure 29. Estimate of  $f_{23}$  by MVE Parameter Estimator - Constant Bottom with Passing Ship Example.

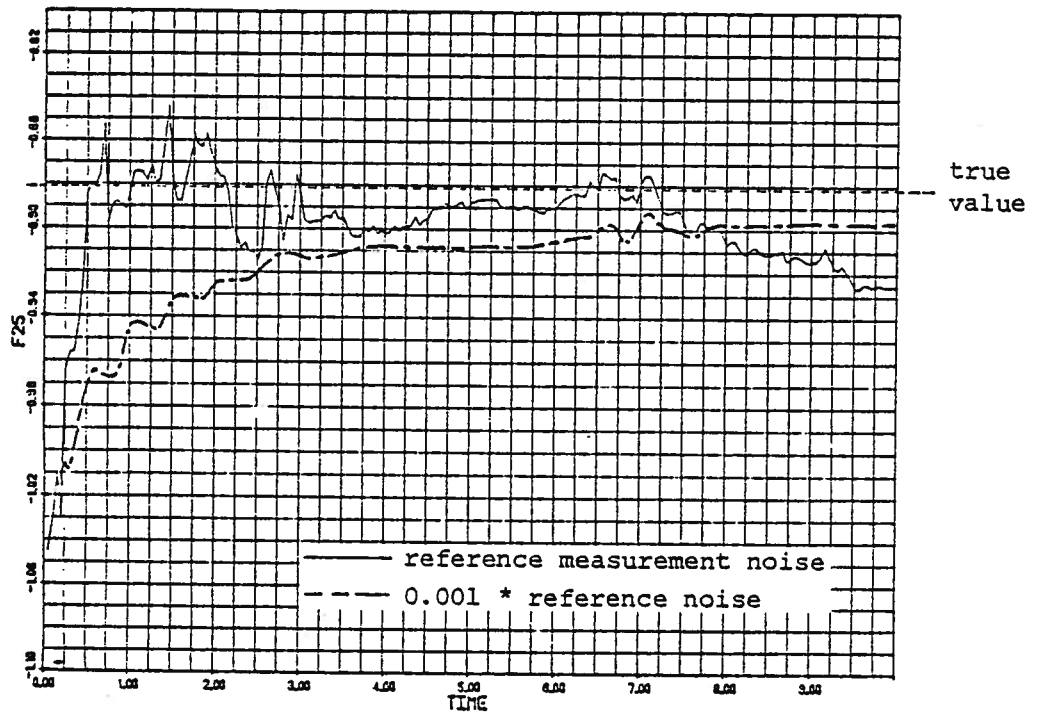


Figure 30. Estimate of  $f_{25}$  by MVE Parameter Estimator — Constant Bottom with Passing Ship Example

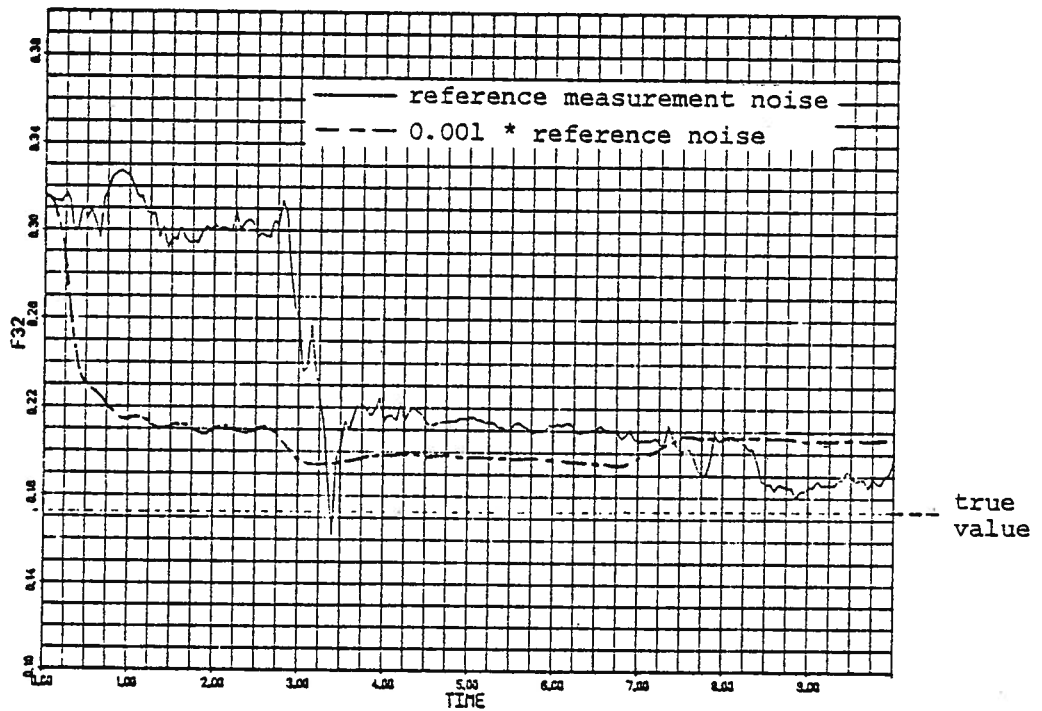


Figure 31. Estimate of  $f_{32}$  by MVE Parameter Estimator — Constant Bottom with Passing Ship Example

The simulations presented in this section show that the MVE ship parameter estimator can be effective in estimating the two parameters needed by an adaptive path controller,  $f_{23}$  and  $f_{25}$ , when these parameters are constant. This performance does not deteriorate with significant zero-mean disturbances. The performance with time-varying parameters is evaluated in the next section.

#### 5.4 Time-Varying Parameters Performance

In this section, we evaluate the performance of the MVE ship parameter estimator when the parameters are time-varying. As in Section 4.3.1, we use the water depth as the independent variable which defines the changing parameters. We simulated the *Tokyo Maru* under the control of an adaptive path controller using the MVE parameter estimator while sailing over two bottom configurations. The controller design was identical to that developed for the *Tokyo Maru* in the previous section except that it was extended to accommodate the time-varying parameters. Two design changes are necessary. First, non-zero parameter variances  $\alpha_i^2$  must be utilized when the weighted covariance matrix  $U_{k-1}$  is calculated in accordance with eq. (106). We utilized the square of half the range of each parameter in Table 2 as the assumed variance. Finally, a non-zero, diffusion coefficient matrix  $\Phi$  must be included in the parameter estimator equation, eq. (114), and in the estimate error covariance propagation equation, eq. (103). This diagonal matrix is composed of the diffusion coefficients for the Brownian motion processes which were used to model the parameters in eq. (83).

The diffusion coefficient matrix  $\Phi$  can be established using the properties of the Brownian motion process developed in Section 3.3. There we showed that the power spectral density of the continuous white noise in the Brownian motion models for the disturbances could be approximated by,

$$q = \Delta t S^2, \quad (66)$$

where  $S$  is the expected rate or change or slope of the continuous process being modeled and  $\Delta t$  is the integration stepsize used in the Euler integration discretization of the continuous process. Now in the derivation of the MVE parameter estimator we modeled the parameters by discrete models, eq. (83),

where the discrete time step is the estimation period or  $\ell\Delta t$ . The element  $\phi_{ii}$  if the diffusion coefficient matrix is the variance of the white sequence  $\eta_i$  in eq. (83) so using eq. (64) we have,

$$\phi_{ii} = \bar{q} = \frac{q}{\ell\Delta t} ,$$

or using eq. (66),

$$\phi_{ii} = \frac{S^2}{\ell} . \tag{119}$$

We approximated the  $\phi_{ii}$  using eq. (119) by assuming that the parameters could diffuse the difference between their values at  $H/T = 1.89$  and  $H/T = \infty$  in Table 2 in the nondimensional time of about 1.5 ship length. The results are summarized in Table 17 for  $\ell = 10$ .

	difference	slope S	$\phi_{ii}$
$p_1 = f_{22}$	0.196	0.1314	$1.726 \times 10^{-3}$
$p_2 = f_{23}$	2.716	1.8218	$3.319 \times 10^{-1}$
$p_3 = f_{25}$	0.169	0.1133	$1.284 \times 10^{-3}$
$p_4 = f_{32}$	0.151	0.1011	$1.023 \times 10^{-3}$
$p_5 = f_{33}$	0.114	0.0770	$5.924 \times 10^{-4}$
$p_6 = f_{35}$	0.00586	0.00393	$1.545 \times 10^{-6}$

Table 17. Design Diffusion Coefficient Matrix

We simulated the *Tokyo Maru* under control of an adaptive path controller using the MVE parameter estimator while sailing over a rising bottom and a falling bottom. These simulations were performed (1) without external disturbances and (2) with the passing ship disturbance shown in Fig. 3 with the ship passing beam-to-beam at  $t'=7$ . The simulations were begun with zero initial conditions; i.e.,  $\underline{x} = \hat{\underline{x}} = 0$ . The dither signal had a 0.5 rad. magnitude and 0.5 ship length period. The periods of open-loop control using the dither signal and closed-loop control using the path controller were the same as used in the previous section. The reference measurement noise level from Table 9 was utilized. For these simulations, the initial parameter estimates were assumed known and, therefore, the initial estimate error covariance  $P_0$  was taken as zero in lieu of using eq. (117).

For the rising bottom example, the bottom was assumed to start at a depth-to-draft ratio  $H/T=10.0$  (corresponding to deep water characteristics). The depth then decreased one draft per ship length until  $t'=8.7$  at which point it reached  $H/T=1.30$  and remained constant. This corresponds to an upward bottom slope of 5.5 percent. The simulation conditions and the approximate ship path for the simulation with the passing ship disturbance are summarized in Fig. 32. Even though the bottom was smoothly rising, the parameter profiles were more irregular. The resulting parameter histories show two regimes; i.e.,

- a slowly varying region from  $H/T=10.0$  to 2.5;
- a quickly varying region from  $H/T=2.5$  to 1.30.

This example was, therefore, very demanding of the MVE parameter estimator. If the MVE is designed for the more slowly varying parameters, the estimator is too slow to track the variation in the second phase. On the other hand, if it is designed for large parameter variations, its estimates are more sensitive to noise and random disturbances. The MVE design studied here, as reflected in the parameter variation slopes used to obtain  $\phi$  in Table 17 is more appropriate for the parameter variation in the first phase of this example.

In the rising bottom example, the parameter estimator was initialized with the correct deep water parameters. The simulation was performed for 15 ship lengths. The results of the first 10 ship lengths of the two rising bottom simulations are summarized in the upper half of Table 18. The table shows the initial value, final value, and true final value for each parameter. The RMS error in each estimate calculated using eq. (118) is also shown as a basis for evaluating the effect of the passing ship disturbance on the estimator performance. Again recall that the control loop requires effective estimates of only the two most sensitive parameters,  $f_{23}$  and  $f_{25}$ . In general, the presence of the passing ship disturbance helps to improve the accuracy of most parameter estimates. This behavior can be explained by noting that the ships pass beam-to-beam at  $t'=7$  so the disturbance, occurring mostly during the duration of the second dither signal, increased the ship motion. It, therefore, increased the information content in the innovation vector. It can be seen from these simulations that  $f_{33}$  and  $f_{35}$  are insensitive parameters; their estimates tend to stay near the initial values. Parameter  $f_{22}$  is also fairly insensitive. Parameter  $f_{32}$  is slightly



more sensitive. Parameters  $f_{23}$  and  $f_{25}$  are the most identifiable parameters as expected from the sensitivity study.

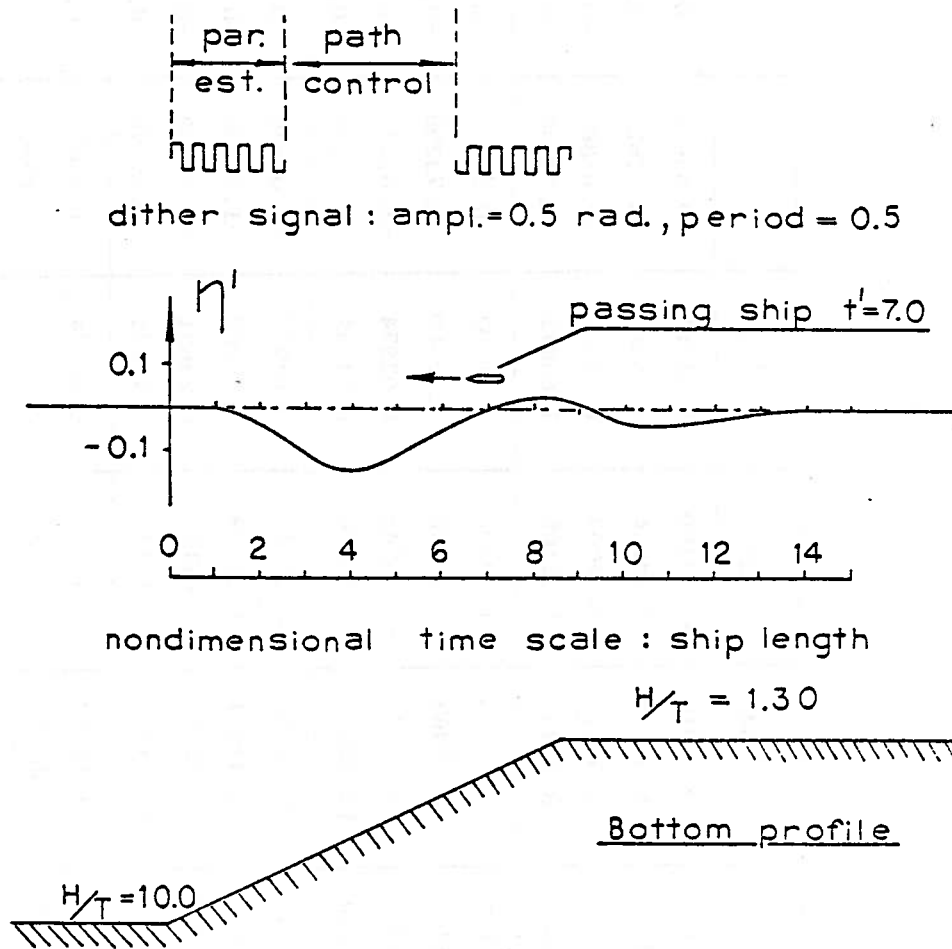


Figure 32. Simulation Conditions and Approximate Ship Path - Rising Bottom Example.

The paths of the parameter estimates  $\hat{f}_{23}$  and  $\hat{f}_{25}$  produced by the MVE parameter estimator are shown as solid lines in Fig. 33 and Fig. 34, respectively, for all 15 ship lengths of the rising bottom simulation with the passing ship disturbance. The correct parameter values are shown as dashed lines on these figures. The assumed parameter variation slopes used to establish the diffusion coefficient matrix  $\phi$  in Table 17 are also shown as solid straight lines for reference. The very rapid parameter change at about  $t'=7.5$  is clearly seen. The estimates  $\hat{f}_{23}$  and  $\hat{f}_{25}$  follow the true parameter values fairly well during the slowly varying portion of the simulation. The

case	parameter	f <sub>22</sub>	f <sub>23</sub>	f <sub>25</sub>	f <sub>32</sub>	f <sub>33</sub>	f <sub>35</sub>
rising bottom no distur- bance	initial value	-1.95150	3.15910	-1.04100	0.31507	-0.63651	-0.16163
	final value	-1.77147	5.84033	-0.64216	-0.09307	-0.68624	-0.15873
	true final value	-1.6508	9.3157	-0.55543	0.02974	-1.0388	-0.09995
	RMS error	1.81469	28.7273	1.82165	1.65872	2.22200	0.32896
rising bottom passing ship at t'=7.0	initial value	-1.95150	3.15910	-1.04100	0.31507	-0.63651	-0.16163
	final value	-1.58717	8.69467	-0.76530	0.12960	-0.73299	-0.16184
	true final value	-1.6508	9.3157	-0.55543	0.02974	-1.0388	-0.09995
	RMS error	1.17260	16.4762	2.17846	0.74142	2.01359	0.34036
falling bottom no distur- bance	initial value	-1.65080	9.31570	-0.55543	0.02974	-1.03880	-0.09995
	final value	-1.88917	3.32914	-1.02159	0.11867	-1.06758	-0.10161
	true final value	-1.8177	4.6112	-1.0416	0.23621	-0.54560	-0.16639
	RMS error	0.62136	19.7372	1.45374	1.41425	6.48168	0.72539
falling bottom passing ship at t'=7.0	initial value	-1.65080	9.31570	0.55543	0.02974	-1.03880	-0.09995
	final value	-1.66669	3.80705	-1.15704	-0.00316	-1.10983	-0.10208
	true final value	-1.8177	4.6112	-1.0416	0.23621	-0.54560	-0.16639
	RMS error	1.06749	20.9118	1.69383	2.17843	6.65488	0.72552

Table 18. Parameter Estimates from MVE Parameter Estimator -- Sloping Bottom Examples

effect of the passing ship disturbance can be seen beginning at about  $t'=5.5$ . The passing ship disturbance ends at  $t'=8.5$ . The MVE is unable to track the rapid rise in parameters beginning at  $t'=7.5$ . It is able to follow  $f_{23}$  well up to the very rapid change which begins at about  $t'=8.5$ . At this point, the parameter change becomes more rapid and the dither signal is stopped.

The estimate of  $f_{25}$  is worse in this period. The parameter estimator was still reacting to the passing ship when the rapid change in the parameters began to occur and required a few ship lengths to catch up. Recall that the ship is very stable at the final water depth and, therefore, the dither signal excites less ship motion and the parameters are specially hard to estimate in the final condition.

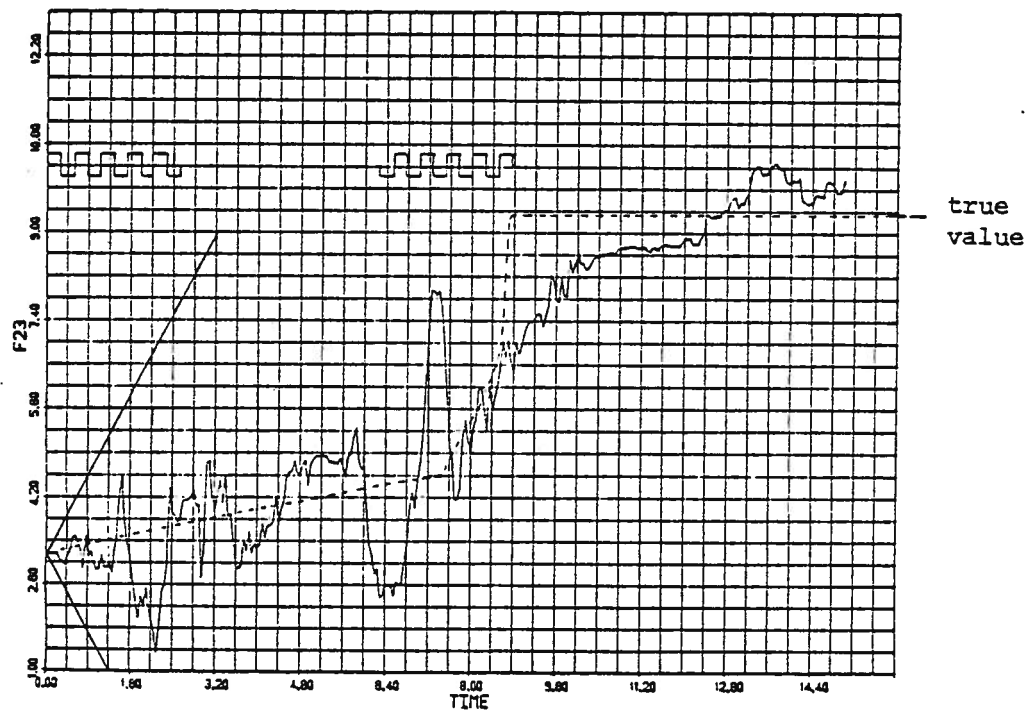


Figure 33. Estimate of  $f_{23}$  by MVE Parameter Estimator -- Rising Bottom with Passing Ship Example

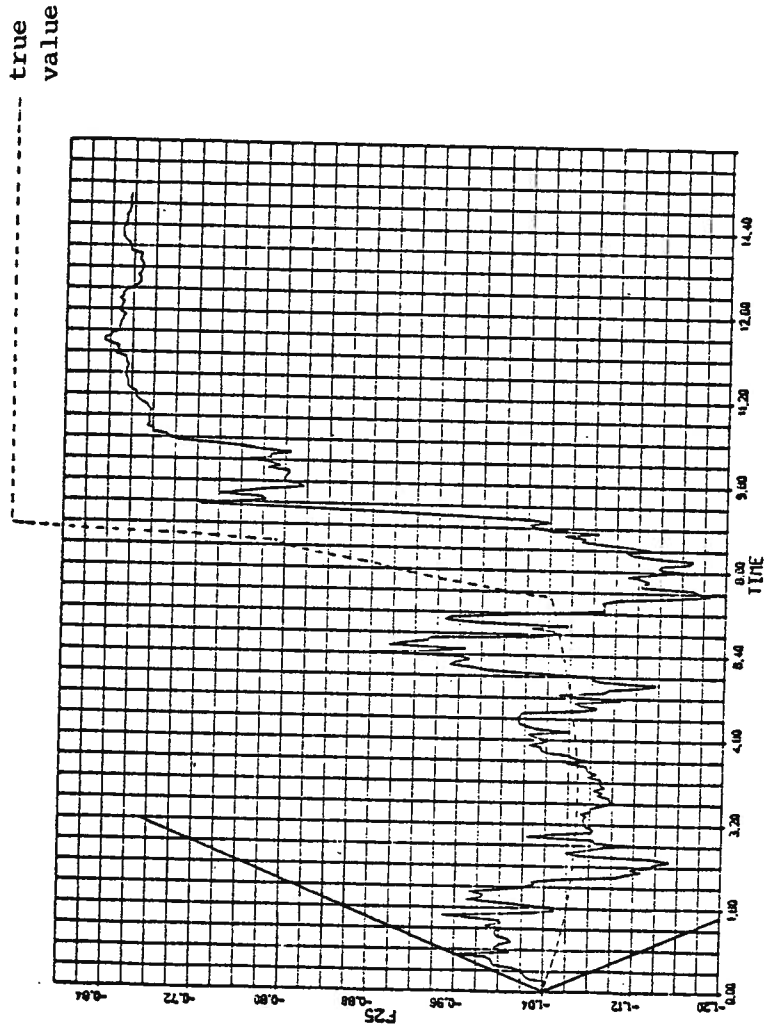


Figure 34. Estimate of  $f_{25}$  by MVE Parameter Estimator -- Rising Bottom with Passing Ship Example

For the falling bottom example, the water depth was assumed to increase such that the depth-to-draft ratio increased linearly from  $H/T=1.30$  to  $H/T=2.50$  in 10 ship lengths. This is a much less drastic change in ship characteristics than present in the rising bottom example. The simulation conditions and the approximate ship path for the simulation with the passing ship disturbance are summarized in Fig. 35. The parameter estimator was initialized with the correct ship parameters and the simulation was run for the 10 ship lengths. The results of the two falling bottom simulations are summarized in the lower half of Table 18. In general, the RMS errors are greater with the passing ship disturbance. The final value of the

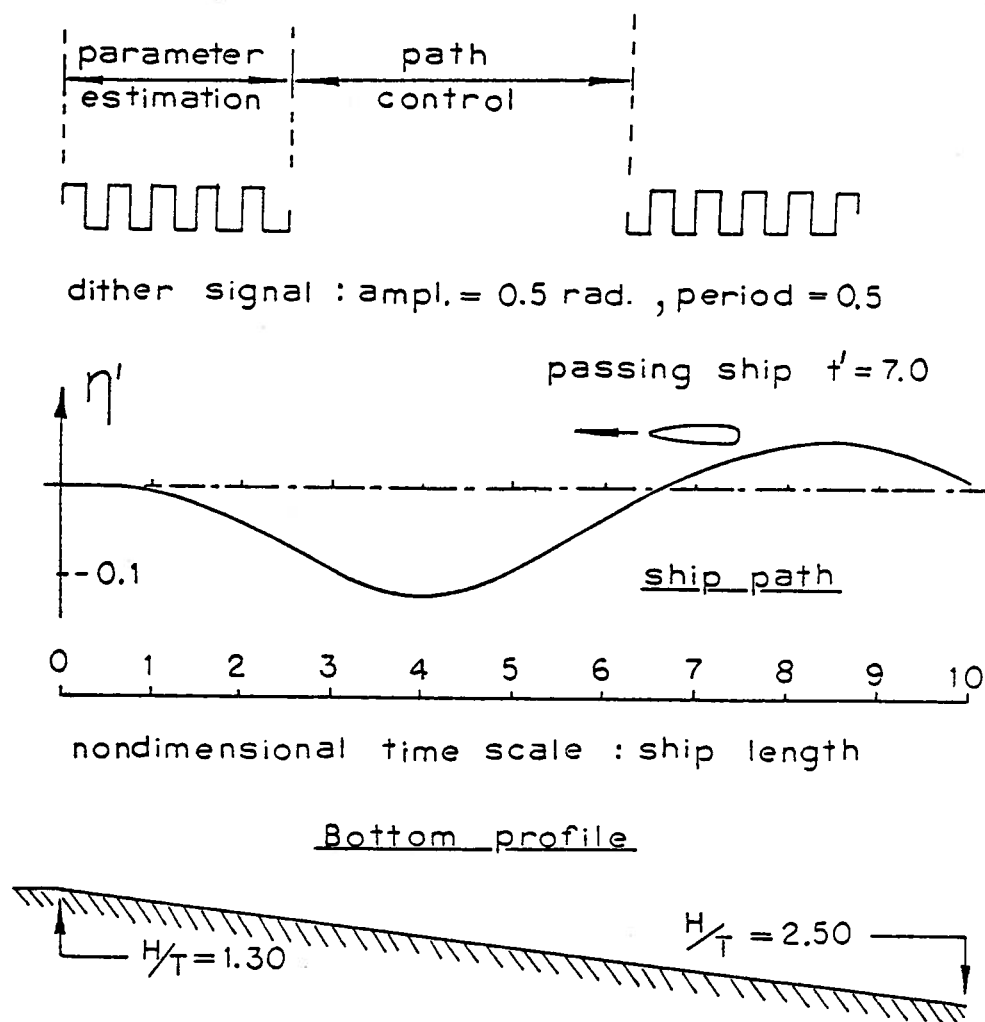


Figure 35. Simulation Conditions and Approximate Ship Path - Falling Bottom Example.

estimate of  $f_{23}$  is, however, closer the true value with the disturbance. As observed before,  $f_{23}$  and  $f_{25}$  are the needed and the most identifiable parameters.

The paths of the parameter estimates  $\hat{f}_{23}$  and  $\hat{f}_{25}$  produced by the MVE parameter estimator are shown as solid lines in Fig. 36 and Fig. 37, respectively, for the falling bottom simulation with the passing ship disturbance. The correct parameter values are shown as dashed lines on these figures. The assumed parameter variation slopes used to establish the diffusion coefficient matrix  $\Phi$  in Table 17 are also shown as solid straight lines for reference. The estimates follow the true values fairly well. At the beginning of the simulation, the ship is so stable that the dither signal has little effect. As a result there is little ship motion and very little information available to the parameter estimator. The estimates tend to stay near their initial values. After about 2 to 3 ship lengths, the ship motion becomes large enough that the estimates  $\hat{f}_{23}$  and  $\hat{f}_{25}$  start tracking the true parameter profiles. The effect of the passing ship disturbance, which is felt from  $5.5 < t' < 8.5$ , is clearly evident.

In general, these simulations show that a MVE ship parameter estimator can be effective in estimating time-varying ship characteristics. The diffusion coefficient matrix  $\Phi$  selection must, however, be consistent with the rate of parameter change encountered by the ship. The estimator performance degrades during periods of external disturbances, but in the long run the ship motion caused by the disturbances can result in improved parameter estimates.

### 5.5 Parameter Identifiability and Measurement Importance

A useful by-product of the study of the MVE ship parameter estimator is a rough indication of the identifiability of each parameter and the relative importance of the various measurements to the estimation of the unknown parameters. The numerical values of the optimal parameter gain matrix  $K_k$  give this information. The principal part of the parameter estimating scheme is given by eq. (96); i.e.,

$$\hat{p}_k = \hat{p}_{k-l} + K_k \cdot I_k, \quad (96)$$

where,

$$I_k = [i_1, i_2, i_3, i_4]_k^T.$$

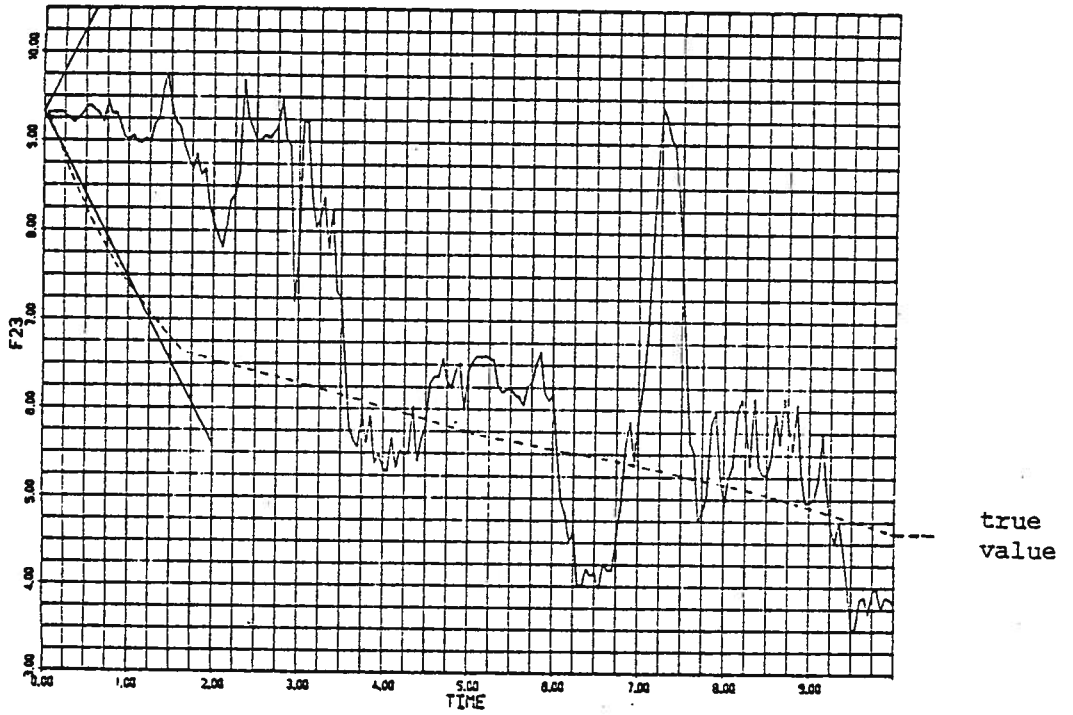


Figure 36. Estimate of  $f_{23}$  by MVE Parameter Estimator -- Falling Bottom with Passing Ship Example

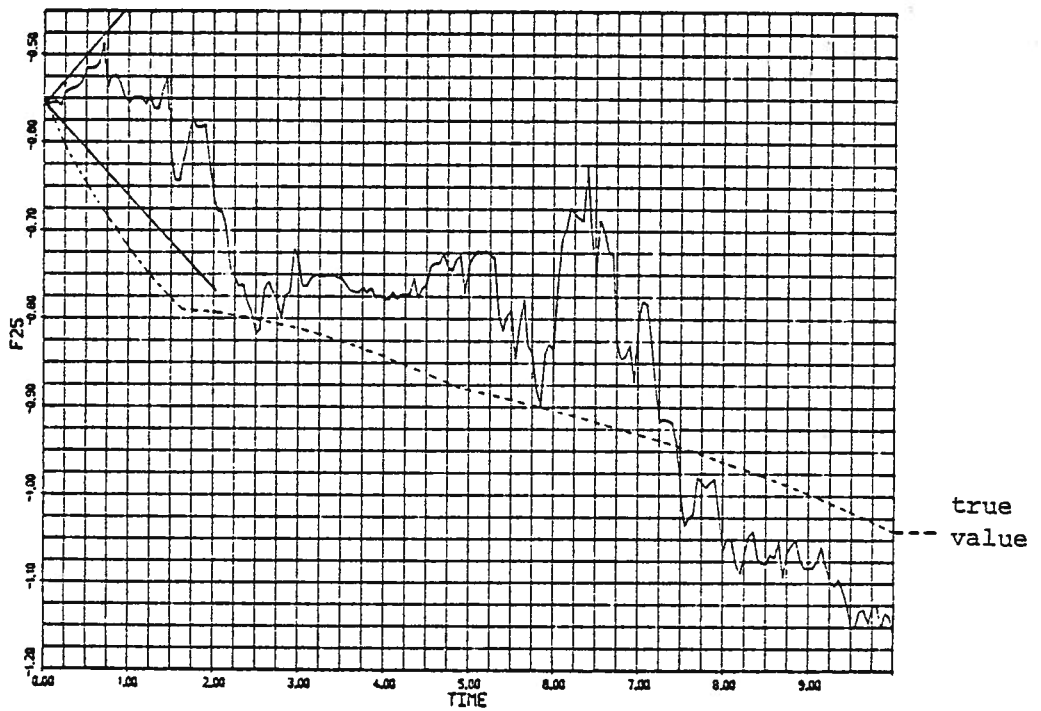


Figure 37. Estimate of  $f_{25}$  by MVE Parameter Estimator -- Falling Bottom with Passing Ship Example

At any time step  $k'$ , each element  $k_{mn}$  of the gain matrix  $K_k$ , represents an optimal weighting factor on the innovation  $i_n$  with respect to the parameter estimate  $\hat{p}_m$ . Furthermore, the innovation  $i_1$  relates to the measurement of  $\psi'$ ,  $i_2$  to the measurement of  $r'$ ,  $i_3$  to the measurement of  $\beta'$ , and  $i_4$  to the measurement of  $\eta'$ . Hence, the magnitudes of  $k_{m1}$ ,  $k_{m2}$ ,  $k_{m3}$ , and  $k_{m4}$  give an indication of the relative importance of these four measurements to the estimate  $p_m$ .

Since the various measurements have different magnitude scales, the most revealing form of  $K_k$ , is to "normalize" each column of the gain matrix by the existing magnitude of the associated measurement. Likewise, since each unknown parameter has its own magnitude scale we can further "normalize" each row of the gain matrix by the existing magnitude of the associated parameter. A typical result is shown in Table 19. In general, the magnitudes of the rows of Table 19 compared vertically indicates the relative identifiability of each of the associated parameters. Coefficients  $f_{32}$ ,  $f_{23}$ , and  $f_{25}$  are therefore the most easily estimated parameters. The magnitudes in the columns of Table 19 compared horizontally indicate the relative importance of each of the associated measurements to the estimation of each of the associated parameters. This indicates roughly where money should be spent to improve the accuracy of the measurements. Since the control loop needs effective estimates of only  $f_{23}$  and  $f_{25}$ , an adaptive ship path controller requires high accuracy and low noise in the measurements of  $r'$  and  $\beta'$ . It is encouraging to note that the measurement of the lateral offset  $\eta'$  is relatively unimportant in this context.

associated parameter	associated measurement			
	$\psi'$	$r'$	$\beta'$	$\eta'$
$p_1 = f_{22}$	0.679	126.075	17.638	0.080
$p_2 = f_{23}$	9.838	1959.550	274.758	1.247
$p_3 = f_{25}$	4.627	921.259	131.861	0.600
$p_4 = f_{32}$	0.118	24.397	6119.733	29.948
$p_5 = f_{33}$	0.006	1.213	303.119	1.486
$p_6 = f_{35}$	0.001	0.032	63.715	0.311

Table 19. Typical "Normalized" Optimal Parameter Estimator Gain Matrix



## 5.6 Computational Requirements

As noted in the introduction to this section, the MVE ship parameter estimator would require less than 100 dynamic storage locations in the implementation. The estimator would also require very little CPU time. The subroutine used in our work was not specifically designed to minimize operations but was timed to require an average of only 12 milliseconds per parameter estimation cycle on the University of Michigan Amdahl 470/V7 computer. This very small load on an onboard computer would make the MVE parameter estimator an attractive candidate for the parameter estimator component of an adaptive ship path control system. In such arrangement, the MVE algorithm could be readily implemented in a time-sharing mode on a main and general-purpose computer onboard a ship. It could also be programmed in a dedicated minicomputer. This arrangement might be advantageous when an independent and/or portable real-time parameter estimator is desired.

## 6. Conclusions

The research summarized in this report has concerned the development and evaluation of techniques which could be utilized in adaptive path control systems for surface ships in restricted waters. In this section, we will review some of the principal conclusions and observations based on this work.

- The example vessel used in this work was the *Tokyo Maru*, a 290m tanker, for which sufficient hydrodynamic data was available from the work of Fujino. The characteristics of this ship undergo significant changes depending upon its operating condition and environment. This type of ship is either course stable or unstable depending upon water depth. Further, the longest time constant of this ship is very long compared with the time scale of importance in path control in restricted waters. The example vessel, therefore, reflects many of the most challenging requirements for an adaptive ship path control system.

- The basic concept of a two-loop adaptive path control system as shown in Fig. 1 appears feasible. The inner or control loop performs the state estimation and control generation continuously as a high priority task. The outer or gain update loop can estimate the system parameters and calculate updated controller and state estimator gains at a slower rate or batchwise. In general, the two loops must function independently.

- A very effective control loop can be designed using random-walk, or more correctly Brownian motion, models for the unknown yawing moment and lateral force disturbances which act upon the ship. These controllers are effective with short-term, zero mean disturbances and with more slowly varying, non-zero mean disturbances. These controllers have the integral control property necessary to accommodate bias disturbances without a constant offset from the desired track. Severe disturbance transients such as the entrance to the SNAME H-10 Panel ABC harbor (Fig. 5) would, however, require some type of supplemental, anticipatory controller. The random walk disturbance model control loops can be designed as statistical steady-state Kalman-Bucy filters and optimal state feedback controllers using Potter's algorithm provided a small numerical parameter is included in the design equations to eliminate otherwise zero eigenvalues. Their performance is not severely degraded

by changing ship coefficients. When designed using incorrect ship parameters, the transient performance of the control loop is degraded but its mean steady-state condition is unchanged.

- The Brownian motion process is a useful concept which can be used as a model for disturbances or processes which are constant (bias) or contain unknown, slowly varying components. The properties of the Brownian motion process can be used to provide a practical design approach for establishing the diffusion coefficient of these models. Instead of estimating both a correlation time and a variance to establish the power spectral density for a first-order shaping filter model, the single modeling parameter, the diffusion coefficient, can be estimated by eq. (65), (66) or (119) using the expected rate of change or diffusion of the process being modeled.

- An adaptive ship path controller needs effective on-line estimation of only two of the ten coefficients of the state equations which change with ship conditions and environment. Adapting for changes in only  $f_{23}$  and  $f_{25}$  allows the recovery of the most important part of the transient response performance which is lost by not using exact ship characteristics. Coefficient  $f_{23}$  is the coefficient of  $\beta'$  and  $f_{25}$  is the coefficient of  $\delta'$ , respectively, in the  $\dot{r}$ -equation. This fact should be recognized in the evaluation of the effectiveness of parameter estimators intended for use in an adaptive ship path controller.

- The degree of difficulty of the adaptive control problem depends on the signal-to-noise ratio. For a surface ship, this ratio is very small when viewed on the time scale of importance in restricted waters. As a result, the adaptive path control of surface ships becomes a very difficult problem.

- An open-loop dither signal is required for successful ship parameter estimation. During the estimation period, the control command has to be independent of disturbances and the ship motion has to be maintained at a sufficient amplitude. Adaptive path control can be achieved by performing the parameter estimation phase and the path control phase alternately. This creates a major tradeoff in design since the improved path following performance achieved by having improved estimates of the ship coefficients must offset the loss in path following performance needed to allow the estimation of the characteristics. A "robust" ship path controller design which is

insensitive to errors in the ship equations of motion would likely prove superior.

- The degree of estimation accuracy depends strongly on the relative levels of information and noise (process and measurement). The amount of information can be increased significantly by lengthening the dither signal period and the length of time it operates. This, however, is restricted due to the path control consideration. It was found that the square wave rudder command dither signal of 0.5 rad. amplitude and 0.5 ship length period operating for over 2 ship lengths gave reasonable results with the linear ship model studied here. Design tradeoff studies would be needed to establish the best tradeoff. In general, we used low levels of measurement noise but demanded more parameter estimate accuracy than really needed by the control loop.

- In very shallow water, the *Tokyo Maru* becomes so stable that the dither signal used here has a relatively small effect on the ship. As a result, there is less ship motion and a lower signal-to-noise ratio. Parameter estimation is, therefore, much more difficult in this situation.

- The parameters  $f_{22}$ ,  $f_{23}$ , and  $f_{25}$  in the  $\dot{r}$ -equation are closely associated with the shorter time constant of the ship which is about 0.4 ship length. The parameters  $f_{32}$ ,  $f_{33}$ , and  $f_{35}$  in the  $\dot{\beta}$ -equation are more closely associated with the longest time constant of the ship which is about 10 ship lengths. As a result, a short (0.5 ship length) dither period can be effective in exciting the ship in the shorter time constant mode allowing reasonable estimation of parameters  $f_{22}$ ,  $f_{23}$ , and  $f_{25}$ . The short dither period is much less effective in exciting the longer time constant mode making estimation of parameters  $f_{32}$ ,  $f_{33}$ , and  $f_{35}$  less effective. Longer dither periods which would be needed to more effectively excite the longer time constant mode would be incompatible with a path control objective. Fortunately, the control loop only really needs accurate estimates of  $f_{23}$  and  $f_{25}$  to achieve an effective level of adaptation.

- The choice of parameters and the availability of measurements are of critical importance to the Weighted Least-Squares (WLS) parameter estimator. Given a data window length acceptable in a path control application, the WLS cost function is extremely sensitive to the measurement noise and the system

model. We found that all states must be measured and that all six of the coefficients  $f_{ij}$  in the open-loop dynamics matrix and control distribution matrix in eq. (71) must be included in the parameter vector. Since the cost function is much more sensitive to external disturbances than ship coefficient changes, the unknown external disturbances must also be included in the parameter vector. The WLS algorithm could not effectively handle linear combinations of parameters or products of parameters so it was necessary to assign the coefficients  $\gamma_{ij}$  in the disturbance distribution matrix assumed, constant values.

- With a 2.5 ship length data window, the WLS parameter estimator can effectively estimate the coefficients  $f_{ij}$  when the ship characteristics and external disturbances are essentially constant during the data window loading period. A major design tradeoff exists in the choice of the data window length. With a longer data window and therefore a longer period of open-loop dither signal operation, the information content of the data base is increased allowing better parameter estimate accuracy but the ship is given a greater offset from the desired path. The improved control loop performance achieved with more accurate parameter estimates must offset the loss in path following performance caused by the dither signal. With our experience to date, we must conclude that the performance of the control loop designs studied in Chapter 3 are good enough with incorrect ship parameters that we would not expect an adaptive capability using a WLS parameter estimator to prove worthwhile.

- The WLS parameter estimator could not effectively estimate the coefficients  $f_{ij}$  when either the ship characteristics or the external disturbances changed significantly during the data window loading period. In path control situations in restricted waters, both would be expected to change during at 2.5 ship length data window. The WLS parameter estimator studied here could, however, be of value in other applications where constant ship characteristics and disturbances could be reasonably expected.

- The Doesn't Use Derivatives (DUD) algorithm used here to minimize the WLS cost function proved to be an effective and efficient search algorithm. In retrospect, however, it requires an excessive amount of dynamic data storage. Thus, it is more suited for an off-line application than for an

on-line application as part of an adaptive system. It did prove effective for the purposes of this study. Alternative search algorithms with more reasonable storage requirements are available for on-line applications. The stopping conditions of any algorithm would have to be tuned to be compatible with the noise content of the data window.

- The Minimum Variance (MVE) parameter estimator can effectively estimate the time-varying coefficients  $f_{23}$  and  $f_{25}$  needed by an adaptive path controller when the ship is not subjected to bias disturbances. The algorithm is recursive and highly efficient both in dynamic data storage and computation time. The MVE algorithm requires ship motion to obtain information about the ship's characteristics so the tradeoff associated with the use of an open-loop dither signal exists with this method as it would with any alternative. The method does show promise and is worthy of further consideration for possible use in an adaptive ship path controller.

- The principal weakness of the MVE parameter estimator as studied here is its inability to accommodate bias disturbances. We initially tried to incorporate consideration of these disturbances by modeling the disturbances as Brownian motion processes in lieu of white noise in the derivation of the disturbance power matrix  $\Gamma'Q_w\Gamma'^T$ . This approach produces a disturbance power matrix which grows continuously with time and this causes the parameter estimator gain matrix to asymptotically approach zero. An alternative, which could not be included in the scope of this study, would be to follow an approach parallel to that used with the WLS parameter estimator. The unknown yawing moment and lateral force disturbances could be included as additional parameters; i.e. the parameter vector could be chosen as eq. (74) in lieu of eq. (78) and the entire MVE algorithm could be rederived. We now feel this should be successful and intend to study this possibility in future work.

- The three major design choices in the development of the MVE algorithm are the estimation frequency  $\ell$ , the assumed disturbance power spectral densities  $q_N^i$  and  $q_Y^i$ , and the parameter model diffusion coefficient matrix  $\phi$ . The derivation requires that the parameters not be estimated more frequently than every two sample times; i.e.  $\ell \geq 2$ . Our work showed little value in estimating the ship parameters more often than  $\ell=10$  or about 2.4 seconds. An even longer estimation period would probably be acceptable. The choice of

the disturbance power spectral densities directly affects the speed of response of the MVE algorithm. If they are assumed too high, the MVE parameter estimator is much too slow to respond to be of value in a path control application. The parameter model diffusion coefficient matrix  $\Phi$  can be selected using the properties of the Brownian motion process as reflected in eq. (119). This choice also affects the response rate of the MVE parameter estimator. If the  $\phi_{ii}$  are too small, the estimator cannot follow more rapidly changing parameters. If the  $\phi_{ii}$  are too large, the estimator will be overly sensitive to noise and disturbances.

- The consideration of the optimal MVE estimator gain matrices shows that in order to effectively estimate the coefficients  $f_{23}$  and  $f_{25}$  needed by an adaptive path controller the measurements  $r$  and  $\beta$  are the most important. The lateral offset from the path, which would be the most difficult to measure accurately, is of much less importance. The development of an adaptive ship controller should, therefore, emphasize accuracy and noise reduction in the measurements of yaw rate and lateral velocity.

## 7. References

1. Parsons, M.G., and Cuong, H.T., "Optimal Stochastic Path Control of Surface Ships in Shallow Water," The University of Michigan, Department of Naval Architecture and Marine Engineering, Report No. 189/ONR Report ONR-CR215-249-2F, 15 Aug. 1977.
2. Honderd, G., and Winkelman, J.E.W., "An Adaptive Autopilot for Ships," Third Ship Control Systems Symposium, Paper III B-1, Bath, U.K., September 1972.
3. van Amerongen, J., and Udink ten Cate, A.J., "Adaptive Autopilots for Ships," Proceedings of the IFAC/IFIP Symposium on Ship Operation Automation, Oslo, Norway, July, 1973.
4. van Amerongen, J., and Verstoep, N.D.L., "Improvement of Ship Maneuverability by means of Automation," Proceedings of the Symposium on Ship Handling, Wageningen, The Netherlands, Nov., 1973, pp. XV, 1-XV, 16.
5. van Amerongen, J., Neiuwenhuis, H.C., and Udink ten Cate, A.J., "Gradient Based Model Reference Adaptive Autopilot for Ships," Paper 58.1 IFAC 6th Triennial World Congress, Boston/Cambridge, Mass., August 24-30, 1975.
6. van Amerongen, J., and van Nauta Lemke, H.R., "Optimum Steering of Ships with an Adaptive Autopilot," Proceedings of the Fifth Ship Control Systems Symposium, Vol. 3, Annapolis, MD., Oct. 30-Nov. 3, 1978, pp. J2 4-1 to J2 4-15.
7. Oldenburg, J., "Experiment with a New Adaptive Autopilot Intended to Control Turns as Well as for Straight Course Steering," Proceedings of the Fourth Ship Control Symposium, Den Helder, The Netherlands, Oct. 27-31, 1975, pp. 1-152 to 1-160.
8. Ware, J.R., Fields, A.S., and Bozzi, P.J., "Design Procedures for a Surface Ship Steering Control System," Proceedings of the Fifth Ship Control System Symposium, Vol. 1, Annapolis, MD., Oct. 30-Nov. 3, 1978, pp. C 4-1 to C 4-22.
9. Sugimoto, A., and Kojima, T., "A New Autopilot System with Condition Adaptivity," Proceedings of the Fifth Ship Control Systems Symposium, Vol. 4, Annapolis, MD., Oct. 30-Nov. 3, 1978, pp. P 1-1 to P 1-13.
10. Åström, K.J., "Some Aspects of the Control of Large Tankers," presented at the International Symposium on New Trends in Systems Analysis, Rocquencourt, France, Déc. 13-17, 1976.
11. Åström, K.J., and Wittenmark, B., "On Self-Tuning Regulators," Automatica, Vol. 9, 1973, pp. 185-199.
12. Åström, K.J., Ljung, L., Borisson, U., and Wittenmark, B., "Theory and Applications of Adaptive Regulators Based on Recursive Parameter Estimation," Paper 50.1, IFAC 6th Triennial World Congress, Boston/Cambridge, Mass., August 24-30, 1975.




13. Källström, C.G., Åström, K.J., Thoreu, N.E., Eriksson, J., and Sten, L., "Adaptive Autopilots for Steering of Large Tankers," Lund Institute of Technology, Technical Report TFRT 3145, 1977.
14. Volta, E., and Tiano, A., "The Route Keeping and Steering Control of Merchant Ships," Proceedings of the International Symposium on Cybernetics in Modern Science and Society, Zagreb, 1975, pp. 73-77.
15. Brink, A.W., Baas, G.E., Tiano, A., and Volta, E., "Adaptive Automatic Course-Keeping Control of a Supertanker and a Containership - A Simulation Study," Proceedings of the Fifth Ship Control System Symposium, Vol. 4, Annapolis, MD., Oct. 30-Nov. 3, 1978, pp. P 4-1 to P 4-38.
16. Abkowitz, M.A., "Systems Identification Techniques for Ship Maneuvering Trials," Proceedings of the Symposium on Control Theory and Navy Applications, July 15-17, 1975, Monterey, CA, pp. 337-392.
17. Åström, K.J., Källström, C.G., Norrbin, N.H., and Byström, L., "The Identification of Linear Ship Steering Dynamics Using Maximum Likelihood Parameter Estimation," Swedish State Shipbuilding Experimental Tank, Report Nr. 75, Gothenberg, Sweden, 1975.
18. Åström, K.J., and Källström, C.G., "Identification of Ship-steering Dynamics," Automatica, Vol. 12, 1976, pp. 9-22.
19. Byström, L., and Källström, C.G., "System Identification of Linear and Nonlinear Ship Steering Dynamics," Proceedings of the Fifth Ship Control Systems Symposium, Vol. 3, Annapolis, MD., Oct. 30-Nov. 3, 1978, pp. J2 2-1 to J2 2-21.
20. Trankle, T.L., and Hall, W.E., Jr., "Application of an Advanced Systems Identification Technique to Submarines," Systems Control, Inc. (Vt.) Report to ONR under Contract No. N00014-76-C-0585.
21. David Taylor Naval Ship Research and Development Reports as yet unpublished.
22. Ohtsu, K., Horigome, M., and Kitagawa, G., "On the Prediction and Stochastic Control of Ship's Motion," Proceedings of the 2nd IFAC/IFIP Symposium on Ship Operation Automation, Washington, DC, Aug. 30-Sept 2, 1976, pp. 69-76.
23. Ohtsu, K., Hara, M., and Kitagawa, G., "An Advanced Ship's Autopilot System by a Stochastic Model," Proceedings of the Fifth Ship Control Systems Symposium, Vol. 1, Annapolis, MD., Oct. 30-Nov. 3, 1978, pp. C 2-1 to C 2-11.
24. Fujino, M., "Maneuverability in Restricted Waters: State of the Art," The University of Michigan, Department of Naval Architecture and Marine Engineering, Report No. 184, Aug., 1976.

25. Ogilvie, T.F., "Recent Progress Toward the Understanding and Prediction of Ship Motions," Proceedings of the 5th Symposium on Naval Hydrodynamics, Bergen, Norway, Sept. 10-12, 1964, pp. 3-80.
26. Fujino, M., "The Effect of Frequency Dependence of the Stability Derivatives on Maneuvering Motions," International Shipbuilding Progress, Vol. 22, No. 256, Dec., 1975, pp. 416-432.
27. Fujino, M., "Experimental Studies on Ship Manoeuvrability in Restricted Waters - Part I" International Shipbuilding Progress, Vol. 15, No. 168, Aug. 1968, pp. 279-301, and "-Part II", Vol. 17, No. 186, Feb. 1970, pp. 45-65.
28. Fujino, M., "Studies on Manoeuvrability of Ships in Restricted Waters," Selected Papers from the Journal of the Society of Naval Architects of Japan, Vol. 4, 1970, pp. 157-184.
29. Bryson, A.E., Jr., and Ho, Y.C., Applied Optimal Control, Blaisdell, Waltham, Mass., 1969.
30. Gelb, A. (ed), Applied Optimal Estimation, The MIT Press, Cambridge, Mass., 1974.
31. Parsons, M.G., and Greenblatt, J.E., "SHIPSIM/OPTSIM Simulation Program for Stationary, Linear Optimal Stochastic Control Systems," The University of Michigan, Department of Naval Architecture and Marine Engineering, Report No. 188/ONR Report ONR-CR215-249-1, 23 June 1977.
32. Millers, H.F., "Modern Control Theory Applied to Ship Steering," Proceedings of the IFAC/IFIP Symposium on Ship Operation Automation, Oslo, Norway, July, 1973.
33. Canner, W.H.P., "The Accuracy Requirements of Automatic Path Guidance," Proceedings of the Fourth Ship Control Systems Symposium, Den Helder, The Netherlands, Oct. 27-31, 1975, pp. 1-141 to 1-151.
34. Hooft, J.P., "Maneuvering Large Ships in Shallow Water," The Journal of Navigation, "-I", Vol. 26, No. 2, April, 1973, pp. 189-201, and "-II". Vol. 26, No. 3, July, 1973, pp. 311-319.
35. Newton, R.N., "Interaction Effects Between Ships Close Aboard in Deep Water," DTMB Report 1461, 1960.
36. Yung, T.-W., "Hydrodynamic Interactions Between Ships in Shallow Water," Ph.D. Dissertation, University of Michigan, Department of Naval Architecture and Marine Engineering, Jan., 1977.
37. Abkowitz, M.A., Ashe, G.M., and Fortson, R.M., "Interaction Effects of Ships Operating in Proximity in Deep and Shallow Water," Proceedings of the 11th Symposium on Naval Hydrodynamics, London, UK, March 28-April 2, 1976, pp. VII.37-VII.57.
38. Panel H-10, "Proposed Procedures for Determining Ship Controllability Requirements and Capabilities," Proceedings of First Ship Technology and Research Symposium, Washington, DC., Aug. 26-29, 1975, pp. 4-1 to 4-34.

39. Newman, J.N., "Theoretical Methods in Ship Maneuvering," Proceedings of the International Symposium on Advances in Marine Technology, Trondheim, Norway, June, 1979, pp. 335-359.
40. van Oortmerssen, G., "Influences of the Water Depth on the Maneuvering Characteristics of Ships," Proceedings of the Symposium on Ship Handling, Wageningen, The Netherlands, Nov., 1973, pp. VI,1 to VI,22.
41. Parsons, M.G., "Optimal Control of Linear Systems," University of Michigan, Department of Naval Architecture and Marine Engineering, unpublished class notes, Sept., 1976.
42. MacFarlane, A.G.J., "An Eigenvector Solution of the Optimal Linear Regulator Problem," Journal of Electronics and Control, Vol. 14, No. 6, June, 1963, pp. 643-654.
43. Potter, J.E., "Matrix Quadratic Solutions," SIAM Journal of Applied Mathematics, Vol. 14, No. 3, May, 1966, pp. 496-501.
44. Bryson, A.E., Jr., and Hall, W.E., Jr., "Optimal Control and Filter Synthesis by Eigenvector Decomposition," Stanford University Report SUDAAR No. 436, Nov., 1971.
45. Holley, W.E., and Bryson, A.E., Jr., "Multi-Input, Multi-Output Regulator Design for Constant Disturbances and Non-Zero Set Points with Application to Automatic Landing in a Crosswind," Stanford University Report SUDAAR No. 465, Aug., 1973.
46. Kwatny, H.G., "Optimal Linear Control Theory and a Class of PI Controllers for Process Control," Proceedings of the 13th Joint Automatic Control Conference, Stanford, CA., Aug. 16-18, 1972, pp. 274-281.
47. Balchen, J.G., Endresen, T., Fjeld, M., and Olsen, T.O., "Multivariable PID Estimation and Control in Systems with Biased Disturbances," Automatica, Vol. 9, 1973, pp. 295-307.
48. Jazwinski, A.H., Stochastic Processes and Filtering Theory, Academic Press, New York, 1970.
49. Cuong, H.T., "Investigation of Methods for Adaptive Path Control of Surface Ships," Ph.D. Dissertation, The University of Michigan, 1980.
50. Dunn, H.J., and Montgomery, R.C., "A Moving Window Parameter Adaptive Control System for the F8-DFBW Aircraft," IEEE Transactions on Automatic Control, Vol AC-22, No. 5, Oct., 1977, pp. 788-795
51. Ralston, M.L., "Dud, a Derivative-Free Algorithm for Nonlinear Regression," Ph.D. dissertation, University of California, Los Angeles, 1975.
52. Ralston, M.L., and Jennrich, R.I., "DUD, A Derivative-Free Algorithm for Nonlinear Least Squares," Technometrics, Vol. 20, No. 1, February 1978

53. Parsons, M.G., "Optimization Methods for Use in Computer-Aided Ship Design, "Proceedings of the First Ship Technology and Research (STAR) Symposium, Washington, D.C., August 26-29, 1975.
54. Kotob, S., and Kaufman, H., "Analysis and Applications of Minimum Variance Discrete Linear System Identification," IEEE Transactions on Automatic Control, Vol AC-22, No. 5, Oct., 1977, pp. 807-815.

 The University of Michigan is an equal opportunity/affirmative action employer. Under applicable federal and state laws, including Title IX of the Education Amendments of 1972, the University does not discriminate on the basis of sex, race, or other prohibited matters in employment, in educational programs and activities, or in admissions. Inquiries or complaints may be addressed to the University's Director of Affirmative Action and Title IX Compliance: Dr. Gwendolyn C. Baker, 5072 Administration Building, 763-0235.

